CERN INTC-2003-036 INTC-P-182

Measurement of the neutron capture cross sections of ^{233}U, ^{237}Np, ^{240,242}Pu, ^{241,243}Am and ^{245}Cm with a Total Absorption Calorimeter at n_TOF

Spokesperson: E. González-Romero **Glimos: P. Cennini**

[1]U. Abbondanno, [2]G. Aerts, [3]F. Alvarez, [4]H. Alvarez, [2]S. Andriamonje, [5]J. Andrzejewski, [6]A. Angelopoulos, [6]P. Assimakopoulos, [35]G. Badurek, [9]P. Baumann, [10]F. Becvar, [11]H. Beer, [4]J. Benlliure, [2]E. Berthomieux, [12]C. Borcea, [13]F. Calviño, [3]D. Cano-Ott, [14]R. Capote, [15]P. Cennini, [16]V. Chepel, [15]E. Chiaveri, [17]N. Colonna, [30]P. Conrazier, [13]G. Cortés, [4]D. Cortina, [18]A. Couture, [18]J. Cox, [11]S. Dababneh, [7]S. David, [30]S. Deberles, [19]R. Dolfini, [20]C. Domingo, [4]I. Durán, [6]C. Eleftheriadis, [3]M Embid-Segura, [7]L. Ferrant, [15]A. Ferrari, [16]M.R. Ferreira, [36]H. Frais-Koelbl, [21]W.I. Furman, [22]I.F. Gonçalves, [3]E. González-Romero, [23]A. Goverdovski, [1]F. Gramegna, [36]E. Griesmayer, [2]F. Gunsing, [24]B. Haas, [25]R. Haight, [11]M. Heil, [15]A. Herrera-Martínez, [6]K.G. Ioannides, [7]S. Isaev, [35]E. Jericha, [15]Y. Kadi, [11]F. Käppeler, [6]D. Karadimos, [6]D. Karamanis, [26]A. Kelic, [9]M. Kerveno , [23]V. Ketlerov, [6]G. Kitis, [27]P.E. Koehler, [21]V. Konovalov, [6]E. Kossionides, [10]M. Kritcka, [28]V. Lacoste, [6]C. Lamboudis, [35]H. Leeb, [16]A. Lindote, [16]I.M. Lopes, [17]G. Lorusso, [14]M. Lozano, [9]S. Lukic, [5]J. Marganiec, [17]S. Marrone, [1]P. Mastinu, [15]A. Mengoni, [29]P. Milazzo, [14]A. Molina, [30]F. Musacchio, [16]F. Neves, [8]H. Oberhummer, [18]S. O'Brien, [2]J. Pancin, [6]T. Papaevangelou, [4]C. Paradela, [8]A. Pavlik, [30]P. Pavlopoulos, [34]M. Perlado, [2]L. Perrot, [11]R. Plag, [12]A. Plompen, [13]A. Poch, [16]A. Policarpo, [13]C. Pretel, [14]J.M. Quesada, [11]W. Rapp, [31]T. Rauscher, [25]R. Reifarth, [32]M. Maurizio, [19]C. Rubbia, [9]G. Rudolf, [12]P. Rullhusen, [22]J. Salgado, [6]E. Savvidis, [22]J.C. Soares, [7]C. Stephan, [17]G. Tagliente, [20]J.L. Taín, [7]L. Tassan-Got, [22]L.M.N. Tavora, [17]R. Terlizzi, [6]N. Tsangas, [33]G. Vannini, [22]P. Vaz, [32]A. Ventura, [3]D. Villamarín-Fernández, [3]M.C. Vicente, [15]V. Vlachoudis, [6]R. Vlastou, [11]F. Voss, [15]H. Wendler, [18]M. Wiescher, [11]K. Wisshak, [1]M. Giacchini.

1 INFN – Legnaro
2 CEA – Saclay
3 CIEMAT – Madrid
4 Universidad de Santiago de Compostela
5 University of Lodz
6 Astroparticle Consortium
7 IN2P3 – Orsay
8 Universitaet Wien – Viena
9 IN2P3 – Strasbourg
10 Charles University – Prague
11 Forschungszentrum Karlsruhe – Karlsruhe
12 IRMM – JRC EU Commission
13 Universidad Politécnica de Cataluña
14 University of Sevilla
15 CERN
16 LIP – Coimbra
17 INFN – Bari
18 University of Notre Dame
19 University of Pavia
20 Instituto de Física Corpuscular – Valencia
21 JINR – Dubna
22 ITN – Lisboa
23 IPPE – Obninsk
24 IN2P3 – Bordeaux
25 Los Alamos National Laboratory
26 IN2P3 – Strasbourg / currently at GSI
27 ORNL
28 CEA – Cadarache
29 INFN – Trieste
30 Pôle Universitaire Léonard de Vinci, Paris La Défense
31 University of Basel

32 ENEA – Bologna
33 INFN – Bologna
34 Universidad Politécnica de Madrid – Madrid
35 Technische Universitaet Wien – Viena
36 Fachhochschule Wiener Neustadt – Viena

Abstract

Accurate and reliable neutron capture cross section data for actinides are necessary for the proper design, safety regulation and precise performance assessment of transmutation devices such as Fast Critical Reactors or Accelerator Driven Systems (ADS). The goal of this proposal is the measurement of the neutron capture cross sections of ^{233}U, ^{237}Np, ^{240,242}Pu, ^{241,243}Am and ^{245}Cm at n_TOF with an accuracy of 5%. ^{233}U plays an essential role in the Th fuel cycle, which has been proposed as a safer and cleaner alternative to the U fuel cycle. The capture cross sections of ^{237}Np, ^{240,242}Pu, ^{241,243}Am and ^{245}Cm play a key role in the design and optimization of a strategy for the Nuclear Waste Transmutation. A high accuracy can be achieved at n_TOF in such measurements due to a combination of features unique in the world: high instantaneous neutron fluence and excellent energy resolution of the facility, innovative Data Acquisition System based on flash ADCs and the use of a high performance Total Absorption Calorimeter as a detection device.

1. Introduction

Nuclear waste is one the main problems for the public perception of the nuclear energy production and for the sustainability of this energy source. Although a deep underground repository seems to be a scientifically proven and technologically viable solution for the nuclear waste for the first thousands of years, this option presents difficulties for social acceptability. For this reason, nuclear waste transmutation has been proposed as a way to reduce substantially (in a factor of 1/100 or more) the inventory of the long lived component of the nuclear waste, mainly the trans-uranium actinides.

Actinide transmutation is proposed to take place by fission in nuclear systems like critical reactors or subcritical Accelerator Driven Systems (ADS). In most of the scenarios, the use of fast neutron energy spectra and specific fuel compositions, highly enriched in high mass trans-uranium actinides, are proposed. In addition, the transmutation of Long Lived Fission Fragments has also been proposed using neutron absorption (mainly by radioactive capture) normally in thermal and epithermal neutron energy spectra.

The actual knowledge on the neutron cross sections of actinides is mainly related to the exploitation of the U-Pu cycle in nuclear reactors with a thermal neutron spectrum and the design and operation of experimental fast U-Pu nuclear reactors. In addition, the currently existing nuclear databases can be used for the conceptual design of the transmutation oriented nuclear devices – critical reactors or ADS – and for the first order evaluation of the impact of the transmutation technology in the nuclear waste management.

However, the detailed engineering designs, safety evaluations and the detailed performance assessment of dedicated transmutation ADS and critical reactors (i.e. with fuels highly enriched in transuranic isotopes) require more precise and complete basic nuclear data [1].

Of crucial importance is the composition of the fuels proposed for transmutation devices, with a large concentration of minor actinides and high mass plutonium isotopes. These isotopes with little relevance for the operation of present reactors will play an important role in the neutronics of the transmuters. Figure 1 shows the strong differences in the fuel composition of nuclear plants – including the typical PWR fresh and irradiated fuels – and the fuel for the typical transmutation devices for two scenarios: the equilibrium cycle in a version of the double strata and a scenario for the phase-out of the nuclear electricity production [1].

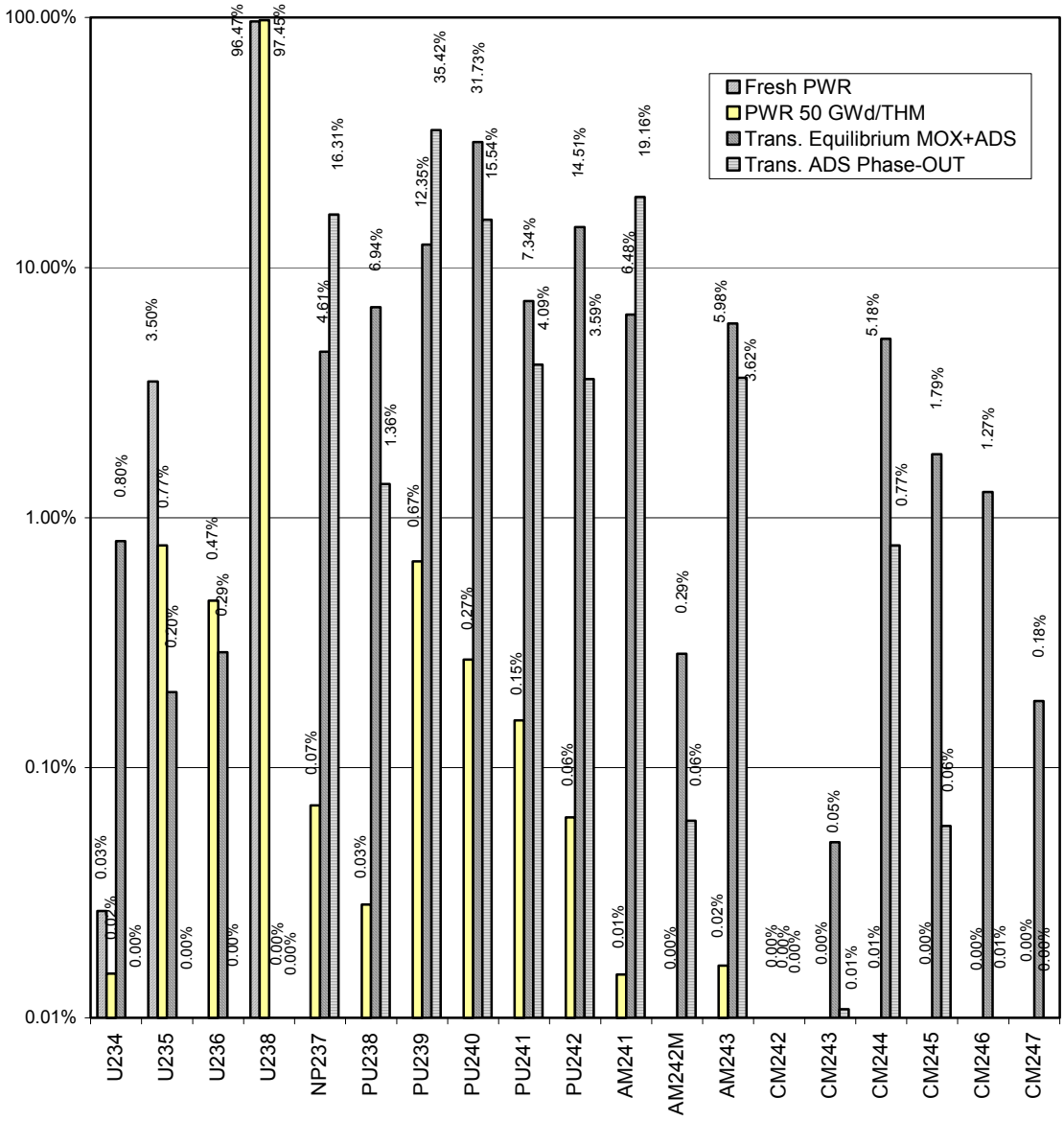

Figure 1. Comparison of the composition of the fuels for different nuclear plants: PWR (fresh and irradiated fuels) and for two Transmutation devices.

The new fuel compositions modify severely the role of the different isotopes for the global operation of the reactor and, in particular, for its transmutation performance. Figure 2 shows the relative contribution to the total number of captures from the different isotopes in the fuels previously described. Several key isotopes for the transmutation scenarios showing significant capture fractions can be identified: ^{237}Np, ^{238,239,240,241,242}Pu, ^{241,243}Am and ^{244,245}Cm.

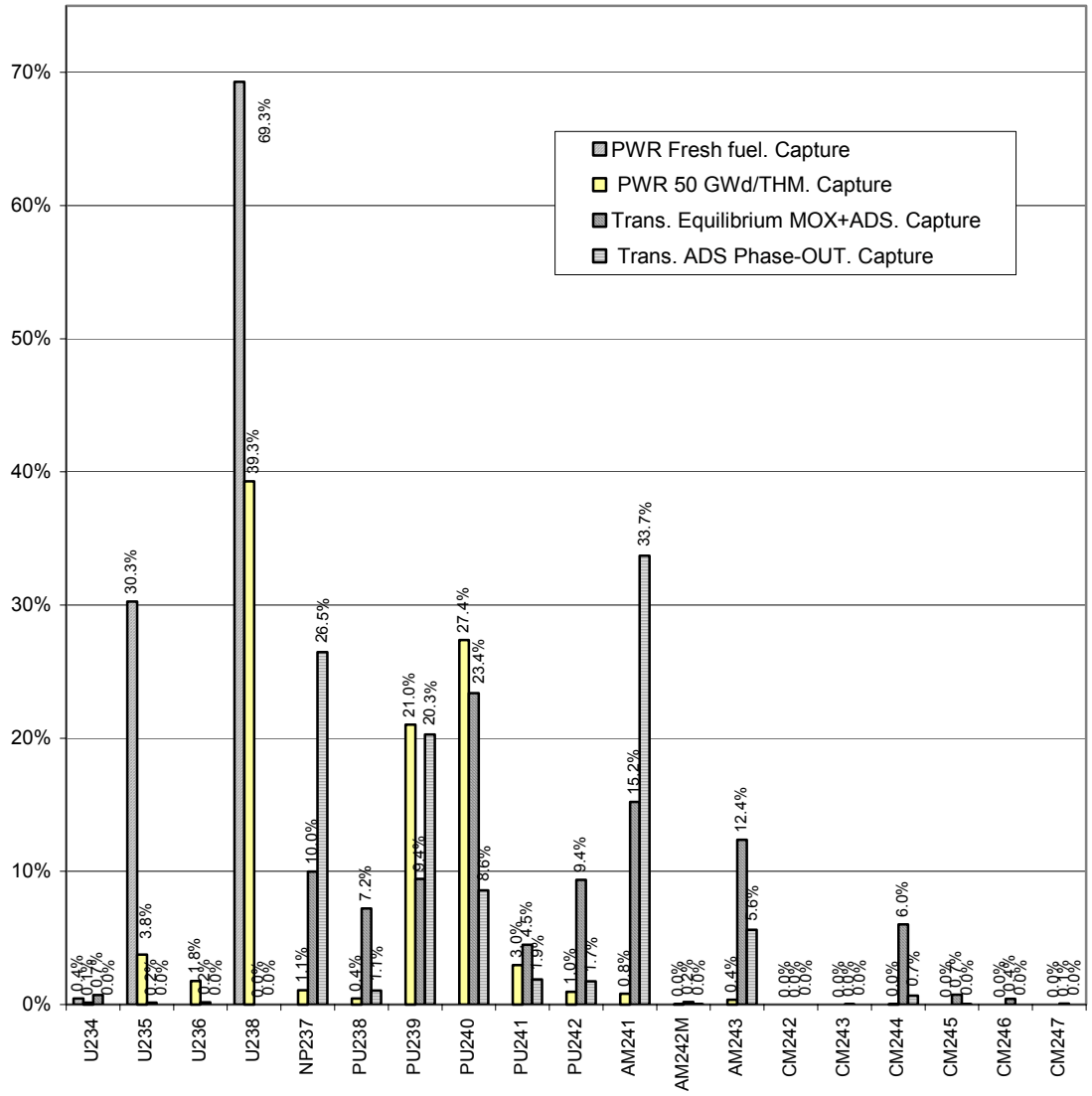

Figure 2. Contribution to capture from the isotopes present in the fuels for different nuclear plants: PWR (fresh and irradiated fuels) and for two Transmutation devices.

A selection criterion based on the impact on the transmuter neutronics and availability of capture cross section data (see Section 2 for details), allows to set a lower priority to the capture measurements of ^{239,241}Pu. In addition, the extreme difficulties involved in the capture measurements of the highly radioactive isotopes like ^{238}Pu($T_{1/2}$ = 87.74 a) and ^{244}Cm ($T_{1/2}$ = 18.1 a) reduces furtherly the list of possible measurements to ^{237}Np, ^{240,242}Pu, ^{241,243}Am and ^{245}Cm.

As a particular scenario, the Th fuel cycle has been proposed as an alternative to the nuclear energy production based on the U/Pu fuel cycle. The main reactions involved in the Th fuels are the neutron capture in ^{232}Th that, after fast series of radioactive decays breeds ^{233}U, which finally undergoes neutron induced fission and provides the necessary neutron multiplication. ^{232}Th has a smaller nuclear mass than ^{238}U. As a consequence, its neutron irradiation produces mainly uranium isotopes and much less trans-uranium actinides (protactinium is also produced), which results into a better tractable nuclear waste.

Not only the isotope list but also the energy range in which the capture cross sections has to be measured needs to be extended. For the U/Pu fuel cycle, the knowledge on the capture cross sections is mainly focused at thermal and epithermal neutron energies. On the contrary, in a fast reactor or ADS core, the neutron captures of fast neutrons play an essential role. Figure 3 shows the cumulative capture rate in several isotopes of interest for transmutation as a function of the neutron energy. A typical ADS neutron energy flux spectrum was adopted for the calculation. As it can be observed in the figure, energies up to 1 MeV have to be considered in order to take into account up to 99% of the neutron captures in the ADS core.

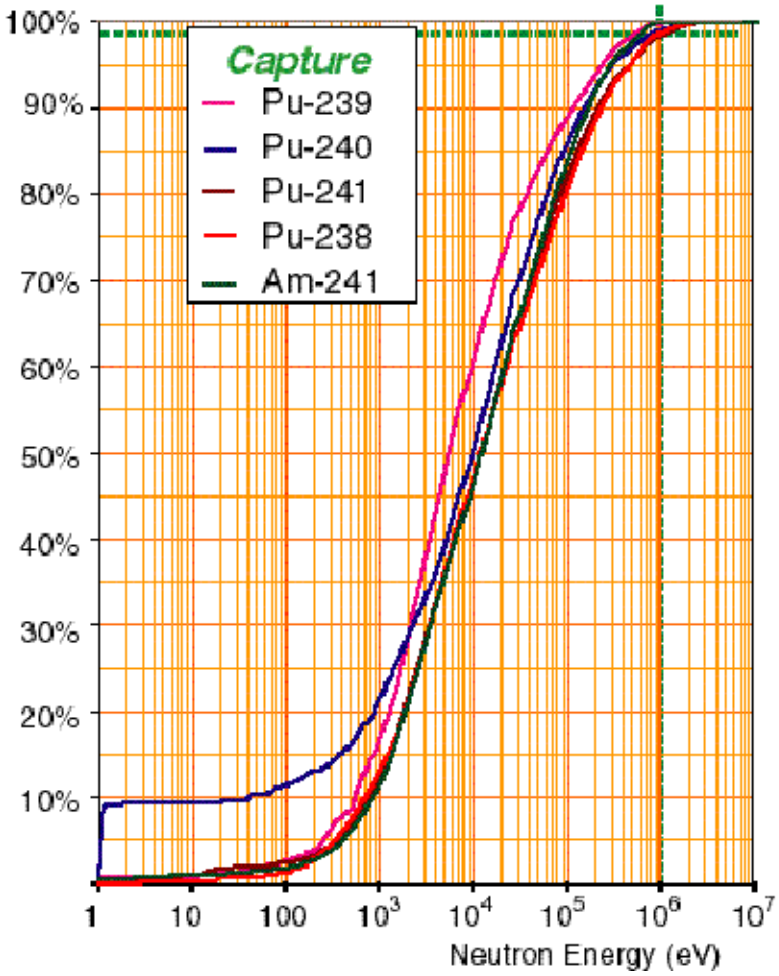

Figure 3. Capture energy range of interest in transmutation devices (Th-based fast ADS). To reach 99% of the full capture rate neutron energy has to be integrated up to 1 MeV.

A recent neutron sensitivity analysis [3] has evidenced the need of determining the neutron capture cross sections of the isotopes listed above with an accuracy better or equal than 5% in the energy range from thermal energies up to 1 MeV. In addition, the neutron sensitivity analysis allows to establish the dependence of several physical quantities describing the behavior of a transmuter on a large number of reaction channels. Thus, the overall uncertainties in such quantities can be largely reduced by performing highly accurate and targeted measurements of specific isotopes and reaction channels.

In addition, deterministic calculations based on multigroup cross sections are evidencing problems in describing changes in the neutron flux spectrum in the reflector of an ADS core [4]. Such problems are attributed to the poor knowledge on the shape of the cross sections in the unresolved resonance region up to 1 MeV. Data with enough resolution, of about 5% or better, are needed in order to determine more accurately the shape of the cross sections at high energies.

For understanding why the available capture cross sections on ^{233}U, ^{237}Np, ^{240,242}Pu, ^{241,243}Am and ^{245}Cm are not sufficient for the optimization of a transmutation device, one has to consider the two steps previous to the release of the corresponding evaluated files. First, the available data sets for ^{233}U, ^{237}Np, ^{240,242}Pu, ^{241,243}Am and ^{245}Cm are not accurate enough, are incompatible in some cases, do not cover the necessary neutron energy range and the resolution provided is not sufficient. Second, the available evaluated cross section files do not agree between themselves as well. More often than it would be desirable the evaluators are forced to question and re-investigate the accuracy of specific data sets in order to reach a self-consistent result in their evaluation for all the reaction channels. Thus, the result on the evaluation depends strongly on the decisions adopted by the evaluator. More accurate measurements are necessary in order to constrain the parameters (such as level densities or optical potential parameters) of the physics models applied.

Data with the necessary accuracy of 5% and resolution in the neutron energy range of 0.1 eV to 1 MeV can be measured at n_TOF due to the following reasons:

- The neutron energy range between 1 eV and 1 MeV is covered in one single measurement with an excellent energy resolution.
- The Total Absorption technique that will be applied for the measurements is particularly well suited for low mass and radioactive samples.
- The sources of background at n_TOF are very well characterized and can be largely suppressed in combination with the Total Absorption Calorimeter.

Details on the availability of capture cross section data are discussed in Section 2. Technical aspects on the characteristics of the targets and the experimental technique are discussed in Section 3 and Section 4 respectively.

For the reasons discussed, the measurement of the neutron capture cross section of ^{233}U, ^{237}Np, ^{240,242}Pu, ^{241,243}Am and ^{245}Cm at n_TOF are proposed in the range from 1 eV to 1 MeV with an accuracy of 5% and an energy resolution in the unresolved resonance region better than 5%. Such measurements are part of the scientific program of the contract FIKW-CT-2000-00107 between the European Commission and the n_TOF collaboration participating institutes. The beam time request is presented in Section 5.

2. Available Experimental Data and Evaluated Cross Sections

An exhaustive study on the availability of previous measurements has been performed. All the experimental cross section data referenced in this section have been obtained from the Experimental Nuclear Reaction Data File (EXFOR [CSISRS]) database [5]. They correspond to the complete sets of data for capture and absorption cross sections (quantity codes CS and RP, see Ref [6] for details) publicly available by the 15th of September 2003. More recent data sets have been obtained from the references found in

the Computer Index of Neutron Data (CINDA) [7]. The evaluated cross section files have been obtained from the most recent releases of the available evaluated cross section libraries ENDF, JEFF, JENDL, BROND and CENDL. Figures showing the experimental data and evaluated cross sections, as well as tables containing technical information about the available data sets are shown in Appendix I.

2.1. ^{240}Pu(n,γ) cross section data

In the resolved resonance region there are experimental radiative resonance parameters determined directly from TOF capture measurements [34] or derived from transmission and fission measurements [35] [36]. For the reported cases, the uncertainties in the radiative and neutron widths are in the range from 5% to 30%.

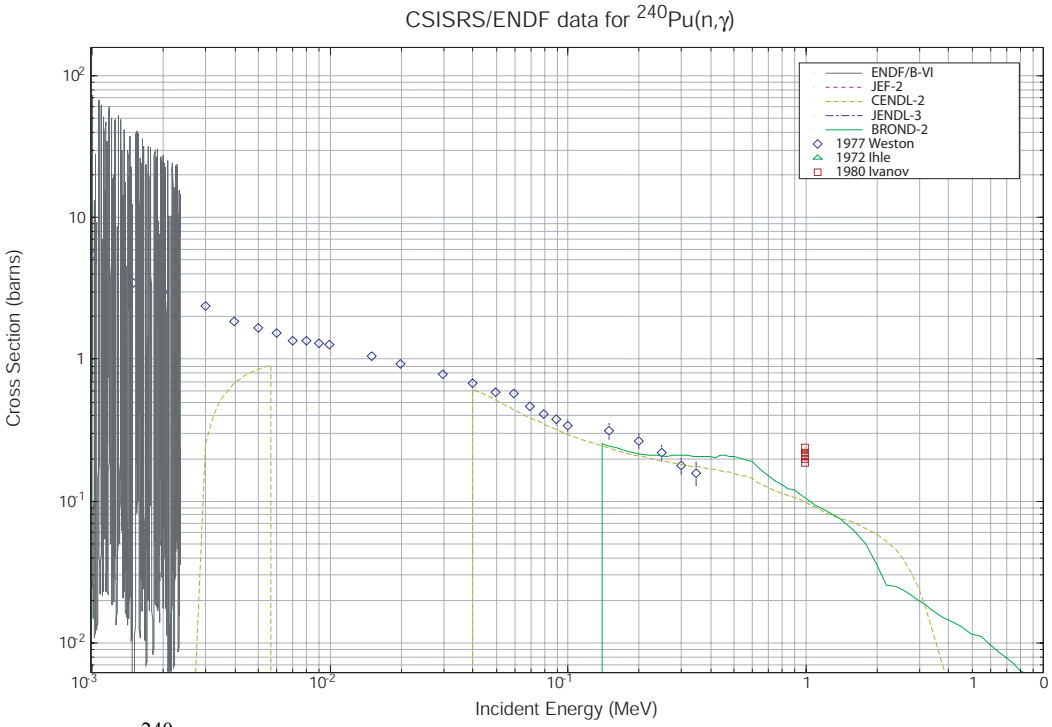

Figure 4. ^{240}Pu(n,γ) evaluated cross sections and EXFOR experimental cross section points in the range from 1 keV eV to 10 MeV.

In the unresolved resonance region, there are only three TOF data sets available. Two are shown in Figure 4 and correspond to the measurements by Weston [32] for neutron energies between 200 eV and 350 keV and Hockenbury [35] for neutron energies between 6 keV and 30 keV. Only Hockenbury reports uncertainties in the range from 7% to 20%. A third set of data relative to the ^{197}Au(n,γ) and ^{238}U(n,γ) cross sections is provided by Wisshak [30][31]. According the to authors, such data are in good agreement with [35] and slightly above but compatible within the uncertainties to [32] in the 10 keV to 30 keV range. The uncertainties estimated range from 5% to 20%. No TOF data are available above 350 keV, although one more additional point coming from activation measurements by Ivanov [33] exists at 1 MeV.

The main goal of the measurement at n_TOF will be to obtain accurate data in the unresolved resonance region (from 1 keV up to 1 MeV) with an energy resolution better

than 5%. In addition, the high resolution of the installation will provide accurate data in the resolved resonance region and allow to extend it up to higher energies.

Al five libraries do contain an evaluation for ^{240}Pu. In the resolved resonance region, there is a good agreement between the different evaluated files up to 250 eV, since all the evaluations share mainly the same recommended list of resonance parameters. In the unresolved resonance region, large discrepancies between the different files are observed. Up to 40 keV, The JEFF cross section is about 6% to 10% below the other evaluations and a discrete jump is observed above 40 keV. Between 40 keV and 250 keV, deviations as large as 25% are observed between the different evaluations. Above 250 keV up to 1 MeV, discrepancies of the order of 100% are found.

2.2. ^{242}Pu(n,γ) cross section data

In the resolved resonance region there are radiative resonance parameters determined directly from TOF capture measurements [50][51] or combined with transmission and fission measurements [51]. For the reported cases, the uncertainties in the neutron and radiative widths range from 5% to 30%.

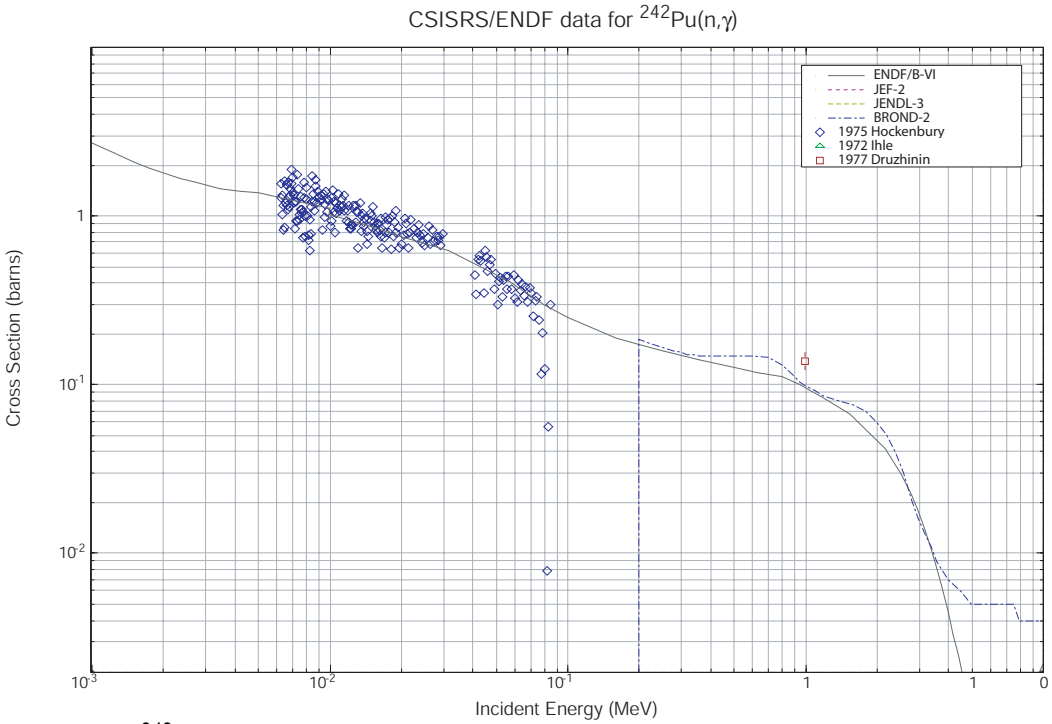

Figure 5. ^{242}Pu(n,γ) evaluated cross sections and EXFOR experimental cross section points in the range from 1 keV to 10 MeV.

In the unresolved resonance region there are only two TOF data sets available. Figure 5 shows the data from Hockenbury [51] from 600 eV to 87 keV. No mention on the uncertainties is made. The data by Wisshak [48][49] from 5 to 90 keV show a good agreement with the data from Hockenbury at the investigated energies. The reported uncertainties range from 5% to 10%. No data are available above 100 keV apart from an activation measurement from Druzhinin [53]. The measurement at n_TOF will improve the available data in the same manner as for the ^{240}Pu case.

The ENDF, JENDL, JEFF and BROND libraries do contain evaluated files for ^{242}Pu. In the resolved resonance region, there is a good agreement between the different evaluations. In the unresolved resonance region up to 200 keV there is a large discrepancy of about 500% between the BROND and the other evaluations. In the same range, the JENDL and JEFF evaluations present an also large discrepancy of about 200% at 4 keV and of 5% to 10% up to 200 keV. Above 200 keV, the average difference between all the evaluations range from 2% to 20%.

2.3. ^{241}Am(n,γ) cross section data

Two different TOF capture data sets are available in the resolved resonance region: the (n,abs) data from Weston [58] and the (n,γ) data from Vanpraet [57]. Both sets correspond to massive and highly radioactive ^{241}Am samples, consisting of 2 g of AmO_2 and 1.7 g of metallic Am respectively.

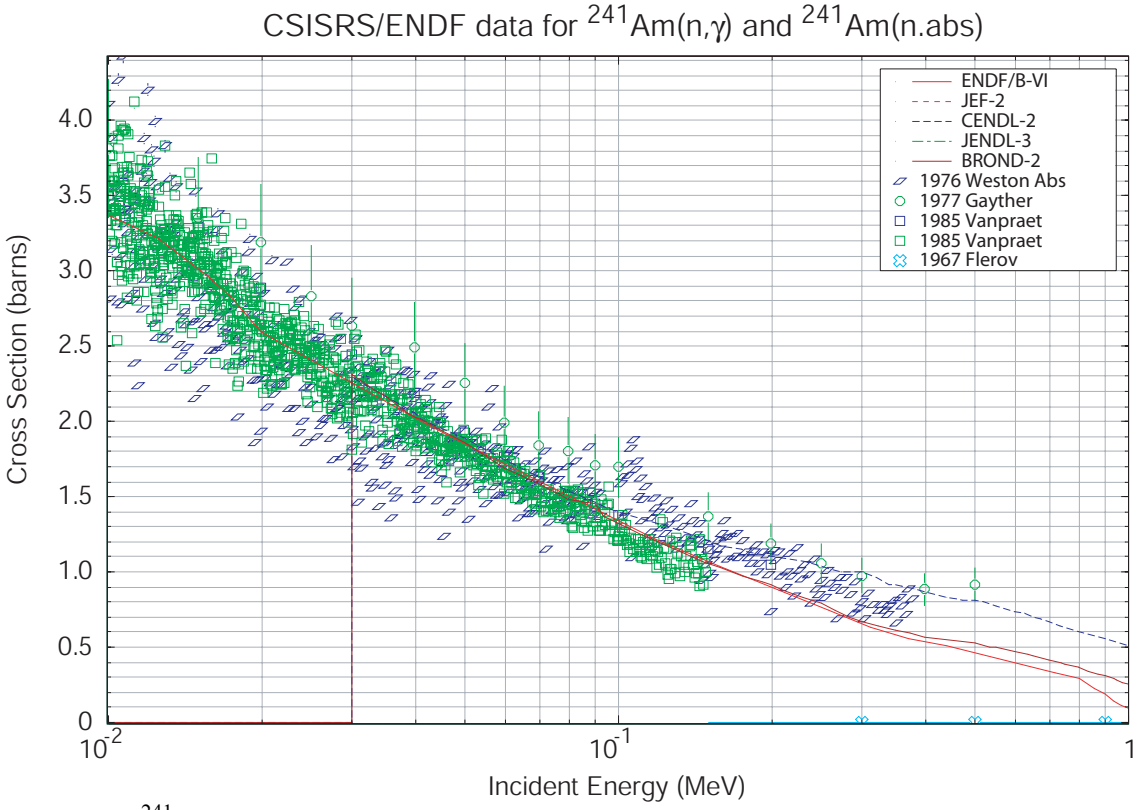

Figure 6. ^{241}Am(n,γ) evaluated cross sections and EXFOR experimental cross section points in the range from 10 keV to 1 MeV.

Large differences up to 30% are found between the two data sets since Vanpraet´s values are not corrected for self-screening effects. Additional experimental resonance parameters have been obtained from direct absorption [58] and indirect transmission/fission [59] measurements.

In the unresolved resonance region two additional sets of TOF data from Gayther [60] and Wisshak [54] are available. Gayther´s data show a good agreement with those from Vanpraet and Weston up to 2 keV, where differences start to be sizeable. According to the authors, the uncertainties of the measurements are of the order of 10% or higher. As it can be seen in Figure 6, above 2 keV the data from Gayther start to deviate

systematicaly by 10% or more. Such a discrepancy could be attributed to uncertainties in the normalization, as suggested in a recent evaluation work from Ignatyuk [65]. The data by Wisshak [54] range from 10 keV to 250 keV and are in good agreement with Gayther's measurement within the uncertainties of 5% to 20%. No other experimental points are available above 400 keV except the data from Flerov, standing for the ^{241m}Am isomeric state capture cross section, and the values from several activation measurements [56][61][28].

The measurement at n_TOF will allow to obtain accurate data in the unresolved resonance region (from 1 keV up to 1 MeV) with an energy resolution better than 5%. The data in the resolved resonance region will be much less affected by the thickness of the ^{241}Am sample and its intrinsic radioactivity. In addition, it will allow to extend the resonance region up to higher energies.

All five libraries do contain an evaluation for ^{241}Am. Differences are found in the shape of the resonances in the energy region between 1 and 10 eV. The BROND evaluated file includes some large resonances not appearing in the other evaluations. In the unresolved resonance region, the average deviation between the different evaluated files is about 5% up to 20 keV and 10% or larger above. An alternative evaluation work from Ignatyuk [65] shows a preference for the data from Wisshak and Gayther, and therefore shows a 5% to 10% increase of the capture cross section in the region above 10 keV.

2.4. ^{243}Am(n,γ) cross section data

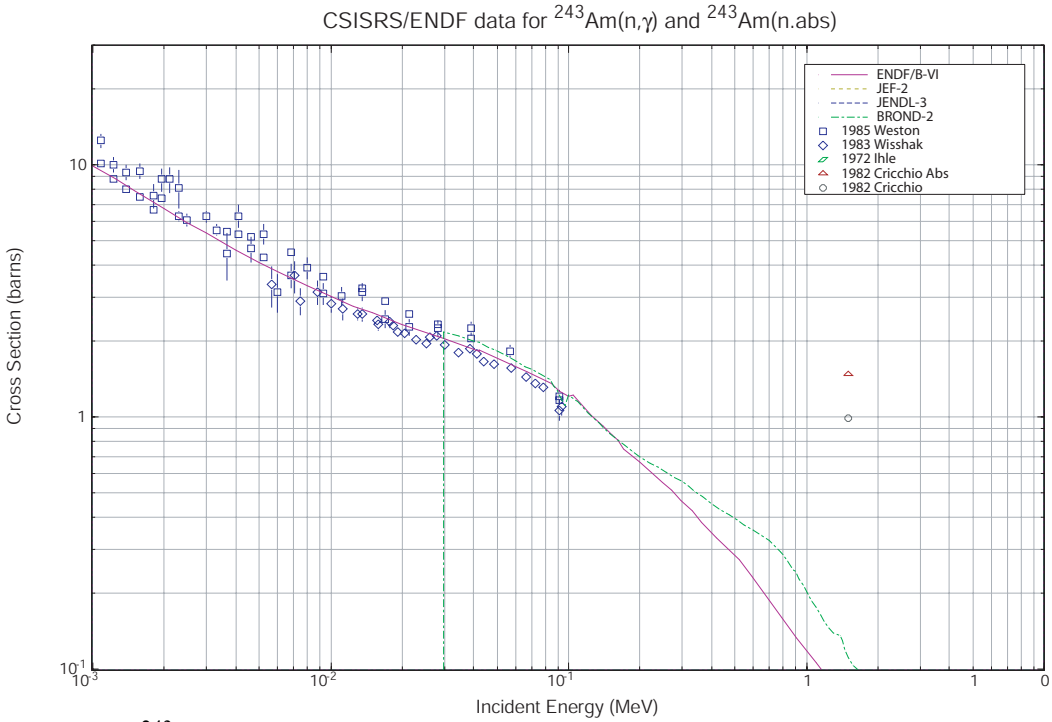

Figure 7. ^{243}Am(n,γ) evaluated cross sections and EXFOR experimental cross section points in the range from 1 keV to 10 MeV.

The amount of available data for ^{243}Am(n,γ) is scarce. In the resolved resonance region, experimental radiative widths have been obtained indirectly from transmission and

fission TOF measurements [67][68][69]. No direct TOF cross section data have been found.

In the unresolved resonance region up to 1 MeV there exist only two TOF data sets by Wisshak [66] and Weston [70], ranging from 0.3 keV to 100 keV and 5 keV to 100 keV respectively. No data are available above 100 keV. As it is shown in Figure 7, there is a systematic bias between the two data sets of about 10%. One more experimental point for the neutron capture cross section is available above 1 MeV from an activation measurement [28].

The measurement at n_TOF will be the first one providing direct capture data in the resolved resonance region.

The ENDF, JENDL, JEFF and BROND libraries do contain evaluated files for ^{243}Am. The discrepancies between libraries in the unresolved resonance region are mainly due to the preference of the evaluators for one of the two data sets [71] and constraints imposed from the other reaction channels. Differences as high as 20% to 30% at 200 keV and 60% at 1 MeV can be observed.

2.5. ^{245}Cm(n,γ) cross section data

No data are available in the EXFOR databank for the ^{245}Cm capture cross section in the energy range from 0.1 eV to 1 MeV. Only four different points at thermal energies [72] [73][74][75] have been measured by activation techniques.

The ENDF, JENDL and JEFF libraries do contain evaluated files for ^{245}Cm. In the resolved resonance region, large differences in the resonance parameters are found. Such differences are attributed to the use of different (n,f) and transmission data sets [77]. In the unresolved resonance region up to a few hundred keV, the JENDL and JEFF evaluations (with a common origin in the evaluation [77]) differ by 30 % to 60 % up to 1 MeV.

The measurement proposed at n_TOF will be the first providing experimental data on the ^{245}Cm(n,γ) reaction.

2.6. ^{233}U(n,γ) cross section data

The resonance parameters up to 150 eV are based on a selected number of data sets containing total cross section measurements [12][13][14][15], fission measurements [16] [17][18][19][20] and capture [16][17]. For higher energies, experimental capture data are scarce. Unresolved resonance parameters have been added from 150 eV to 30 keV and from 30 keV to 1 MeV the evaluation is based on a capture to fission ratio experiment [21].

2.7. ^{237}Np(n,γ) cross section data

The amount of available data for ^{237}Np is larger than for the rest of isotopes in this proposal. In the resolved resonance region, experimental radiative widths have been obtained from capture, transmission and fission TOF measurements [37][38][39][40][41]

[42]. For the reported cases, the uncertainties in the neutron and radiative widths range from 2% to 50%.

Two large data sets by Weston [38] and Hoffmann [46] are available from epithermal energies up to 220 keV and 20 eV to 250 keV respectively. Both measurements used massive (2g) and highly radioactive samples. The uncertainties in Weston's data range from 2% to 20% and are comparable to the ones in Hoffmann's data, ranging from 2% to 30%. Both data sets show huge discrepancies up to 200%, particularly at energies above 1 keV. Above 200 keV and up to 1.2 MeV, there are additional capture data from activation measurements by Buleeva [43], Trofimov [44], Lindner [45] and Stupegia [47]. The data of Buleeva and Trofimov agree within the uncertainties, while the values from Stupeggia differ by 50% to 100% at energies around 1 MeV.

The measurement at n_TOF will provide the necessary high accuracy data in both resolved and unresolved resonance regions.

The ENDF, JENDL, JEFF and CENDL libraries do contain evaluated files for ^{237}Np. The JEFF and ENDF evaluations are nearly identical. In the unresolved resonance region, there are differences between the ENDF and JENDL libraries up to 10%, mainly in the tails between the resonances. The CENDL evaluation shows larger deviations up to 50% with respect to the ENDF and JENDL files. In the unresolved resonance region, the CENDL evaluation is 20% larger than all other three files up to 20 keV. Above 100 keV, the JENDL evaluation is about 10% to 20% below the ENDF, JEFF and CENDL cross sections.

2.8. Summary and conclusions

The amount and accuracy of the available experimental capture cross section data for ^{233}U, ^{237}Np, ^{240,242}Pu, ^{241,243}Am and ^{245}Cm is not sufficient. As it is described in Appendix I, the experimental techniques employed in those measurements (Moxon Rae detectors, liquid scintillators and total energy detectors) require large corrections for determining the counting efficiencies, estimating the backgrounds, in particular due to the radioactivity of the samples, and discriminating the different reaction channels. Therefore, larger systematic uncertainties than the reported ones should not be excluded, as it has been pointed out already in several evaluations. The measurements at n_TOF will be performed in better experimental conditions and the following goals will be achieved:

- Provide the first capture data for ^{245}Cm.
- Provide the first high resolution capture data in the resolved resonance region for ^{243}Am.
- Obtain accurate data in the unresolved resonance region (from 1 keV up to 1 MeV) with an energy resolution better than 5%.
- Obtain accurate data in the resolved resonance region and extend it up to higher energies.
- Provide high quality data in the region from 1 keV to 1 MeV for constraining the physics models used in the evaluations.

3. Targets

The ^{237}Np, ^{233}U, ^{240}Pu and ^{241,243}Am targets for the neutron capture measurements will be provided by IPPE OBNINSK under a contract signed between the n_TOF collaboration and IPPE OBNINSK. The Oak Ridge Target laboratory, Russian Federation laboratories and ITU-FZK are being consulted for the manufacture of the ^{245}Cm and ^{242}Pu targets.

All targets will be made with isotopically enriched material with a purity typically larger than 99.9% according to the manufacturer. The contamination in the capture measurements due to decay products grown after the isotopic separation has been calculated and is well below 1%.

Isotope	Density (g/cm^3)	Available mass (mg)	Sample diameter (cm)	Sample surface (cm^2)	Sample thickness (at/barn)	Sample thickness (μm)
^{233}U	18.95	100	1	7.85E-01	3.29E-04	6.72E+01
^{237}Np	20.45	20	1	7.85E-01	6.47E-05	1.25E+01
^{240}Pu	19.84	20	1	7.85E-01	6.39E-05	1.28E+01
^{242}Pu	19.84	20	1	7.85E-01	6.34E-05	1.28E+01
^{241}Am	13.6	25	1	7.85E-01	7.95E-05	2.34E+01
^{243}Am	13.6	25	1	7.85E-01	7.89E-05	2.34E+01
^{245}Cm	13.511	10	1	7.85E-01	3.13E-05	9.42E+00
Samples for reference and background measurements and structural materials						
^{197}Au	19.32	100	1	7.85E-01	3.89E-04	6.59E+01
^{nat}C	2.62	100	1	7.85E-01	6.39E-03	4.86E+02
^{208}Pb	11.34	300	1	7.85E-01	1.11E-03	3.37E+02
^{27}Al	2.702	2.1	1	7.85E-01	6.029E-05	1.000E+01

Table 1. Description of the physical characteristics of the actinide samples, reference samples and structural materials (canning and sample backings)

The isotopically enriched samples will be deposited on a thin backing of Al and encapsulated inside an (Al or Ti) canning fulfilling the ISO 2919 norm for sealed containers. The appropriate certification will be provided by the manufacturer and delivered to the CERN Radioprotection authorities, thus fulfilling the CERN radiation protection requirements on the use of radioactive sources. The canning will be made of a mechanically resistant low Z and low capture/elastic cross section material (Al or Ti) with thin entrance windows.

Table 1 shows the details of the isotopic enriched targets such as masses and geometric characteristics. Two groups are distinguished: the actinide samples and reference samples or structural materials.

The activity of each actinide sample has been calculated for determining the magnitude of the background in the capture measurements due to decay gamma rays. The full decay chains for each isotope were considered. The complete list of gamma rays for each decay mode was taken into account and adopted from the detailed Evaluated Nuclear Structure Data Files (ENSDF). The conclusion of the study is that, even for the most radioactive samples, the background rates in the calorimeter will be acceptable. Detailed results on the activities for each isotope can be found in Appendix II. A discussion on the influence of the background due to the sample activity follows in Section 4.

4. Experimental Technique

The combination of the n_TOF facility, the innovative n_TOF Data Acquisition System (DAQ) and the use of a powerful Total Absorption Calorimeter of BaF_2 make n_TOF to be at present time a unique installation for studying neutron capture cross sections of highly radioactive materials available in low quantities. The magnitude and good control mechanisms of possible sources of systematic uncertainties associated to the experimental technique is discussed in Subsections 4.1, 4.2 and 4.3.

4.1. Advantages of the n_TOF facility

The n_TOF facility [79] provides an excellent energy resolution of 10^{-3} to 10^{-4} at a 185 m flight path between the Pb spallation target and the counting station. For capture measurements with a 4 cm diameter neutron beam spot, the instantaneous fluence amounts to 10^5 neutrons/cm^2/pulse for neutron energies between 0.1 eV and 20 GeV. This is one of the key features for measuring the (n,γ) cross section of low mass and highly radioactive isotopes such as ^{233}U, ^{240,242}Pu, ^{241,243}Am and ^{245}Cm with a good signal to noise ratio. The repetition rate can be as large as 5 – 6 proton pulses for a PS supercycle of 16.4 s.

The capture cross section measurements at n_TOF will be done relative to the standard reference cross section ^{197}Au(n,γ) for neutron capture. For this reason, several independent monitors are used permanently for a proper normalization between the ^{197}Au(n,γ) and main measurements [79]:

- Silicon Flux Monitor, based on the ^{6}Li(n,α) reaction. It monitors constantly the neutron beam before the capture setups.
- PS proton beam information. It is used to correlate the proton beam intensity at the spallation target and the neutron yield.
- Wall current monitor. Its response is proportional to the proton beam intensity on the spallation target, which is correlated to the neutron yield.
- BF_3 array at the neutron escape lane used as a beam on/off flag.

It has been determined experimentally that the systematic uncertainties due to normalization between the reference and capture measurements is about 1%.

4.2. The Data Acquisition System (DAQ) at n_TOF

The n_TOF DAQ is based on 64 channels of high performance flash ADCs. Each channel [80] has 8 Mbytes memory and is operated at a sampling rate of 500

Msamples/s, thus allowing to record the full detector history for neutron energy ranges between 0.3 eV and 20 GeV.

After zero suppression and data formatting, the raw data are transferred to CASTOR [81] via several fast Gigabit links. In parallel, specially designed pulse shape analysis routines extract from the digitized detector signals the necessary information for the data analysis.

The n_TOF DAQ offers unique features such as an extremely low dead time (< 10 ns), excellent signal analysis and pileup discrimination among others, resulting in an excellent mechanism for controlling all kind of systematic uncertainties associated to the detector's behavior. As an example, the quality of the reconstruction [84] for a C_6D_6 liquid scintillator is shown in Figure 8: flash ADC data (in black) and reconstructed signals by means of a pulse shape fitting analysis routine (in red). Pileups are easily detected and the parameters such as time and amplitude are correctly determined. Similar techniques will be applied to the analysis of the BaF_2 signals, thus allowing to reduce the systematic uncertainties due to dead time and pileup to 3%.

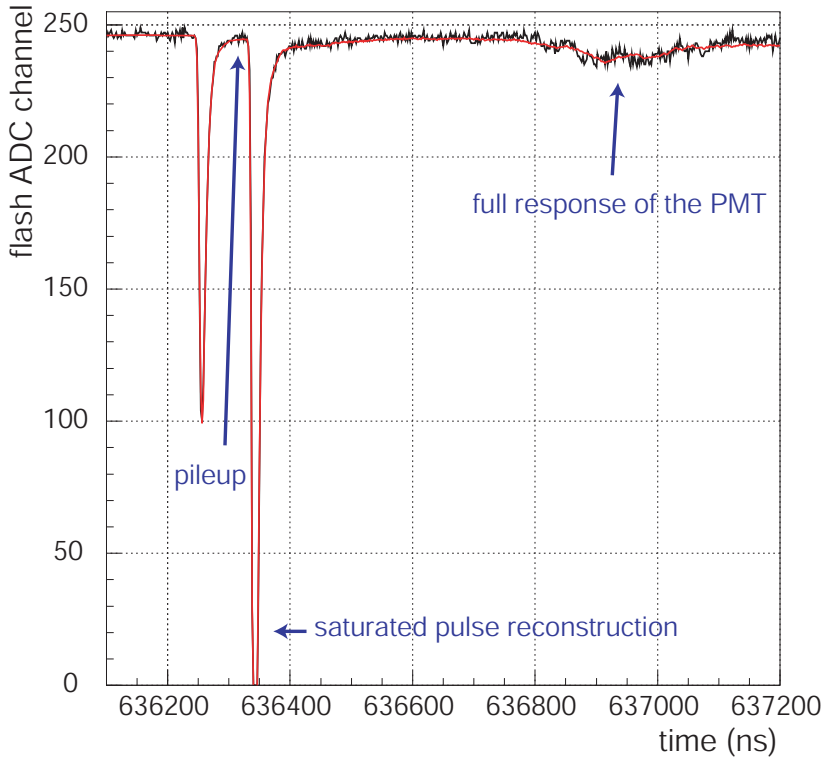

Figure 8. Flash ADC data (black) and reconstructed (red) pulse shapes of a C_6D_6 liquid scintillator.

4.3. Total Absorption Calorimetry at n_TOF

The total absorption technique is a powerful tool for investigating the electromagnetic de-excitation of isotopic species independently from their particular de-excitation pattern. It has been successfully applied in the measurement of neutron capture cross sections both with large liquid scintillator tanks and more recently with inorganic scintillators [10][11].

The use of a Total Absorption Calorimeter in neutron capture measurements allows to add up all the gamma rays de-exciting the compound nucleus after the neutron capture has occurred. In this way, a total absorption sum peak is observed in the energy deposition TAC spectra at an energy corresponding to the neutron separation energy of the compound nucleus S_n added to the energy of the captured neutron. In such a way, the signal due to capture can be largely discriminated from all possible sources of background. In addition, the use of beam time is highly optimized, since the total detection efficiency is nearly 100%.

Total Absorption Calorimetry has significant advantages over alternative techniques commonly employed in neutron capture cross section measurements such as the Moxon-Rae [8] and the Pulse Height Weighting technique [29]:

- High efficiency of nearly 100% versus 0.1% for the Moxon-Rae detectors and 5% for the total energy detectors (like C_6D_6).
- Good energy resolution which allows the recognition of structures in the energy spectra.
- Direct background suppression mechanisms based on combined multiplicity and energy deposition analysis.
- Low systematic uncertainties associated to the counting efficiency are at the level of 1%

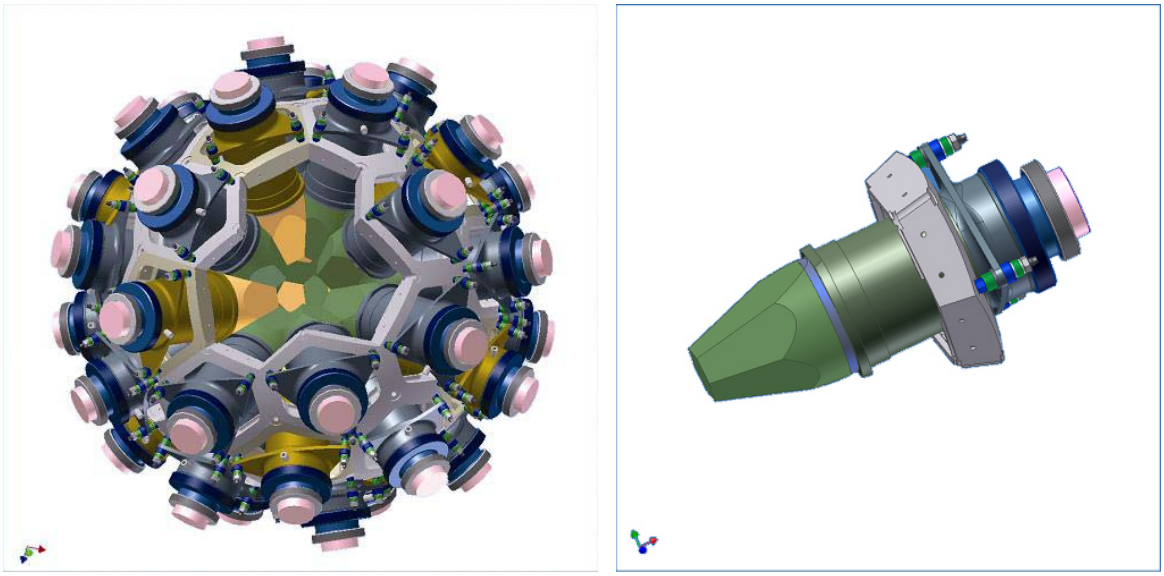

Figure 9. Left: CAD drawing of the complete TAC assembly. Right: CAD drawing of an hexagonal module with housing, support and photomultiplier housing.

A Total Absorption Calorimeter is being built at n_TOF and will be fully operative in early Spring 2004. Figure 9 shows the CAD drawings of the full TAC assembly (left) and a complete module (right). The TAC at n_TOF is nearly identical to the one already existing at FZK [10] and shown in the left part of Figure 10. The 4π geometry consists of 42 BaF_2 crystals, 12 of them having a pentagonal shape and the rest an hexagonal shape. Both pentagons and hexagons have a 15 cm thickness and cover the same solid angle with respect to the geometric center of the TAC at 10 cm from the front face of the crystals. At n_TOF only 40 crystals will be used for leaving two holes along the entrance and exit points for the neutron beam, respectively.

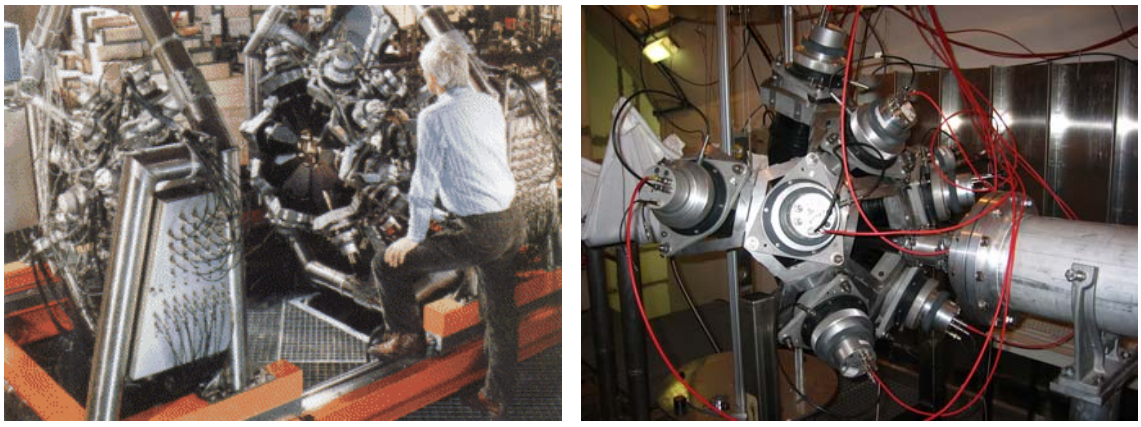

Figure 10. Left: Setup of the 4π BaF_2 installed at the VdG facility in FZK (Karlsruhe). Right: Setup of a 1p subassembly at n_TOF during the test-beam performed in July 2003.

Figure 11 shows a scheme of the experimental setup for the (n,γ) measurements with the TAC. The neutron beam is monitored first with the Silicon Flux Monitor and afterwards interacts with the targets located in the center of the TAC. The large fraction of beam not interacting with the samples (>95%) exits the experimental area and is dumped on a polyethylene block at the end of the TOF line at a 200 m flight path.

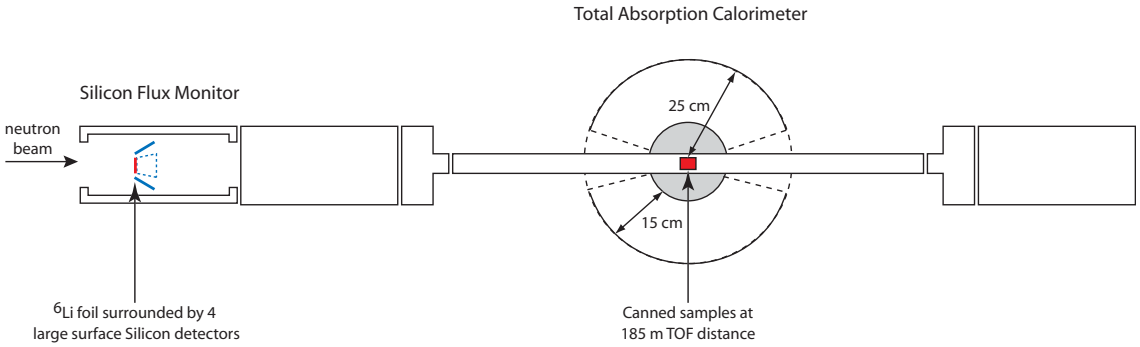

Figure 11. Schematic view of the TAC setup at the n_TOF experimental area.

A test beam with 9 crystals, covering approximately 1π solid angle, has been performed at n_TOF in July 2003 . The good operation of the crystals was demonstrated.

The sources of systematic uncertainties in the capture measurements with the TAC at n_TOF are mainly coming from the different types of background. They can be summarized as follows:

- The n_TOF environmental background and beam related background outside the beam line: it has been determined both by Monte Carlo simulations [86][87][88] and experimentally [78] that the fluence of neutrons and gamma rays outside the beam pipe is 5 orders of magnitude lower than the neutron beam fluence. In addition, the iron shielding against ultrarelativistic μ installed along the n_TOF tunnel will be completed during the PS winter shutdown in 2003.

- The sample related background. The main sources of background at n_TOF are due to the samples placed in the neutron beam:

a.) in-beam gamma rays. It has been determined that there is a sizeable source of background due to gamma rays propagating inside the neutron beam line and scattered at the samples. It originates at the n_TOF spallation target and is mainly due to thermal or epithermal neutron capture in the hydrogen of the H_2O moderator, which produces 2.2 MeV gamma rays. For the measurements with the TAC such a component can be highly suppressed by energy discrimination. In addition, it can be measured and subtracted from the data.

b.) scattered neutrons. In every capture experiment there is always a contribution due to neutrons elastically scattered at the samples and captured in the detectors and surrounding materials. For the measurements to be performed with the TAC, the probability of detecting a scattered neutron which is subsequently captured ranges from 2% to 20%, depending on the neutron energy. Such a source of background is of particular importance at neutron energies for which the elastic scattering cross section dominates over the capture and has been investigated by Monte Carlo simulations [92][93][94][95]. It can be highly suppressed at neutron energies between 0.1 eV and 1 keV by using a neutron absorber of ^{6}LiH inside the TAC. In addition, it can be measured and subtracted from the data.

c.) inelastic channels. At neutron energies above the 1st excited state of the isotope being measured, there is a contribution of gamma rays due to inelastic scattering. Such a component can be easily suppressed in capture measurements with a TAC by setting a threshold in the deposited energy of 1 MeV.

d.) neutron induced fission gamma rays and neutrons. Gamma rays and neutrons emitted in the fission process are the dominant background in (n,γ) measurements at neutron energies where fission dominates over capture. Such is the case of ^{233}U and ^{245}Cm in the whole neutron energy range and for ^{237}Np, ^{240,242}Pu, ^{241,243}Am above the fission thresholds. The contribution of the fission background has been investigated both experimentally [96] and by Monte Carlo simulations [95] and the conclusion is that it can be greatly suppressed by applying a combination of multiplicity and energy thresholds. Furthermore, it can be measured by using a fission tagging.

e.) Capture and elastic reactions in the canning. The cannings of the samples used will be as thin as possible. In addition, their effect will be measured (with an empty canning) and subtracted from the data.

- radioactivity of the samples. The gamma activity of the actinide samples can be divided in two components. First, the dominant component due to X-rays and low energy gamma rays (< 100 keV) MeV. Second, the much weaker component (by several orders of magnitude) due to gamma rays associated to beta decay and with average energies of several hundred keVs up to MeVs. The first component can be suppressed during the pulse shape analysis by treating it

as a baseline shift. The second component can be discriminated by adequate thresholds on the total energy deposited in the TAC.

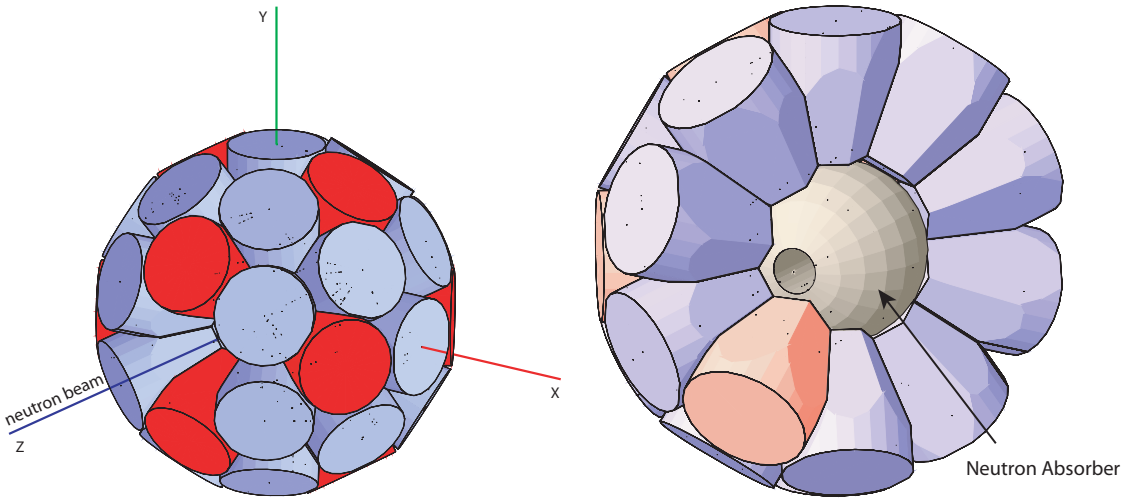

Figure 12. Left: geometry of the TAC with 40 crystals. Right: geometry of the TAC with a 10 cm radius ^{6}LiH absorber inside.

Two different configurations will be used in the capture measurements at n_TOF: the TAC with a neutron absorber surrounding the samples and the bare TAC without the absorber. Figure 12 shows the two different geometries.

The use of ^{6}LiH allows to largely suppress the scattered neutron background in the neutron energy regions where the largest contribution to the background is due to scattered neutrons. Such is the case for ^{237}Np, ^{240,242}Pu and ^{241,243}Am below the fission threshold (at about 200 keV).

As it can be observed in Figure 13 for a reference ^{197}Au sample, the suppression of the scattered neutron background is nearly complete at neutron energies below 100 eV and about a factor of 4 at neutron energies above 1 keV.

For fissile nuclei like ^{233}U and ^{245}Cm, the largest background will be due to the neutron induced fission channel. As can be observed in Figure 14 for the case of ^{245}Cm, the use of the absorber has several negative side effects:

- reduction of the magnitude of the total absorption peaks
- reduction of the average multiplicities of fission events
- enhancement of gamma ray fission background in the TAC energy spectra in the region of interest for the capture events.

For this reason, the measurements with the absorber will be combined with measurements without absorber for making a rigorous comparative analysis that will allow to extract the cross section with the necessary accuracy.

Last, if a fission tagging will be available at the time of the measurements, the background due to fission gamma rays will be directly measured and subtracted from the data.

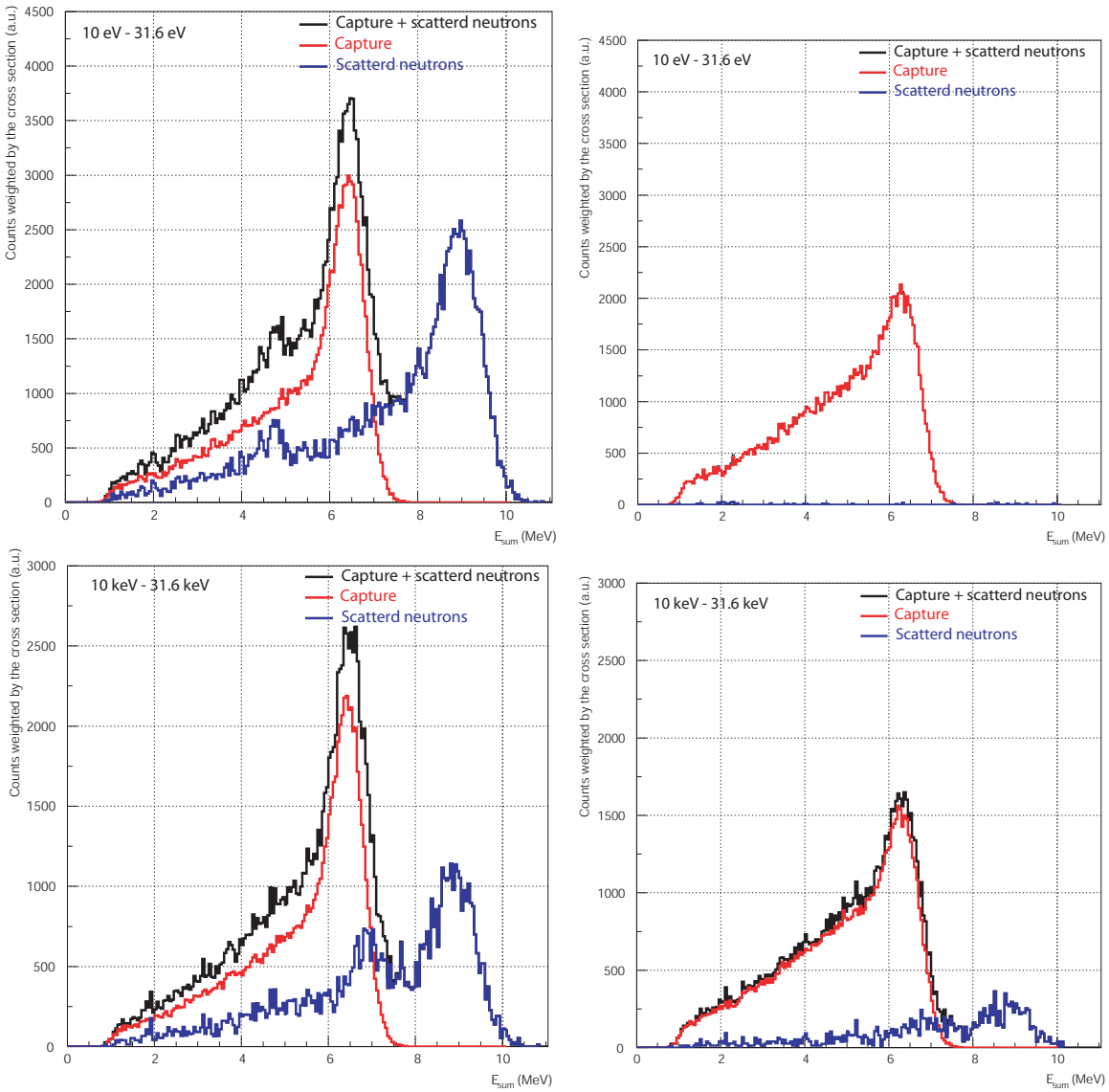

Figure 13. Monte Carlo simulated response of the TAC to a ^{197}Au(n,γ) electromagnetic cascade (in red), scattered neutrons (in blue) and total (in black) for neutron energies between 10 keV and 31.6 keV. Left: without absorber. Right: with a ^{6}LiH absorber.

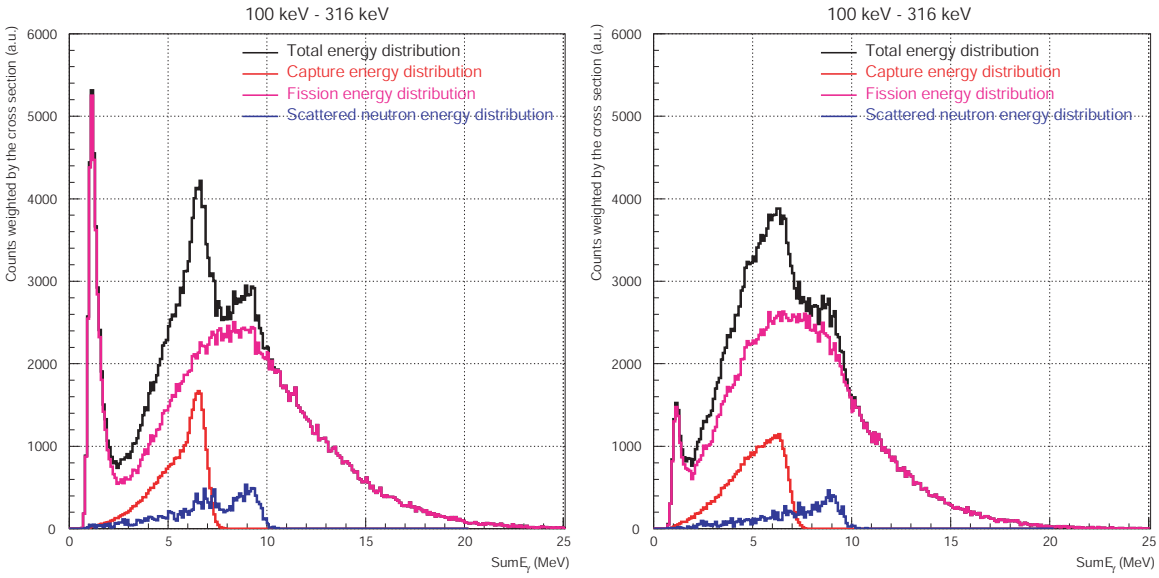

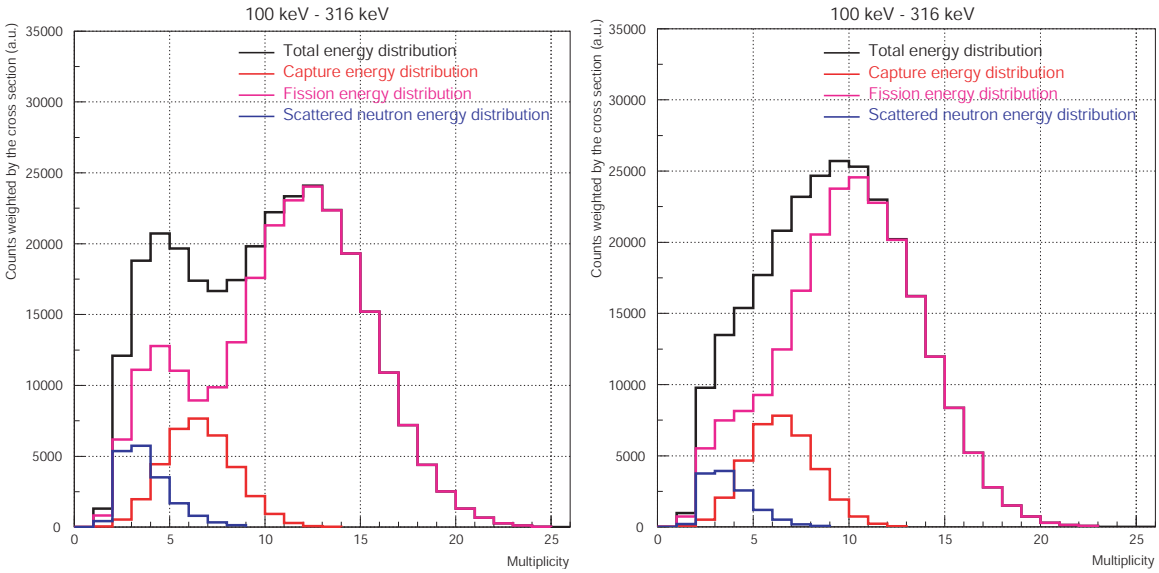

Figure 14. Top: Monte Carlo simulated response of the TAC without (left) and with ^{6}LiH absorber (right) to a ^{245}Cm(n,γ) electromagnetic cascade (in red), scattered neutrons (in blue), neutron induced fission (in magenta) and total (in black) for neutron energies between 100 keV and 316 keV. Bottom: Multiplicities measured in the TAC without (left) and with ^{6}LiH absorber (right).

4.4. Conclusions

The final uncertainties in the measurements proposed at n_TOF are defined by:

- The uncertainty in the recommended standard capture cross section of ^{197}Au.
- The uncertainty in the normalization between the reference and main measurement of 1%.
- The systematic uncertainty due to the dead time and pileup below 3%.
- The systematic uncertainties associated to the experimental technique below 5%.
- The statistical uncertainties in the capture data.

For this reason, a 5% overall uncertainty will be achieved if sufficient statistics is provided in each measurement.

5. Rate Estimates and Beam Time Request

The following series of measurements are proposed:

- ^{233}U, ^{237}Np, ^{240,242}Pu, ^{241,243}Am and ^{245}Cm (n,γ) measurements with and without neutron absorber.
- Sample radioactivity measurements without beam, for subtracting the contribution due to the intrinsic activity of the samples.
- ^{197}Au reference measurement at the beginning of each run for determining the shape and magnitude of the neutron fluence. The cross section measurement of each actinide isotope will be referred to the ^{197}Au measured in the same experimental conditions and with the same statistical uncertainties.
- Empty canning for determining the background due to the canning.
- Carbon sample for determining with sufficient accuracy the neutron sensitivity of the TAC as a function of the neutron energy.

- Pb sample for determining with sufficient accuracy the background due to in-beam gamma rays scattered at the samples.

For making the beam time request, the rate distributions as a function of the neutron energy have been calculated for all isotopes of interest. The following experimental conditions were taken into account:

- Neutron beam optics adjusted for a narrow beam of 4 cm diameter.
- Shape and magnitude of the n_TOF neutron energy distribution from 0.1 eV to 1 MeV.
- Beam interception fraction of 20% for 1cm diameter samples.
- ENDF BVI.8 cross section files at 300 Kelvin.
- A PS supercycle of 16.4 s and an average number of 3.5 TOF pulses per supercycle.
- A TAC detection efficiency of 90%.

	Count rate per PS pulse of $7\cdot10^{12}$ protons at different energies							**Request**	
	1 - 10 eV	**10 - 100 eV**	**100 eV - 1 keV**	**1 - 10 keV**	**10 - 100 keV**	**100 keV - 1 MeV**	**Total number of counts**	**Beam Time (d)**	**Protons**
^{233}U (capture)	92.92	24.62	6.57	2.49	1.16	1.75	129.51	10.4	$1.34\cdot10^{18}$
^{237}Np (capture)	59.45	36.99	10.55	3.30	1.46	1.18	112.93	8.3	$1.07\cdot10^{18}$
^{240}Pu (capture)	396.69	21.19	6.00	0.95	0.49	0.36	425.68	24.5	$3.17\cdot10^{18}$
^{242}Pu (capture)	134.52	5.40	3.23	0.89	0.42	0.32	144.78	28.8	$3.71\cdot10^{18}$
^{241}Am (capture)	153.27	32.23	14.59	4.50	1.95	1.61	208.16	24.7	$3.19\cdot10^{18}$
^{243}Am (capture)	292.43	40.95	13.22	3.79	1.79	1.30	353.48	27.0	$3.48\cdot10^{18}$
^{245}Cm (capture)	5.74	1.53	1.50	0.48	0.23	0.24	9.73	25.7	$3.32\cdot10^{18}$
							Subtotal	**149.4**	**$1.93\cdot10^{19}$**
^{197}Au (capture)	544.33	33.29	37.29	10.03	2.55	2.23	629.71	28.24	$3.66\cdot10^{18}$
						Reference and background measurements	Empty canning	5	$3.69\cdot10^{17}$
							Carbon sample	3	$2.21\cdot10^{17}$
							Pb sample	3	$2.21\cdot10^{17}$
							Total	**188.64**	**$2.38\cdot10^{19}$**

Table 2. Count rate for all isotopes in 7 different energy intervals and the requested beam time expressed in number of PS pulses, days and number of protons.

The rate distributions as a function of the neutron energy shown in Appendix III. Table 2 presents the count rate for all isotopes in 7 different energy intervals and the requested beam time expressed in days and number of protons. The requested beam will allow the reach the goals of the proposal:

- Determine the neutron capture cross section of ^{233}U, ^{237}Np, ^{240,242}Pu, ^{241,243}Am and ^{245}Cm with an overall accuracy of 5% dominated by the systematic uncertainties associated to the experimental technique.
- In the resolved resonance region, the resonances will be measured with a 1% to 3% statistical uncertainty with an energy resolution of 10^{-3}.
- The capture cross section in the unresolved resonance region will be measured with a statistical uncertainty better than 2% and an energy resolution of 3%.
- The reference cross section of ^{197}Au will be determined with the same statistical uncertainty as the actinide cross sections.
- The main sources of background necessary for correcting the data will be measured as well with an accuracy below 5%.

To summarise, a number of $1.93 \cdot 10^{19}$ protons is requested for the capture cross section measurements of ^{233}U, ^{237}Np, ^{240,242}Pu, ^{241,243}Am and ^{245}Cm. A total number of $4.7 \cdot 10^{18}$ protons is requested for the reference and background measurements with ^{197}Au, C, Pb samples and an empty canning. The grand total of protons requested in the proposal amounts to $2.38 \cdot 10^{19}$.

6. Key codes

CAD: Computer Aided Design
CS: Cross Section values
CSR: Cross Section Ratio values
RP: Resonance Parameters
TAC: Total Absorption Calorimeter
TOF: Time of Flight

7. References

[1] Accelerator Driven Systems and Fast Reactors in Advanced Nuclear Fuel Cycles, ISBN 92-64-18482-1 ENEA/OECD Report, 2002

[2] E. González on behalf of the n_TOF collaboration, Proceedings of "Astrophysics, Symmetries and Applied Physics at Spallation Neutron Sources", World Scientific 2002, ISBN 981-238-249-6

[3] M. Salvatores, "A systematic approach to Nuclear Data Uncertainties and their Impact on Transmutation strategies", proceedings of the Workshop on Nuclear Data for the Transmutation of Nuclear Waste, GSI – Darmstadt, 2 – 5 September, 2003.

[4] E. González, private communication

[5] http://www-nds.iaea.or.at/exfor/

[6] http://www-nds.iaea.or.at/reports/nds-206.pdf, V. McLane, EXFOR Basics, IAEA NDS-206 (2000)

[7] http://www-nds.iaea.or.at/cinda/cinda.html

[8] M.C. Moxon, E.R. Rae, Nucl. Instr. Meth. 24, (1963) 445

[9] Macklin, J.H. Gibbons, Phys. Rev. 159 (1967) 1007
[10] K. Wisshak, F. Käppeler, Nucl. Instr. Meth 227 (1984) 91
[11] G.W. Muradyan, Yu. V. Adamchuk, Yu.G. Shchepkin, M.A. Voskanyan, Nucl. Sci. Eng. 90 (1985) 60
[12] Pattenden et al., Nucl. Sci. and Eng., 17, 404 (1963)
[13] M.S. Moore, C.W. Reich, Phys. Rev. 118 (1960) 718
[14] Kolar et al., 1970 HELSINKI, VOL.I, 387 (1970)
[15] Harvey et al., 1979 KNOXVILLE, P.690 (1979)
[16] L.W. Weston, R. Gwin, G. De Sausurre, R.R. Fullwood, R.W. Hockenbury, Nucl. Sci. Eng. 34 (1968) 1
[17] L.W. Weston, R. Gwin, G. De Sausurre, R.W. Iingle, J.H. Todd, C.W. Craven, R.W. Hockenbury, R.C. Block, Nucl. Sci. Eng. 42 (1970) 143
[18] Blons et al., Nucl. Sci. and Eng., 51, 130 (1973)
[19] Deruyter et al., Nucl. Sci. and Eng., 54, 423 (1974)
[20] Wagemans et al.,1988 MITO, 91 (1988)
[21] J.C. Hopkins, B.C. Diven, Nucl. Sci. and Eng., 12, 169 (1962)
[22] G.D. Sauter, C.D. Bowman, Phys. Rev. 174 (1968) 1413
[23] G. De Sausurre,R.B. Perez, H. Derrien, 1970 HELSINKI, 2 (1970) 757(94)
[24] L.G. Miller, J.E. Evans, BAP,1,247(C5),5606
[25] S. Ya. Nikitin, S.I. Sukhoruchkin, K.G. Ignatiev, N.D. Galanina, 55MOSCOW (1955) 87
[26] J.C. Hopkins, B.C. Diven, Nucl. Sci. Eng. 12,169,62
[27] F.D. Brooks, J.E. Joly, M.G. Schomberg, M.G. Sowerby, AERE-M-1709,,6609
[28] A. Cricchio, R. Ernstberger, L. Koch, R. Wellum, 82ANTWER (1982) 175
[29] R.L. Macklin, H.W. Schmitt, J.H. Gibbons, ORNL-2022,5602
[30] K. Wisshak, F. Käppeler, Nucl. Sci. Eng. 69,(1),39,7901
[31] K. Wisshak, F. Käppeler, J,Nucl. Sci. Eng. 76,(3),363,7806
[32] L.W. Weston, J.H. Todd, J,Nucl. Sci. Eng. 63,143,77
[33] V.I. Ivanov, V.A. Tolstikov, YK,1/36,26,8003
[34] M. .Asghar, M.C. Moxon, N.J. Pattenden, EANDC(UK)-103 (1968)
[35] R.W. Hockenbury, W.R. Moyer, R.C. Block, Nucl. Sci. Eng. 49,153,197210
[36] H. Weigmann, J.P. Theobald, JNE 26 (1972) 643
[37] J.J. Scoville, J.W. Rogers, ANS,10,259,6706
[38] L.W. Weston, J.H. Todd, Nucl. Sci. Eng. 79 (1981) 184
[39] L. Mewissen, A. Angeletti, E. Cornelis, F. Poortmans, G. Rohr, G. Vanpraet, H. Weigmann, NSE,70,155,7905
[40] D. Paya, PhD thesis
[41] G.F. Auchampaugh, M.S. Moore, J.D. Moses,R.O. Nelson, C.E. Olsen, R.C. Extermann, N.W. Hill, J.A. Harvey, Phys. Rev. C 29 (1984) 174
[42] F. Gunsing, A. Lepretre, C. Mounier, C. Rapset, A. Brusegan, E . Macavero, F. Corvi, C. Bastian, N. Herault, J. González, V. Gressier, G. Noguere, P. Siegler, NSTS, 2 (2) (2002) 1067
[43] N.N. Buleeva, A.N. Davletshin, O.A. Tipunkov, S.V. Tikhonov, V.A. Tolstikov, AE, 65 (6) (1988) 348
[44] Ju.N. Trofimov, JU.A. Nemilov, 83KIEV,2,142,8310
[45] M. Lindner, R.J. Nagle, J.H. Landrum, Nucl. Sci. Eng. 59 (1976) 381
[46] M.M.Hoffman, W.M. Sanders, M.D. Semon, BAP 21, 655 (JE3) 1976
[47] D.C. Stupegia, M. Schmidt, C.R. Keedy, Nucl. Sci. Eng. 29 (1967) 218
[48] K. Wisshak, F. Käppeler, Nucl. Sci. Eng. 69,(1),39,7901
[49] K. Wisshak, F. Käppeler, Nucl. Sci. Eng. 76,(3),363,7806

[50] F. Poortmans, G. Rohr, J.P. Theobald, H. Weigmann, G.J. Vanpraet, Nucl. Phys. A 207 (1973) 342
[51] F.B. Simpson, O.D. Simpson, H.G.. Miller, J.A. Harvey, N.W. Hill, ORNL-4844 (1973) 90
[52] R.W. Hockenbury, A.J. Sanislo, N.N. Causal, 75WASH,2,584,7503
[53] A.A. Druzhinin, V.K. Grigorev, A.A. Lbov, S.P. Vesnovskij, N.G. Krylov, V.N. Polunov, AE, 42,(4),314,7704
[54] K.Wisshak, F. Käppeler, Nucl. Sci. Eng. 76,(2),148,8011
[55] K.Wisshak, J. Wickenhauser, F. Kappeler, G. Reffo, F. Fabbri, Nucl. Sci. Eng. 81,(3),396,8207
[56] V.I. Ivanov, I.P. Markelov, V.A. Tolstikov, 71KIEV,1,325,7105
[57] G.Vanpraet, E. Cornelis, S. Raman, G. Rohr, 85SANTA,,85
[58] L.W.Weston, J.H. Todd, Nucl. Sci. Eng. 61,356,7611
[59] H. Derrien, B. Lucas, 75WASH,2,637,7503
[60] D.B.Gayther, B.W.Thomas, 77KIEV,3,3,770418
[61] N.I. Ivanova, A.N. Kobzev, N.G. Krylov, A.A. Lbov, N.P. Martynov, A.E. Trikanov, A.I. Shelamkov, AE,30,(4),369,7104
[62] G.N.Flerov, A.A. Pleve, S.M. Polikanov, S.P. Tretyakova, I. Boca, M. Sezon, I. Vilcov, N. Vilcov, Nucl. Phys. A 102 (1967) 443
[63] L.W. Weston, J.H. Todd, Nucl. Sci. Eng. 61 (1976) 356
[64] A. Cricchio, R. Ernstberger, L. Koch, R. Wellum, 82ANTWER,175,8209
[65] A.V. Ignatyuk, A.I. Blokhin, V.P. Lunev, V.N. Manokhin, G.Ya. Tertychny, V.A. Tolstikov, K.I. Zolotarev, INDC(CCP)-424 (1999)
[66] K. Wisshak, F. Käppeler, Nucl. Sci. Eng. 85,251,8311
[67] O.D. Simpson, F.B. Simpson, J.A. Harvey, G.G. Slaughter, R.W. Benjamin, C.E. Ahlfeld, Nucl. Sci. Eng. 55 (1974) 273
[68] J.R.Berreth,F.B.Simpson, IN-1407 (1970) 66
[69] R.E. Cote, L.M. Bollinger, R.F. Barnes, H. Diamond, Phys. Rev. 114 (1959) 505
[70] L.W. Weston, J.H. Todd, Nucl. Sci. Eng. 91 (1985) 444
[71] V.M. Maslov, E.Sh. Sukhovitskij, Yu.V. Porodzinskij, A.B. Klepatskij, G.B. Morogovskij, INDC(BLR)-006
[72] V.D. Gavrilov, V.A. Goncharov, J,AE,44,(3),246,7803 (1978)
[73] J. Halperin, R.E. Druschel, R.E. Eby, P,ORNL-4437,196909 (1969)
[74] C.H. Ice, R,DP-MS-66-69,6610 (1966)
[75] C.M. Stevens, M.H. Studier, P.R. Fields, J.F. Mech, P.A. Sellers, A.M. Friedman, H. Diamond, J.R. Huizenga, Phys. Rev. 94,974,54 (1954)
[76] J.A.Smith, C.J.Banick, R.L. Folger, H.P. Holcomb, I.B. Richter, 68WASH,2,1285,6803
[77] V.M. Maslov, E.Sh. Sukhovitskij, Yu.V. Porodzinskij, A.B. Klepatskij, G.B. Morogovskij, INDC(BLR)-003
[78] S. Lukic, D. Cano-Ott, L. Ferrant, D. Karadimos, L. Lourenco, S. O´Brien, C. Paradela, L. Perrot, V. Vlachoudis, C. Domingo, J.L. Tain, n_TOF analysis group report (2002)
[79] U. Abbondano et al., "n_TOF Performance Report", CERN/INTC-O-011, INTC-2002-037
[80] http://www.acqiris.com
[81] http://castor.web.cern.ch/castor
[82] ORIGEN
[83] Nuclides

[84] D. Cano-Ott, "Development of a new pulse shape analysis routine for the C_6D_6 flash ADC data analysis", n_TOF collaboration meeting, Lisboa 2002.
[85] D. Cano-Ott, "Preliminary result of the TAC 1π test", 2nd TAC meeting, Geneva 2003
[86] D. Cano-Ott, E. González-Romero, M. Embid, DFN/TR-01/II-02
[87] D. Cano-Ott, M. Embid, E. González-Romero, D. Villamarín, DFN/TR-07/II-99
[88] D. Cano-Ott, F. Calviño, G. Cortés, I.F. Goncalves, E. González-Romero, A. Poch, P. Vaz, "Results of the Monte Carlo Simulation of the Neutron and Gamma Background in a Second Experimental Area for Fisión Measurements at n_TOF", n_TOF internal report (2002)
[89] V. Vlachoudis, "Monte Carlo Simulations of alternative moderators/coolants for the n_TOF spallation target", 2nd TAC meeting, Geneva (2003)
[90] GEANT: Detector description and simulation tool, CERN Program Library W5013, Geneve 1994
[91] S. Agostinelli et al., Nucl. Instr. Meth. A 506 (2003) 250 – 503
[92] M. Heil, R. Reifarth, M.M. Fowler, R.C. Haight, F. Käppeler, R.S. Rundberg, E.H. Seabury, J.L. Ullmann, J.B. Wilhelmy, K. Wisshak, Nucl. Instr. Meth. A 459 (2001) 229
[93] R. Plag, "The neutron sensitivity of the 4π BaF_2 detector for n_TOF", n_TOF internal report (2003)
[94] R. Terlizzi, N. Colonna, "Alternative solutions for reducing the neutron background in the Total Absorption Calorimeter, n_TOF, n_TOF internal note BA/02/03 (2003)
[95] D. Cano-Ott, F. Calviño, G. Cortés, E. González, A. Poch, J.L. Taín, "Monte Carlo Simulation of the 4π Total Absorption Calorimeter at n_TOF", n_TOF internal report (2003)
[96] F. Käppeler et al., presentation during the n_TOF winter school in Les Houches (2003)

Appendix I.
Information on the available neutron capture cross section measurements for ^{233}U, ^{237}Np, ^{240,242}Pu, ^{241,243}Am and ^{245}Cm

^{233}U

Figure 15 and Figure 16 show the neutron capture cross sections and absolute cross section experimental data available for ^{233}U.

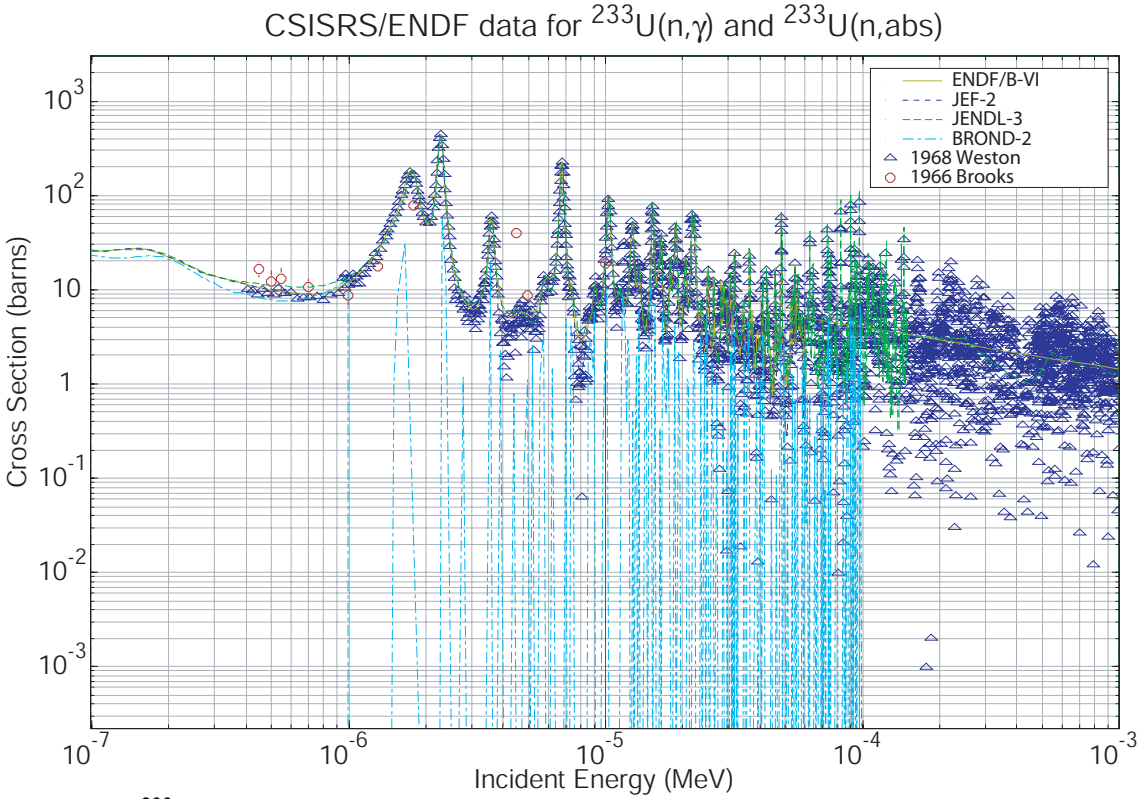

Figure 15. ^{233}U(n,γ) evaluated cross sections and EXFOR experimental cross section points in the range from 0.1 eV to 1 keV.

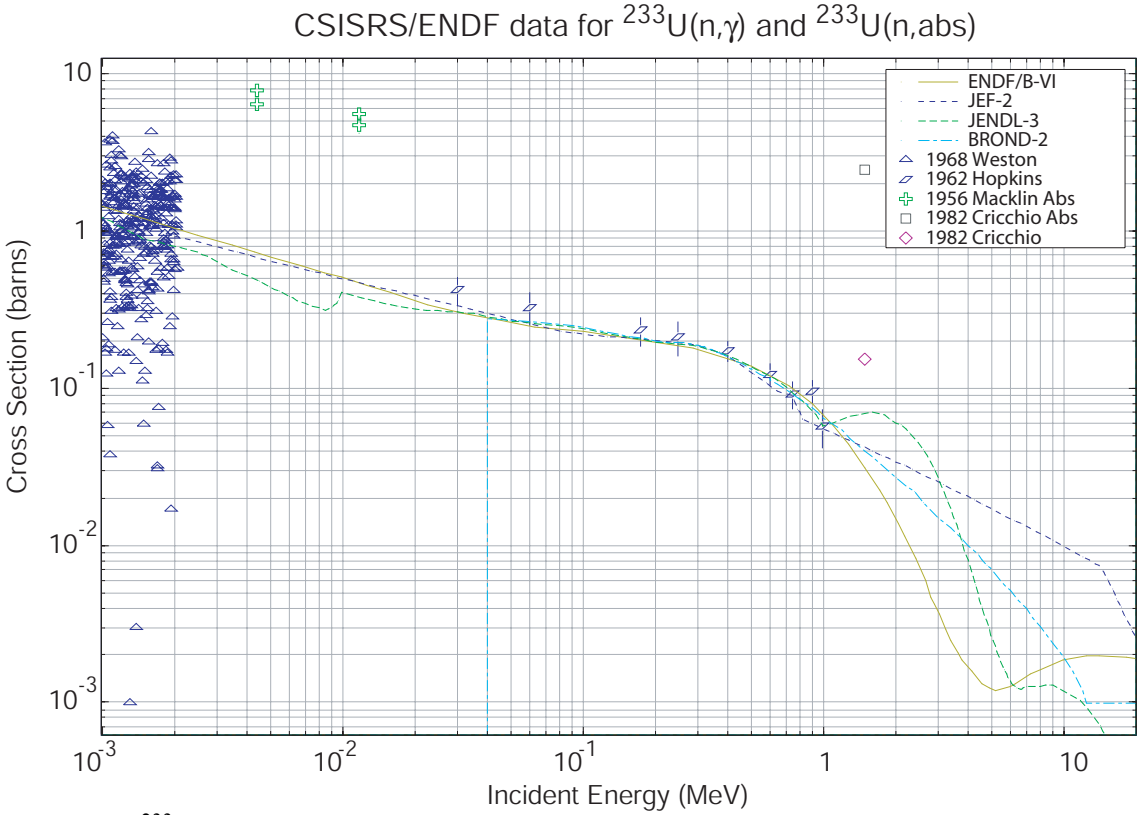

Figure 16. ^{233}U(n,γ) evaluated cross sections and EXFOR experimental cross section points in the range from 0.1 eV to 20 MeV.

Energy Range (eV)	Experimental Technique	Facility/Laboratory and Method	Detectors	Min and Max uncertainty	Experimental data	Ref.
1.59e0 - 3.08e1	Scattering	Data from private communication	Not specified	Not specified	RP: 30	[22] Sauter
2.00e-2 6.43e1	-	Linac/ORELA, TOF	-	Not given	RP: 68	[23] Sausurre
1.95e-1 - 1.05e1	-	-	-	-	RP: 10	[13] Moore
-5.00 - 4.70	Fragment spectrometry.	Widths derived from fission cross section	Crystal spectrometer	-	RP: 7	[24] Miller
1.45 - 1.22e1	Secondary neutron detection	TOF	Neutron detector	-	RP: 3	[25] Nikitin
4.05e-1 - 2.05e+3	-	TOF	-	>2% + 2% on the fission + capture sum	CS: 3423	[16] Sukhorutchkin
3.00e+4 - 1.00e+6	Capture to fission ratio	-	-	-	CS: 9	[26] Hopkins
3.50e-1 - 1.00e+1	Gamma, neutron and FF detection	Linac/Harwell, TOF	Scintillator	20%	CS: 10	[27] Brooks
1.68e-2 - 1.06	Gamma and FF detection	Linac/RPI, TOF	Liq. Scintillator + Fission Chamber + PP BF_3 monitor	No information	CS: 50	[17] Weston

1.50e+6	Activation	Reactor/Cadarache	Mass separation	No information	CS: 1	[28] Cricchio

Table 3. Neutron capture EXFOR data sets for ^{233}U

Energy Range (eV)	Experimental Technique	Facility/Laboratory and Method	Detectors	Min and Max uncertainty	Experimental data	Ref.
4.40e3 - 1.18e4	Shell Transmission	Van de Graaff	Not Specified	10%	CS: 2	[29] Macklin
1.50e+6	Activation + Separation	Reactor/Cadarache	Mass separator	2%	CS: 1	[28] Cricchio

Table 4. Neutron absorption data sets for ^{233}U

Table 5 summarizes the relevant information on the most recently released evaluated cross section libraries. The most recent evaluation of the data for ^{233}U is in the JENDL3.3 evaluated data library.

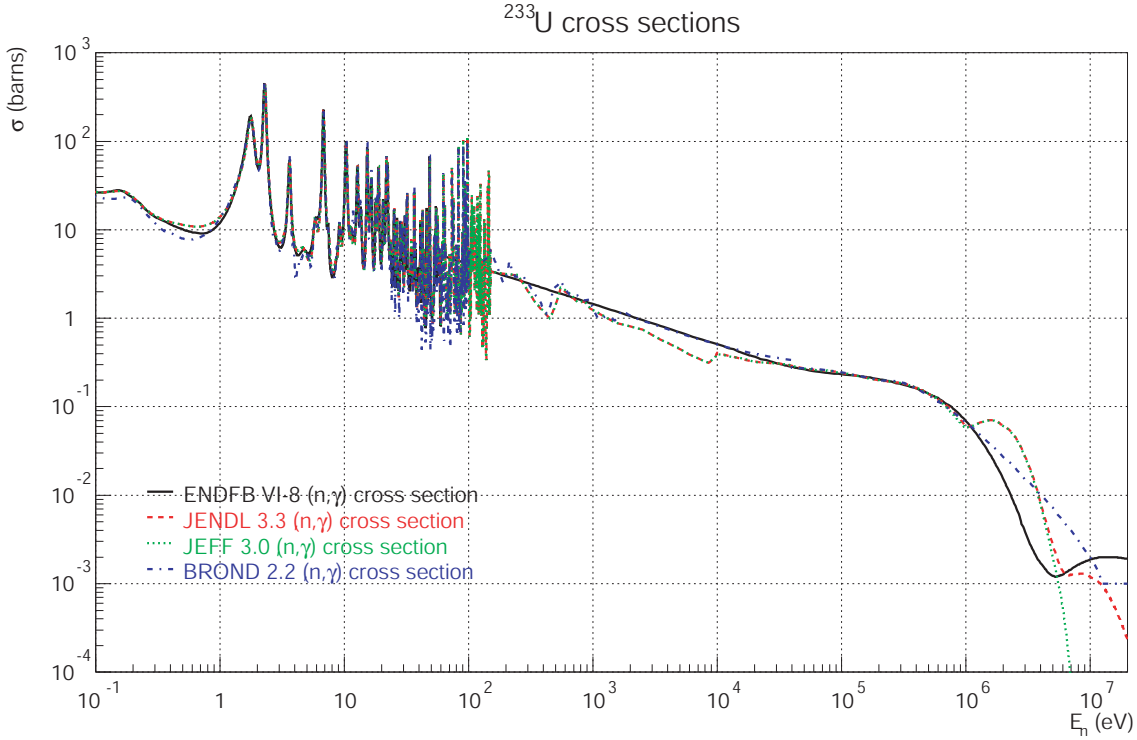

Figure 17. Most recent releases (by September 2003) of evaluated (n,γ) cross sections for ^{233}U.

Library	Lab	Evaluators	Evaluation date	Revision date
ENDF/B-VI.8	LANL / ORNL	Stewart et al + L. Weston	December 78	-
JEFF-3.0	SAEI	H.Matsonubu, T. Nakagawa	March 87	-
CENDL-2.1	-	-	-	-
JENDL-3.3	SAEI	T.Mutsunobu, T. Kawano	March 00	May 00
BROND-2.2	MINSK	Sukhovitskij, Klepatskij	March 90	-

Table 5. Information on the evaluation of the most recent releases (September 2003) of the ENDF, JEFF, CENDL, JENDL and BROND neutron cross section libraries for ^{233}U.

^{237}Np

Energy Range (eV)	Experimental Technique	Facility/Laboratory and Method	Detectors	Min and Max uncertainty	Experimental data	Ref.
0.5	-	Reactor	-	5%	RP : 1	[37] Scoville
1.50e+6	Activation	Reactor/Cadarache	Mass Separator	Not given	CS: 1	[28] Cricchio
4.91e-1 - 1.99e+1	Total Energy Detector	LINAC / ORELA, TOF	NE226	2% - 20%	RP : 17	[38] Weston
8.32e+0 - 2.04e+2	Capture and Transmission	LINAC / CBNM, TOF	^{3}He chamber + C_6F_6	5% - 50%	RP : 25	[39] Mewissen
1.32e+0 - 2.35e+2	Transmission + Capture	LINAC / Saclay, TOF	^{10}B + NaI(Tl)	2% - 30%	RP : 78	[40] Paya
-1.07 - 6.00e+2	Fission	Spallation Neutron Source	-	only statistical	RP:749	[41] Auchampaugh
500	Total Energy detectors	TOF / Gelina	N230	7%	RP : 1	[42] Gunsing
1.66e+5 - 1.14e+6	Activation	Van De Graaff	Germanium (Li)	5%	CS : 13	[43] Buleeva
2.50e+5 - 1.91e+6	Activation	Van De Graaff	Germanium (Li)	5% - 10%	CS:7	[44] Trofimov
9.75e-3- 2.12e+5	Total Energy Detector	LINAC / ORELA, TOF	NE226	2% - 20%	CS: 5325	[38] Weston
1.21e+5 - 2.73e+6	Activation	Van De Graaff	-	3% - 50%	CS:23	[45] Lindner
2.01e+1 - 2.55e+5	Moxon Rae	Underground Nuclear Explosion	^{3}He + Moxon Rae	2% - 30%	CS: 19300	[46] Hoffmann
1.52e+5 - 1.51e+6	Activation	-	-	-	CS:8	[47] Stupegia

Table 6. Neutron capture EXFOR data sets for ^{237}Np.

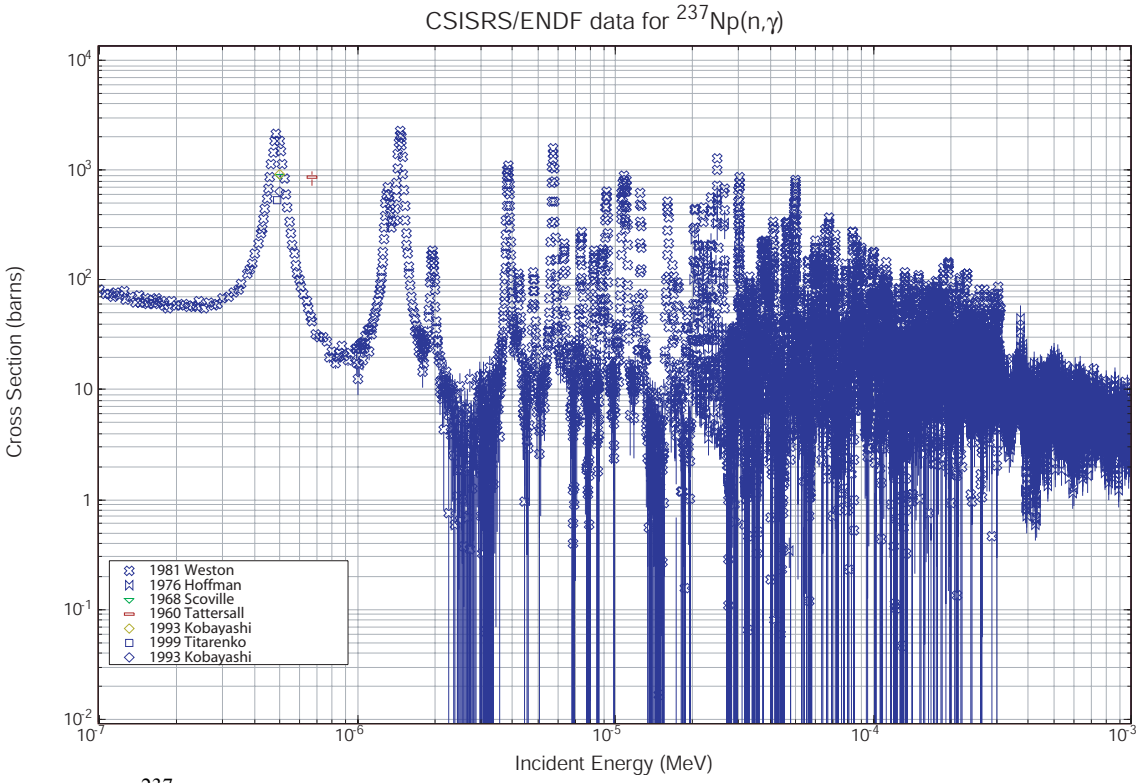

Figure 18. ^{237}Np(n,γ) EXFOR experimental cross section points in the range from 0.1 eV to 1 keV.

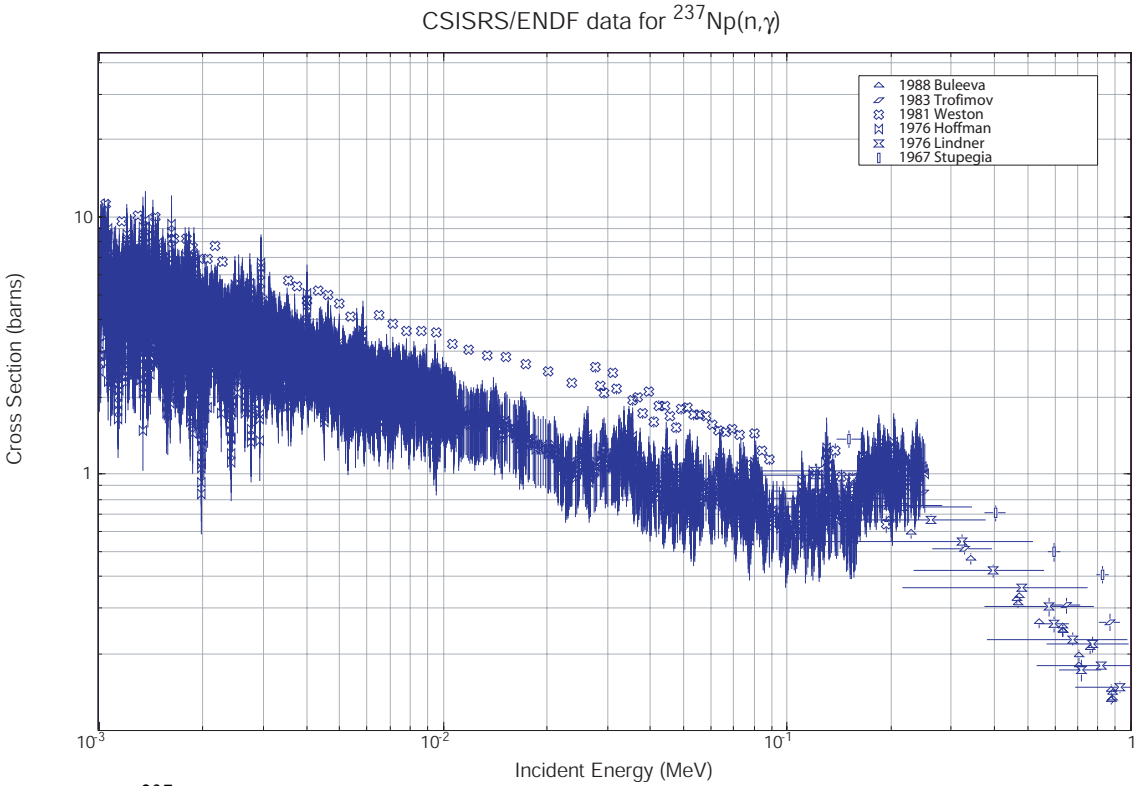

Figure 19. ^{237}Np(n,γ) EXFOR experimental cross section points in the range from 1 keV to 1 MeV.

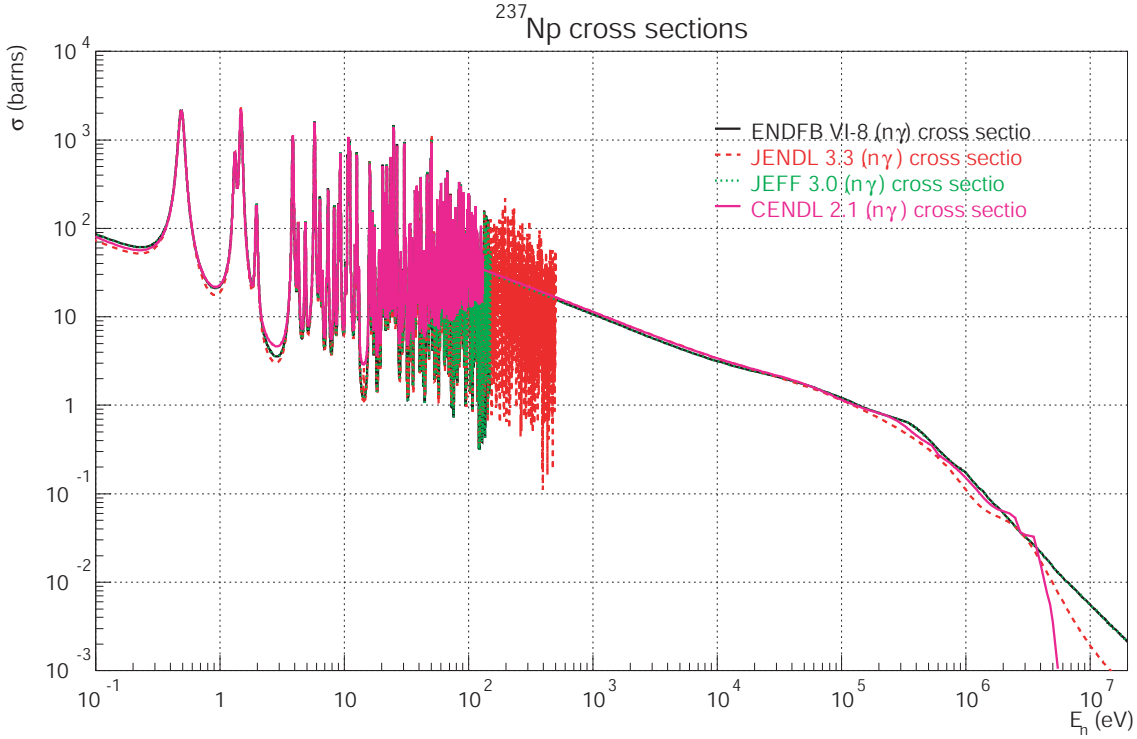

Figure 20. Most recent releases (by September 2003) of evaluated (n,γ) cross sections for ^{237}Np.

Library	Lab	Evaluators	Evaluation date	Revision date
ENDF/B-VI.8	LANL	P. Young, E. Arthur, F. Mann.	April 90	July 91
JEFF-3.0	NEA	P. Young, E. Arthur, F. Mann.	April 90	April 02
CENDL-2.1	PEKING	G.Y. Tang, J.H. Fan, S.L. Bao, W.T. Cao	May 90	June 94
JENDL-3.3	JAERI	T. Nakagawa, O. Iwamoto et al.	January 01	March 02
BROND-2.2	-	-	-	-

Table 7. Information on the evaluation of the most recent releases (September 2003) of the ENDF, JEFF, CENDL, JENDL and BROND neutron cross section libraries for ^{237}Np.

^{240}Pu

Figure 21 shows the neutron capture cross sections and EXFOR capture data available for ^{240}Pu in 1 keV to 20 MeV range. Table 8 contains a summary about the different experimental EXFOR data sets, such as energy ranges, experimental techniques and detectors, number of data points and the corresponding references.

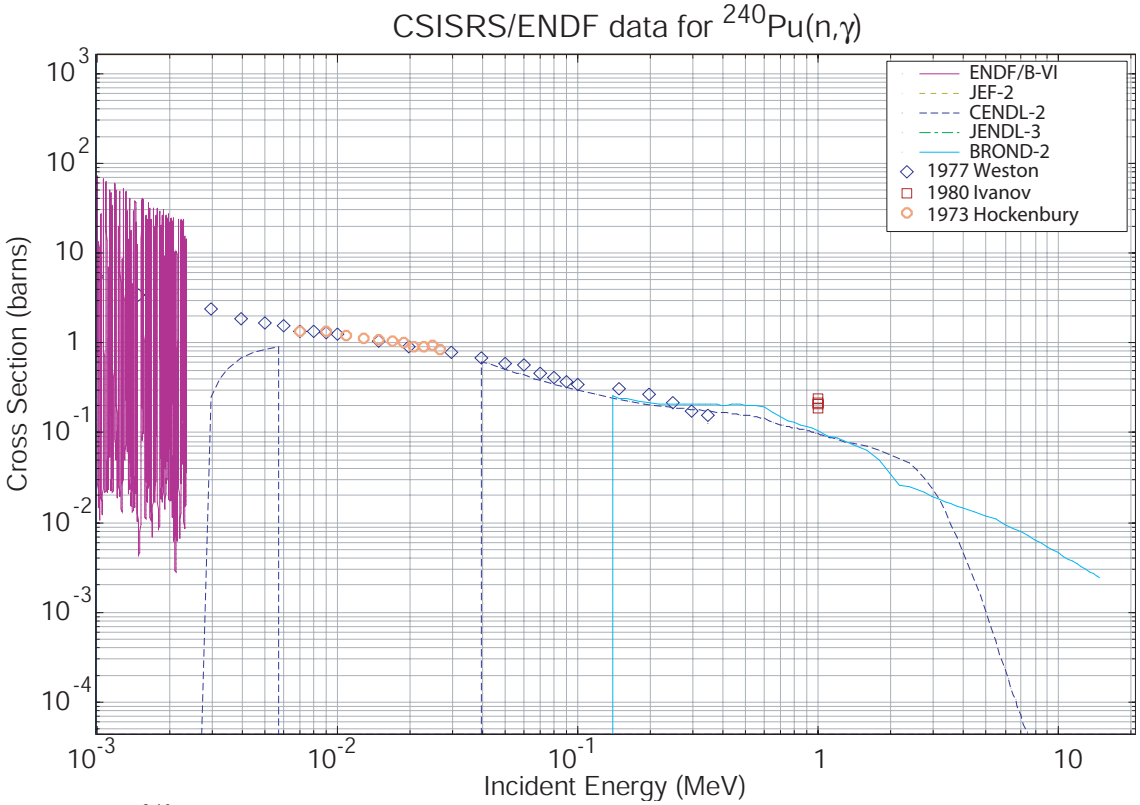

Figure 21. ^{240}Pu(n,γ) evaluated cross sections and EXFOR experimental cross section points in the range from 1 keV eV to 20 MeV.

Energy Range (eV)	Experimental Technique	Facility/Laboratory and Method	Detectors	Min and Max uncertainty	Experimental data	Ref.
4.84e4 – 2.13e5	Moxon Rae + neutron,gamma discrimination	Van de Graff/FZK, TOF	Moxon Rae + Liq. Scint NE213	5% - 10%	CSR: 17	[30] Wisshak
1.19e4 - 8.87e4	Moxon Rae + neutron,gamma discrimination	Van de Graff /FZK, TOF	Moxon Rae + Liq. Scint NE213	5% - 10%	CSR: 34	[31] Wisshak
2.00e2 - 3.50e5	Gamma Total Energy detector + neutron detector	Linac/ORELA, TOF	NE226 + NE213	7% - 20%	CS: 33	[32] Weston
1.e6	Mass separation after irradiation	Fast Reactor/BR-5	Mass spectrometer	> 5%	CS: 1	[33] Ivanov
2.00e1 - 9.50e2	Moxon Rae + Scattering/Transmission	Linac/Harwell, TOF	Moxon Rae + Liq. Scintillator	> 5%	RP: 33	[34] Asghar
2.05e1 - 4.99e2 6.e3 – 3.e4	Hi/lo bias + Transmission	Linac/RPI, TOF	Liq. Scintillator + ^{10}B-NaI	Not reported	RP: 17 + CS	[35] Hockenbury
3.83e1 - 6.66e2	Capture + Transmission	Linac/CBNM,	Not reported	Not reported	RP: 14	[36] Weigmann

Table 8. Neutron capture EXFOR data sets for ^{240}Pu.

Figure 22 shows the most recent releases of the existing evaluated neutron capture cross sections for ^{240}Pu. Table 9 contains the status of the evaluated cross section releases.

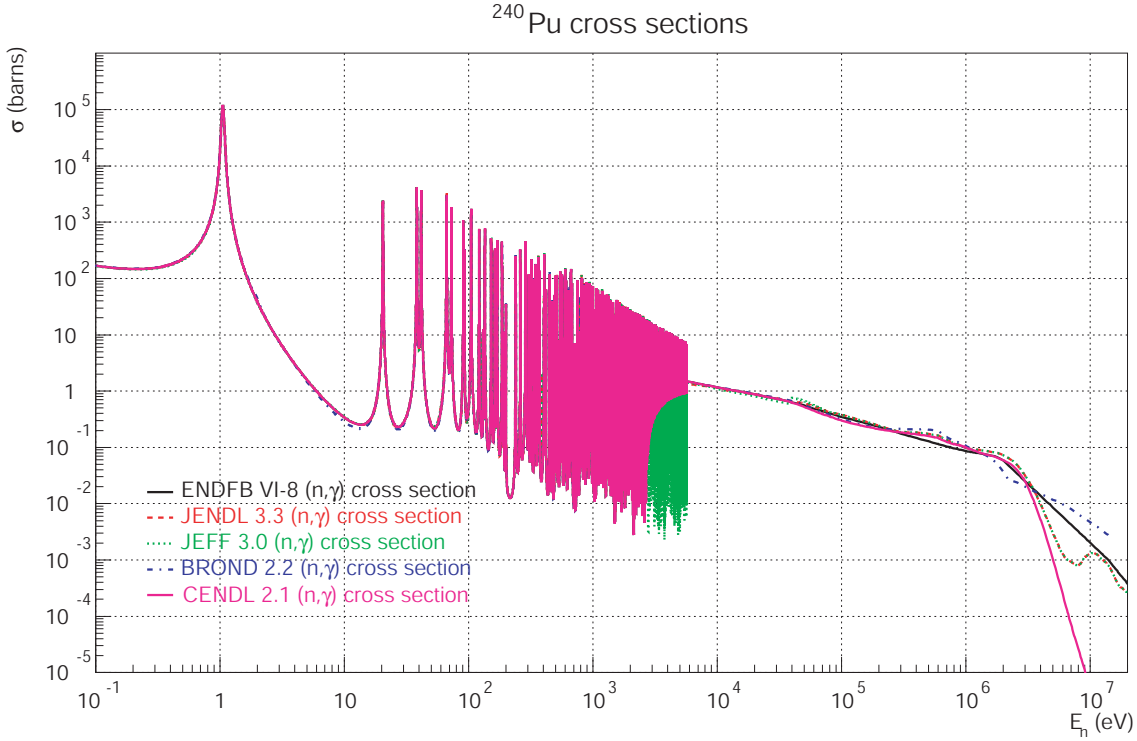

Figure 22. Most recent releases (by September 2003) of evaluated (n,γ) cross sections for ^{240}Pu.

Library	Lab	Evaluators	Evaluation date	Revision date
ENDF/B-VI.8	ORNL	L.W. Weston and E. D. Arthur	August 86	June 93
JEFF-3.0	CEA / NEA	O.Bouland, H.Derrien, S.Masetti	April 2002	-
CENDL-2.1	CNDC	Cai Dunjiu et al.	December 92	June 94
JENDL-3.3	AITEL	T.Murata, T.Kawano, Takagawa	February 00	February 02
BROND-2.2	TMO	Kon'Shin, Sukhovitskij, Antsipov	December 80	June 85

Table 9. Information on the evaluation of the most recent releases (September 2003) of the ENDF, JEFF, CENDL, JENDL and BROND neutron cross section libraries for ^{240}Pu.

^{242}Pu

Figure 23 shows the neutron capture cross sections and EXFOR capture data available for ^{242}Pu in 0.1 eV to 20 MeV range. Table 10 contains a summary about the different experimental EXFOR data sets, such as energy ranges, experimental techniques and detectors, number of data points and the corresponding references.

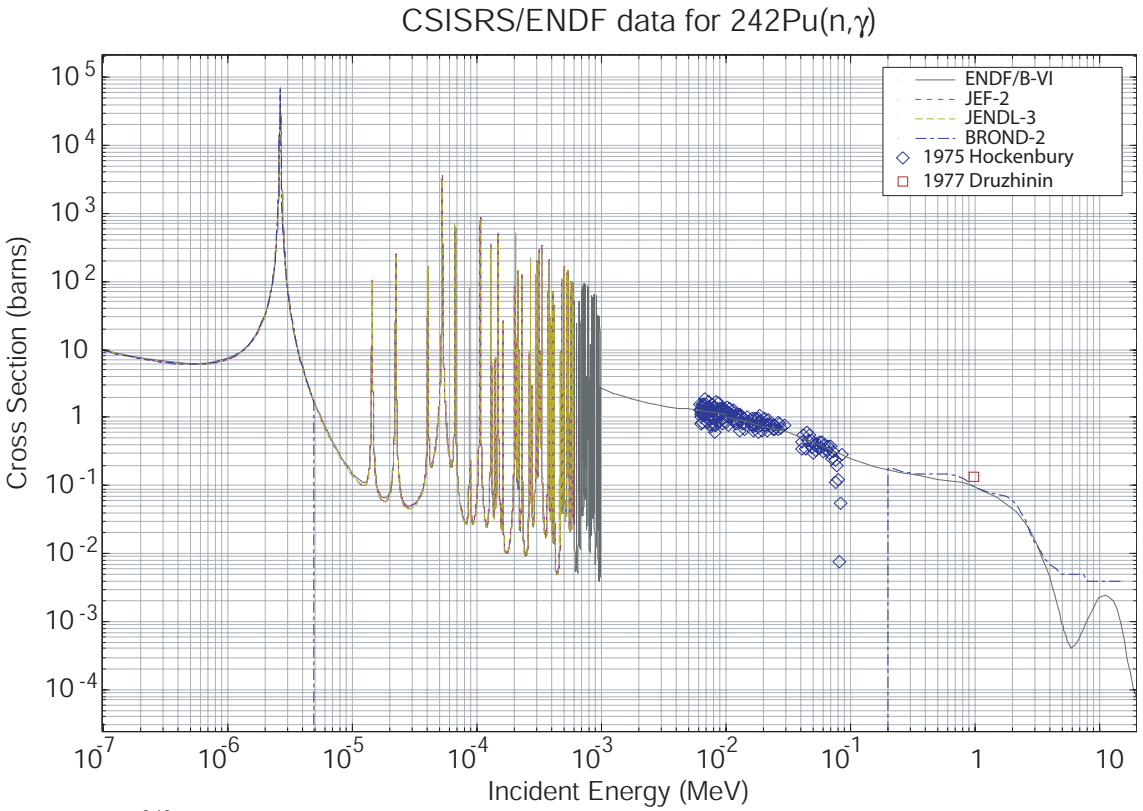

Figure 23. ^{242}Pu(n,γ) evaluated cross sections and EXFOR experimental cross section points in the range from 0.1 eV to 20 MeV.

Energy Range (eV)	Experimental Technique	Facility/Laboratory and Method	Detectors	Min and Max uncertainty	Experimental data	Ref.
5.53e4 - 2.13e5	Moxon Rae + neutron,gamma discrimination	Van de Graff/FZK, TOF,	Moxon Rae + Liq. Scint NE213	5% - 10%	CSR: 16	[48] Wisshak
1.04e4 - 8.89e4	Moxon Rae + neutron,gamma discrimination	Van de Graff/FZK, TOF,	Moxon Rae + Liq. Scint NE213	5% - 10%	CSR: 41	[49] Wisshak
2.02e4 - 7.96e4	Moxon Rae + neutron,gamma discrimination	Van de Graff/FZK, TOF	Moxon Rae + Liq. Scint NE213	5% - 10%	CSR: 21	[49] Wisshak
5.35e1 - 9.49e2	Moxon Rae + Scattering + Transmission	Linac/CBNM, TOF	Moxon Rae + 3He	5% - 10%	RP : 25	[50] Poortmans
2.26e1 -	Transmission	Linac/ORELA,	6Li glass	5% - 30%	RP: 13	[51]

4.95e2		TOF	detector			Simpson
6.27e3 – 8.70e4	Hi/lo bias + Transmission	Linac, TOF	Liq. Scintillator + NaI monitor	Not reported	RP + CS: 251	[51] Hockenbury
1.e6	Activation	Reactor, activation	Scintillator as beta detector	Not reported	CS: 1	[53] Druzhinin

Table 10. Neutron capture EXFOR data sets for ^{242}Pu.

Figure 24 shows the most recent releases of the existing evaluated neutron capture cross sections for ^{242}Pu. Table 11 contains some relevant information on the evaluated cross section releases. No CENDL evaluation has been released for ^{242}Pu.

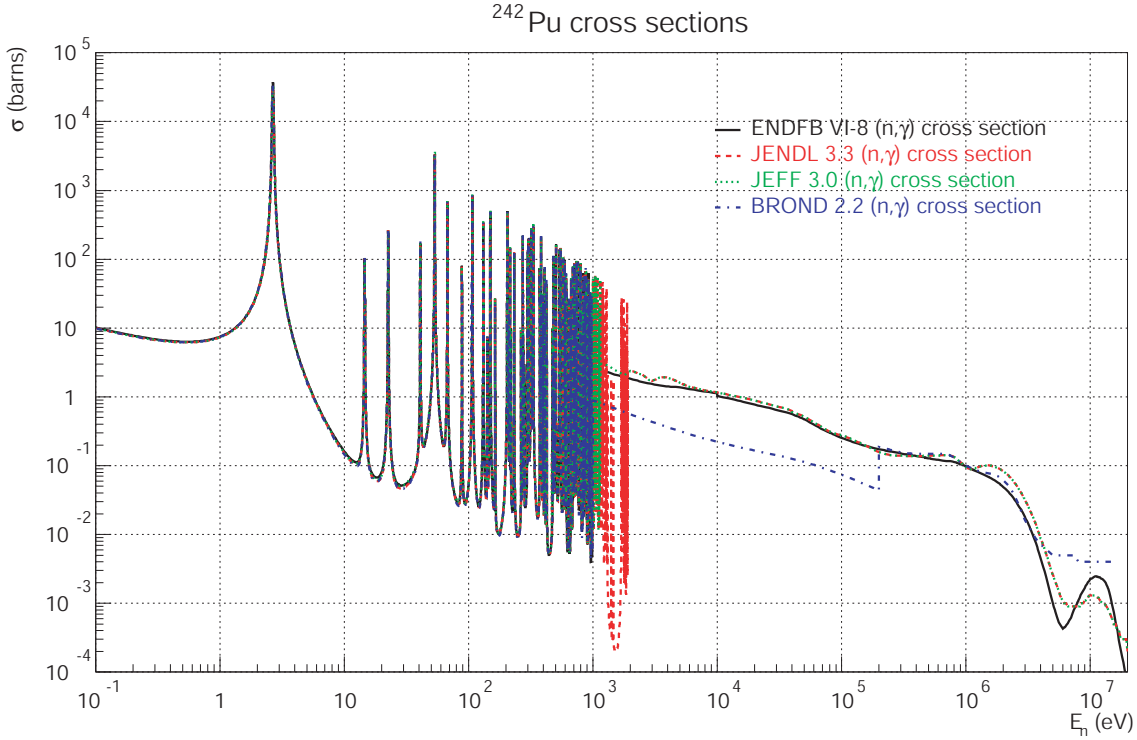

Figure 24. Most recent releases (by September 2003) of evaluated (n,γ) cross sections for ^{242}Pu.

Library	Lab	Evaluators	Evaluation date	Revision date
ENDF/B-VI.8	HEDL	Mann, Benjamin, Madland, Howerton et al.	October 78	February 90
JEFF3.0	ENEA / IJS	A.Ventura, S.Masetti, A.Trkov	October 98	April 02
CENDL-2.1	-	-	-	-
JENDL-3.3	AITEL	T. Murata, T. Kawano	March 00	May 00
BROND-2.2	IHMT	Kon'Shin, Shukovitskij, Antsipov	December 80	December 82

Table 11. Information on the evaluation of the most recent releases (September 2003) of the ENDF, JEFF, CENDL, JENDL and BROND neutron cross section libraries for ^{242}Pu.

^{241}Am

Figure 25 and Figure 26 show the neutron capture cross sections and EXFOR capture and absorption data available for ^{241}Am in different energy ranges. Table 12 and Table 13 contain a summary about the different experimental EXFOR data sets, such as energy ranges, experimental techniques and detectors used, number of data points and the corresponding references.

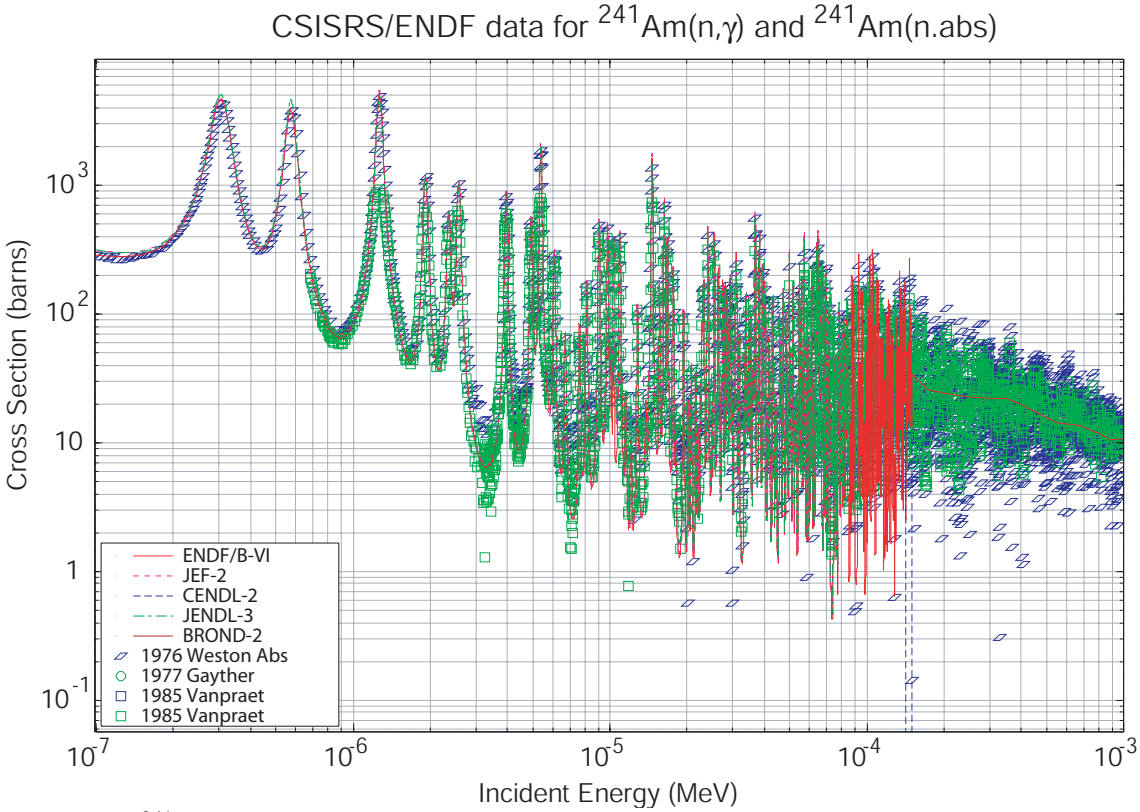

Figure 25. ^{241}Am(n,γ) evaluated cross sections and EXFOR experimental cross section points in the range from 0.1 eV to 1 keV.

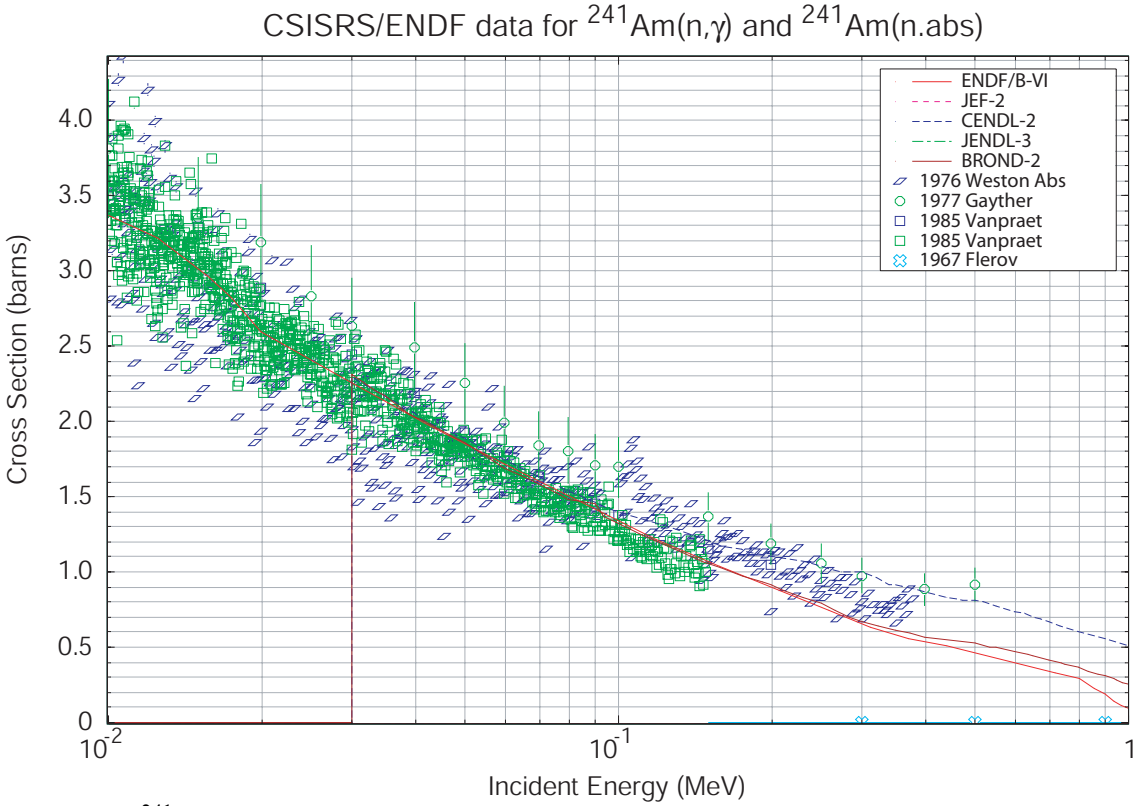

Figure 26. ^{241}Am(n,γ) evaluated cross sections and EXFOR experimental cross section points in the range from 10 keV to 1 MeV.

Energy Range (eV)	Experimental Technique	Facility/Laboratory and Method	Detectors	Min and Max uncertainty	Experimental data	Ref.
1.04e4 - 2.30e5	Moxon Rae + neutron,gamma discrimination	Van de Graff/FZK, TOF	Moxon Rae + Liq. Scint NE213	5% - 10%	CSR: 22	[54] Wisshak
1.48e-2 2.90e4	Activation	Reactor+ Van de Graff/FZK, TOF	Beta detector	5% - 10%	CS: 3	[55] Wisshak
1.00e6	Activation	Reactor	Solid state detector	30%	CSR: 1	[56] Ivanov
6.86e1 - 1.50e5	Total energy detector (Mayer Leibnitz weighting)	Linac/GELINA, TOF	C_6D_6 detector	0.5% + 10% + 5%	CS: 7356	[57] Vanpraet
-2.20e1 - 4.94e1	Total Energy detector	Linac/ORELA, TOF	NE226 Liq. Scintillator	7% + 5%	RP: 7	[58] Weston
1.28 - 1.49e2	Transmission and fission	Linac/Saclay, TOF	^{10}B-NaI + NE213 for neutrons	2% + 5% norm.	RP: 78	[59] Derrien
1.00e2 - 5.00e5	Total energy detector	Linac/Harwell, TOF	Liq. Scintillator tank	> 10%	CS: 39	[60] Gayther
1.e6	Activation	Reactor	Beta counter	15%	CS: 1	[61] Ivanova
1.5e6	Activation	Fast Reactor	Mass separator	Not given	CS: 1	[28] Cricchio
3.00e5 - 6.80e6	Mono energetic source + fission	p-Cyclotron	Fragment detectors	20% - 100%	CS: 9	[62] Flerov

	fragments of 242mAm after capture					

Table 12. Neutron capture EXFOR data sets for ^{241}Am.

Energy Range (eV)	Experimental Technique	Facility/Laboratory and Method	Detectors	Min and Max uncertainty	Experimental data	Ref.
9.84e-3 - 3.77e5	Total Energy detector	Linac/ORELA, TOF	NE226 Liq. Scintillator	5% + 7%	CS: 4968	[63] Weston
1.50e+6	Activation	Reactor	Mass separator	7%	CS: 1	[28] Cricchio

Table 13. Neutron absorption EXFOR data sets for ^{241}Am.

Figure 27 shows the most recent releases of the existing evaluated neutron capture cross sections for ^{241}Am. Only three set are available from the ENDF/B-VI.8, JENDL 3.3 and JEFF 3.0. Table 14 summarizes the relevant information on the most recently released evaluated cross section libraries.

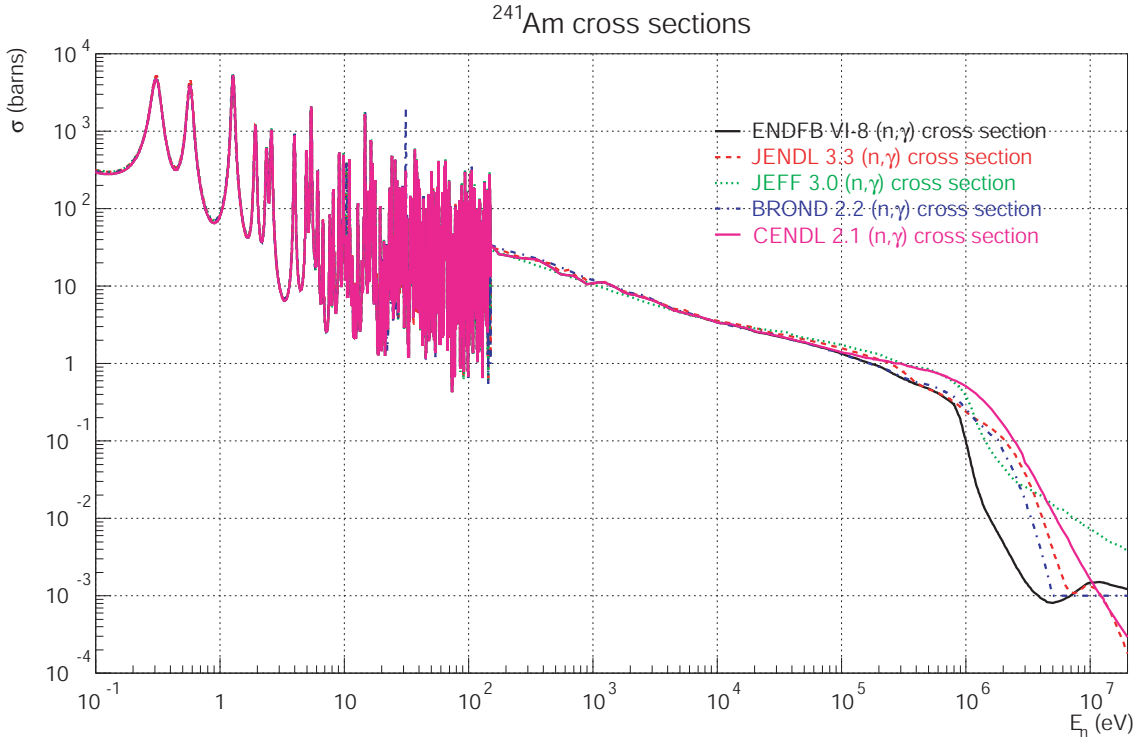

Figure 27. Most recent releases (by September 2003) of evaluated (n,γ) cross sections for ^{241}Am.

Library	Lab	Evaluators	Evaluation date	Revision date
ENDF/B-VI.8	LANL, CNDC	Young, Madland, Zhou et al.	February 94	August 94
JEFF-3.0	NEA	H. Conde	June 82	-
CENDL-2.1	CNDC	Zhou Delin, Gu Fuhua et al.	February 88	June 92
JENDL-3.3	JAERI	T. Nakagawa, O. Iwamoto et al.	March 00	March 01
BROND-2.2	FEI / IJE	A.I.Blokhin, V.M.Maslov	October 90	December 90

Table 14. Information on the evaluation of the most recent releases (September 2003) of the ENDF, JEFF, CENDL, JENDL and BROND neutron cross section libraries for ^{241}Am.

^{243}Am

Figure 28, Figure 30 and Figure 29 show the neutron capture cross sections and EXFOR capture and absorption data available for ^{243}Am in different energy ranges. Table 15 and Table 16 contain a summary about the different experimental EXFOR data sets, such as energy ranges, experimental techniques and detectors, number of data points and the corresponding references.

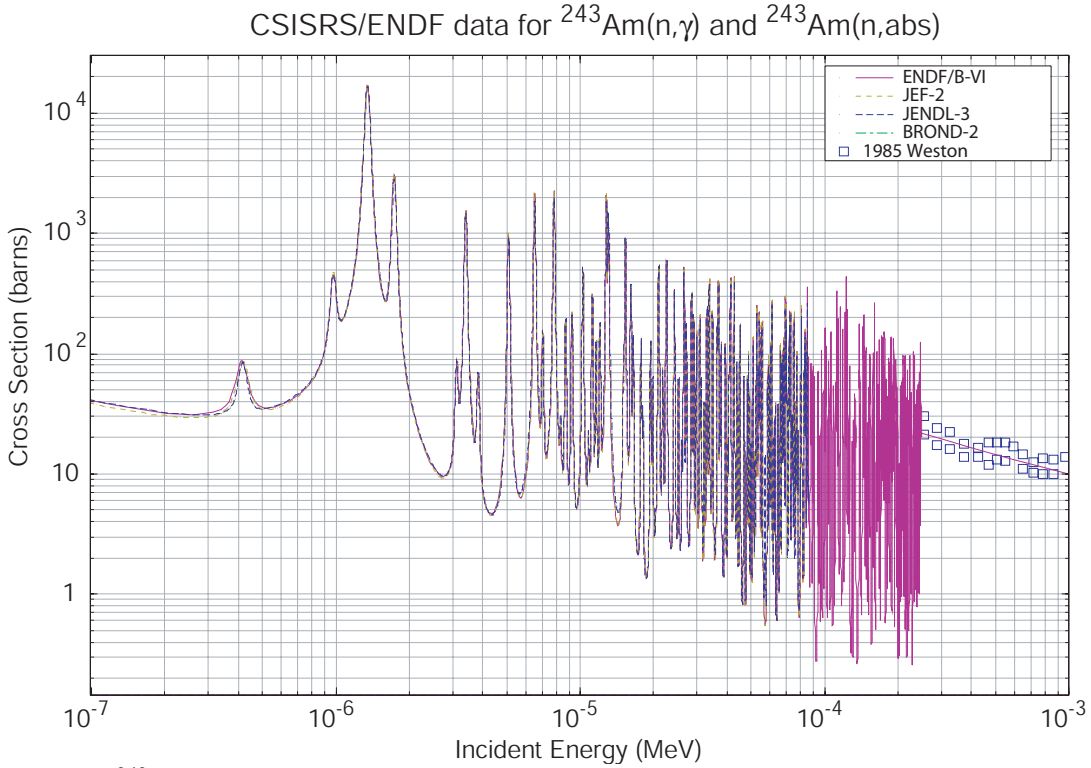

Figure 28. ^{243}Am(n,γ) evaluated cross sections and EXFOR experimental cross section points in the range from 0.1 eV to 1 keV.

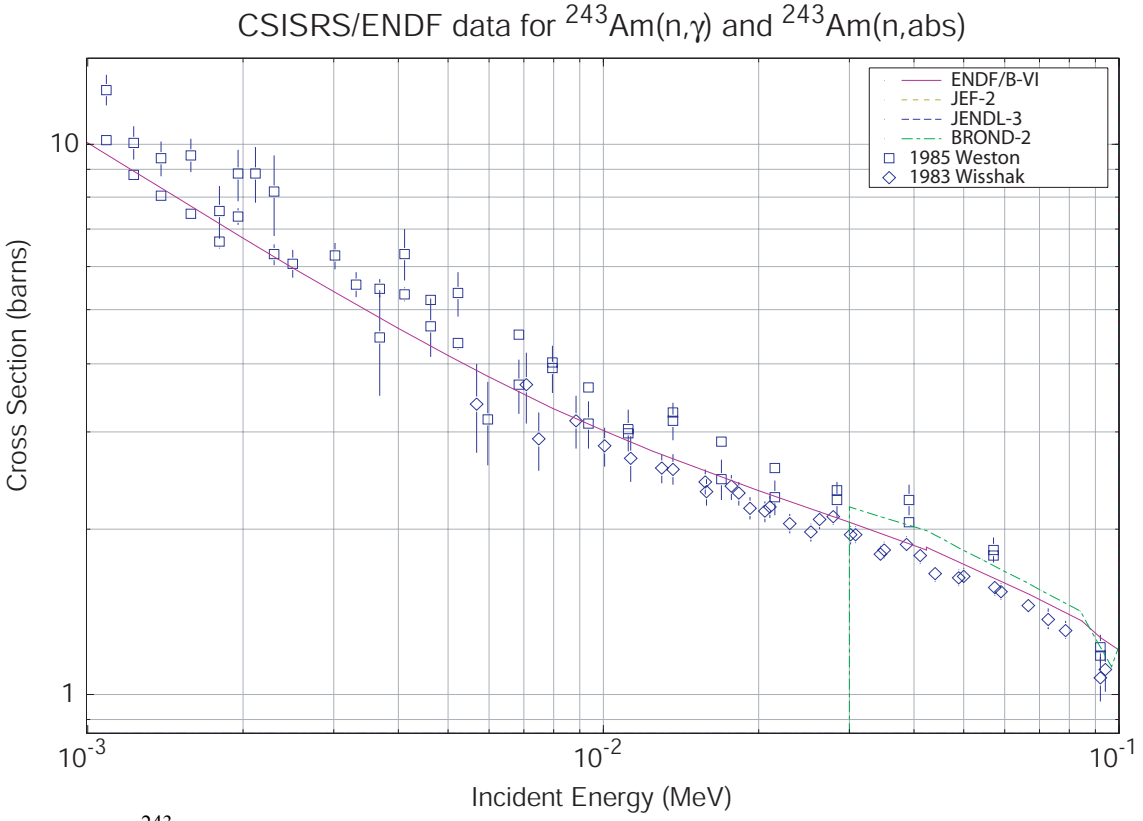

Figure 29. ^{243}Am(n,γ) evaluated cross sections and EXFOR experimental cross section points in the range from 1 keV to 100 keV.

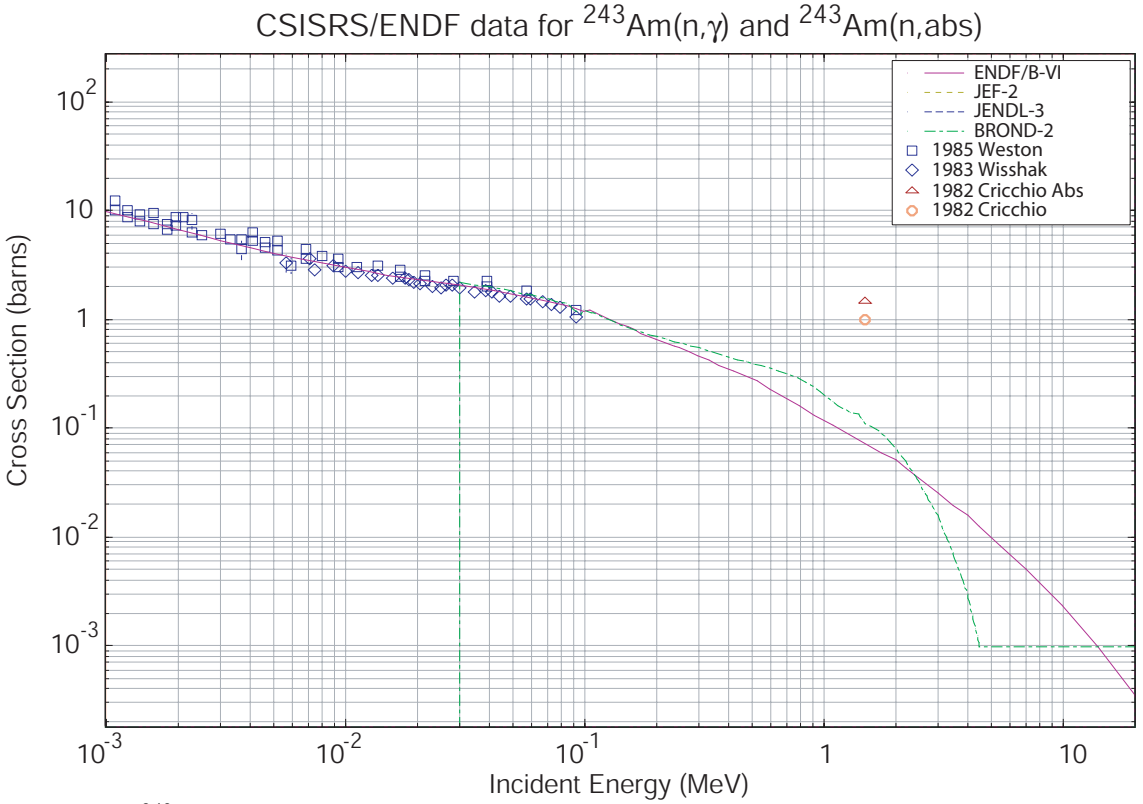

Figure 30. ^{243}Am(n,γ) evaluated cross sections and EXFOR experimental cross section points in the range from 1 keV to 20 MeV.

Energy Range (eV)	Experimental Technique	Facility/Laboratory and Method	Detectors	Min and Max uncertainty	Experimental data	Ref.
5.70e3 - 9.21e4	Moxon Rae + neutron,gamma discrimination	Van de Graff/FZK, TOF	Moxon Rae + Liq. Scint NE213	5% - 20%	CSR: 16 + 10	[66] Wisshak
1.00e6	Activation	Reactor	Solid state detector	30%	CSR: 1	[56] Ivanov
9.83e-1 - 1.99e1	Transmission	Linac/ORELA, TOF	^{6}Li glass Scintillator	10%	RP: 23	[67] Simpson
-2.00 - 2.46e1	Transmission	Reactor, TOF	BF_3	No information	RP: 8	[68] Berreth
9.76e-1 - 1.53	Transmission	Reactor/ANL, TOF	Not specified	10%	RP: 3	[69] Cotre
2.58e2 - 9.21e4	Total energy detector	Linac/ORELA, TOF	NE226 Liq. Scintillator	10%	CS: 38	[70] Weston
5.70e3 - 9.21e4	Moxon Rae + neutron,gamma discrimination	Van de Graff/FZK, TOF	Moxon Rae + Liq. Scint illator NE213	5% - 20%	CS: 16	[66] Wisshak
1.50e+6	Activation	Reactor/Cadarache	Mass Separator	Not given	CS: 1	[28] Cricchio

Table 15. Neutron capture EXFOR data sets for ^{243}Am.

Energy Range (eV)	Experimental Technique	Facility/Laboratory and Method	Detectors	Min and Max uncertainty	Experimental data	Ref.
1.50e+6	Activation	Reactor/Cadarache	Mass Separator	Not given	CS: 1	[28] Cricchio

Table 16. Neutron absorption EXFOR data sets for ^{243}Am.

Figure 31 shows the most recent releases for the existing evaluated ^{243}Am (n,γ) cross sections. No evaluated file exists from the CENDL cross section library. Small differences are found in the unresolved resonance region.

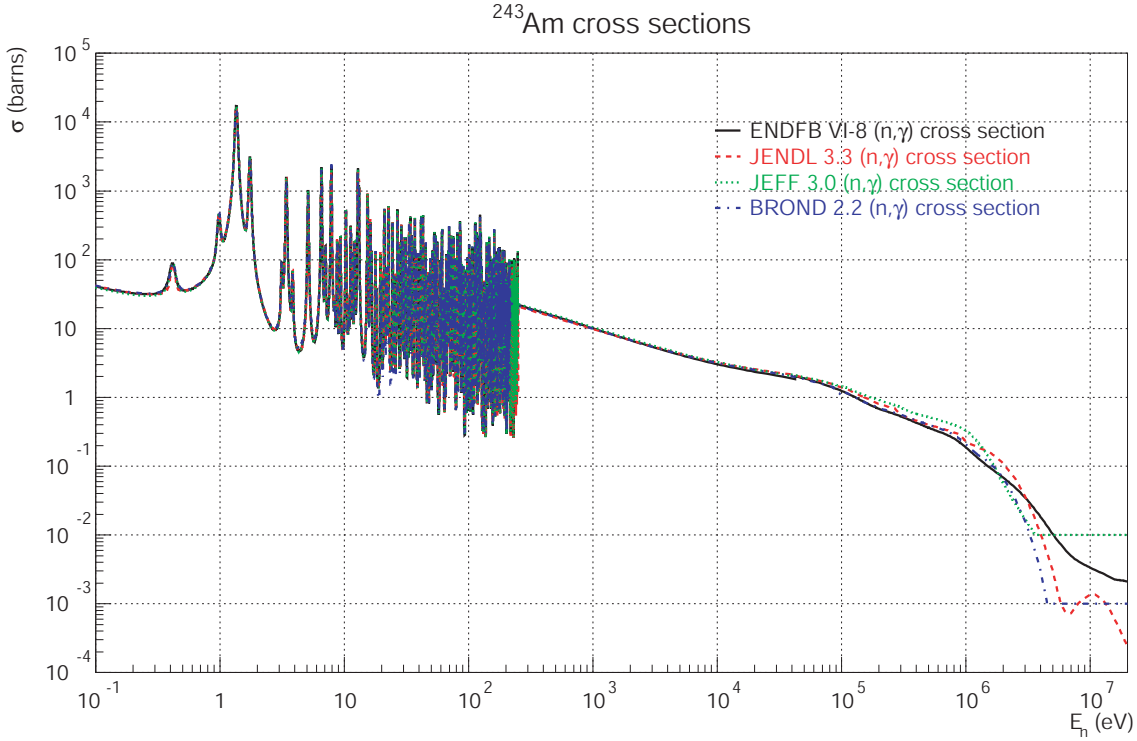

Figure 31. Most recent releases (by September 2003) of evaluated (n,γ) cross sections for ^{243}Am.

Library	Lab	Evaluators	Evaluation date	Revision date
ENDF/B-VI.8	LANL / ORNL	P.G. Young, L.W. Weston	September 96	September 96
JEFF3.0	NEA	H. Conde	June 82	-
CENDL-2.1	-	-	-	-
JENDL-3.3	MINSK / JAERI	V.M. Maslov, T. Nakagawa et al.	January 02	February 02
BROND-2.2	FEI / IJE	A.I. Blokhin, V.M. Maslov	October 90	-

Table 17. Information on the evaluation of the most recent releases (September 2003) of the ENDF, JEFF, CENDL, JENDL and BROND neutron cross section libraries for ^{243}Am.

^{245}Cm

Figure 32 shows the most recent releases of the existing evaluated neutron capture cross sections. Only three sets are available from ENDF/B-VI.8, JENDL 3.3 and JEFF 3.0. Table 18 describes the available evaluated cross section releases.

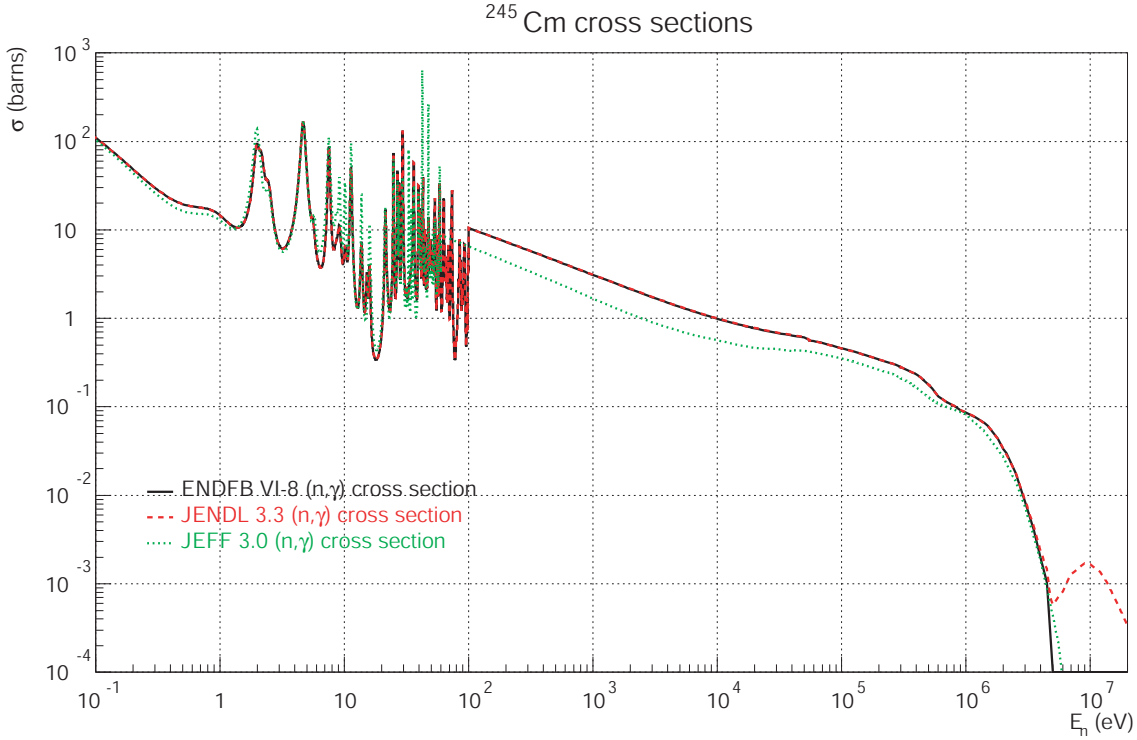

Figure 32. Most recent releases (by September 2003) of evaluated (n,γ) cross sections for ^{245}Cm.

Library	Lab	Evaluators	Evaluation date	Revision date
ENDF/B-VI.8	MINSK	V. Maslov et al.	November 95	-
JEFF-3.0	JAERI	T. Nakagawa	March 98	-
CENDL-2.1	-	-	-	-
JENDL-3.3	MINSK / BYEL	V.M. Maslov et al.	November 95	April 00
BROND-2.2	-	-	-	-

Table 18. Information on the evaluation of the most recent releases (September 2003) of the ENDF, JEFF, CENDL, JENDL and BROND neutron cross section libraries for ^{245}Cm.

Appendix II.
Information on the activity of the ^{233}U, ^{240,242}Pu, ^{241,243}Am and ^{245}Cm samples for neutron capture measurements

Isotope	Activity		γ activity		Average γ energy (keV)	Daughter γ activity (MBq)	Average daughter γ energy (keV)	Gamma Dose Rate at 30 cm (μSv/hr)
	MBq	mCi	MBq	mCi				
^{233}U	35.6	1.0	-	-	-	-	-	13.9
^{237}Np	1.1	3.1e-2	-	-	-	-	-	0.4
^{240}Pu	167.9	4.5	18.6	0.5	13.8	5.0e-7	13.5	13.0
^{242}Pu	2.9	7.9e-2	0.3	7.2e-3	13.8	1.1e-10	103.6	0.2
^{241}Am	3169	85.6	2554	69.0	34.7	2.4e-3	96.3	241.5
^{243}Am	369.2	10.0	498.5	13.5	87.0	319.9	102.4	115.6
^{245}Cm	66.5	1.8	92.5	2.5	71.8	0.4	126.2	17.8

Table 19. Total and gamma activities of the samples after a 1 year decay.

Isotope	Activity		γ activity		Average γ energy (keV)	Daughter γ activity (MBq)	Average daughter γ energy (keV)	Gamma Dose Rate at 30 cm (μSv/hr)
	MBq	mCi	MBq	mCi				
^{233}U	35.8	1.0	-	-	-	-	-	13.9
^{237}Np	1.1	3.1e-2	-	-	-	-	-	0.4
^{240}Pu	167.9	4.5	18.5	0.5	13.8	2.5e-6	13.5	12.9
^{242}Pu	2.9	7.9e-2	0.3	7.2e-3	13.8	6.1e-10	106.5	0.2
^{241}Am	3149	85.1	2538	68.6	34.7	1.3e-2	99.5	240.0
^{243}Am	369.1	10.0	498.3	13.5	87.0	319.8	102.2	115.5
^{245}Cm	77.2	2.1	94.0	2.5	72.6	1.9	124.4	20.9

Table 20. Total and gamma activities of the samples after a 5 years decay.

Isotope	Activity		γ activity		Average γ energy (keV)	Daughter γ activity (MBq)	Average daughter γ energy (keV)	Gamma Dose Rate at 30 cm (μSv/hr)
	MBq	mCi	MBq	mCi				
^{233}U	36.3	1.0	-	-	-	-	-	14.2
^{237}Np	1.1	3.1e-2	-	-	-	-	-	0.4
^{240}Pu	167.4	4.5	18.5	0.5	13.8	1.5e-5	13.5	12.9
^{242}Pu	2.9	7.9e-2	0.3	7.2e-3	13.8	3.6e-9	106.5	0.2
^{241}Am	3025	81.8	2438	65.9	34.7	7.7e-2	99.5	230.6
^{243}Am	368.3	10.0	497.2	13.4	87.0	319.1	102.2	115.3
^{245}Cm	113.3	3.1	99.6	2.7	74.8	7.7	113.1	30.6

Table 21. Total and gamma activities of the samples after a 30 years decay.

^{240}Pu

Z	A	Type of decay	Branch	T1/2 (s)	l (s-1)	Disint /ns	m (g)	#atoms	#g/ns	<Eg> (keV)	% of atoms	<Eg>i *(#g/ns)i (keV/ns)
Th	232	Alpha	1.00E+00	4.43E+17	1.56E-18	1.23E-19	3.02E-14	7.84E+07	3.48E-22	6.95E+01	1.56E-10	2.42E-20
U	236	Alpha	1.00E+00	7.39E+14	9.38E-16	4.97E-09	2.08E-06	5.30E+15	4.97E-10	1.35E+01	1.06E-02	6.72E-09
Pu	240	Alpha	1.00E+00	2.07E+11	3.35E-12	1.68E-01	2.00E-02	5.02E+19	1.86E-02	1.38E+01	1.00E+02	2.56E-01

Table 22. Composition of the ^{240}Pu 1 year the isotopic separation

Z	A	Type of decay	Branch	T1/2 (s)	l (s-1)	Disint /ns	m (g)	#atoms	#g/ns	<Eg> (keV)	% of atoms	<Eγ>i *(#γ/ns)i (keV/ns)
Th	232	Alpha	1.00E+00	4.43E+17	1.56E-18	3.06E-18	7.55E-13	1.96E+09	8.70E-21	6.95E+01	3.91E-09	6.05E-19
U	236	Alpha	1.00E+00	7.39E+14	9.38E-16	2.48E-08	1.04E-05	2.65E+16	2.49E-09	1.35E+01	5.28E-02	3.36E-08
Pu	240	Alpha	1.00E+00	2.07E+11	3.35E-12	1.68E-01	2.00E-02	5.02E+19	1.86E-02	1.38E+01	9.99E+01	2.56E-01

Table 23. Composition of the ^{240}Pu 5 years after the isotopic separation

Z	A	Type of decay	Branch	T1/2 (s)	λ (s-1)	desint/ns	m (g)	#atoms	#γ/ns	<Eγ> (keV)	% of atoms	<Eγ>i *(#γ/ns)i (keV/ns)
Tl	208	Beta	1.00E+00	1.84E+02	3.76E-03	2.18E-17	2.00E-27	5.80E-06	5.22E-17	1.41E+03	1.16E-23	7.33E-14
Pb	208	Stable					5.19E-21	1.50E+01			2.99E-17	0.00E+00
Pb	212	Beta	1.00E+00	3.83E+04	1.81E-05	6.08E-17	1.18E-24	3.36E-03	5.97E-17	1.47E+02	6.69E-21	8.77E-15
Bi	212	Beta	6.41E-01	3.63E+03	1.91E-04	6.08E-17	1.12E-25	3.19E-04	9.79E-18	6.17E+02	6.35E-22	6.04E-15
Bi	212	Alpha	3.59E-01	3.63E+03	1.91E-04	6.08E-17	1.12E-25	3.19E-04	3.02E-18	8.37E+01	6.35E-22	2.53E-16
Po	212	Alpha	1.00E+00	3.00E-07	2.31E+06	3.89E-17	5.93E-36	1.69E-14	1.79E-18	1.72E+03	3.36E-32	3.08E-15
Po	216	Alpha	1.00E+00	1.50E-01	4.62E+00	6.08E-17	4.72E-30	1.32E-08	1.15E-21	8.05E+02	2.62E-26	9.30E-19
Rn	220	Alpha	1.00E+00	5.56E+01	1.25E-02	6.08E-17	1.78E-27	4.88E-06	6.93E-20	5.50E+02	9.71E-24	3.81E-17
Ra	224	Alpha	1.00E+00	3.16E+05	2.19E-06	6.08E-17	1.03E-23	2.77E-02	2.50E-18	2.42E+02	5.53E-20	6.05E-16
Ra	228	Beta	1.00E+00	2.11E+08	3.28E-09	6.08E-17	7.02E-21	1.85E+01	4.32E-18	1.35E+01	3.69E-17	5.84E-17
Ac	228	Beta	1.00E+00	2.21E+04	3.14E-05	6.08E-17	7.33E-25	1.93E-03	9.50E-17	5.54E+02	3.86E-21	5.26E-14
Ac	228	Alpha	5.50E-08	2.21E+04	3.14E-05	6.08E-17	7.33E-25	1.93E-03	1.49E-24	1.11E+01	3.86E-21	1.65E-23
Th	228	Alpha	1.00E+00	6.04E+07	1.15E-08	6.08E-17	2.00E-21	5.29E+00	1.05E-18	1.14E+02	1.05E-17	1.19E-16
Th	232	Alpha	1.00E+00	4.43E+17	1.56E-18	1.10E-16	2.72E-11	7.05E+10	3.13E-19	6.95E+01	1.40E-07	2.18E-17
U	236	Alpha	1.00E+00	7.39E+14	9.38E-16	1.49E-07	6.22E-05	1.59E+17	1.49E-08	1.35E+01	3.16E-01	2.01E-07
Pu	240	Alpha	1.00E+00	2.07E+11	3.35E-12	1.67E-01	1.99E-02	5.00E+19	1.85E-02	1.38E+01	9.97E+01	2.55E-01

Table 24. Composition of the ^{240}Pu 30 years after the isotopic separation

^{242}Pu

Z	A	Type of decay	Branch	T1/2 (s)	λ (s-1)	Disint /ns	m (g)	#atoms	#γ/ns	<Eg> (keV)	% of atoms	<Eγ>I *(#γ/ns)i (keV/ns)
Th	230	Long T1/2		2.38E+12	2.91E-13	0.00E+00		0.00E+00			0.00E+00	0.00E+00
Th	234	Beta	1.00E+00	2.08E+06	3.33E-07	4.11E-13	4.80E-19	1.23E+03	6.32E-14	6.04E+01	2.48E-15	3.82E-12
Pa	234	Beta	1.00E+00	2.41E+04	2.87E-05	5.34E-16	7.23E-24	1.86E-02	1.15E-15	6.70E+02	3.74E-20	7.67E-13
Pa^M	234	Beta	9.98E-01	7.02E+01	9.87E-03	4.11E-13	1.62E-23	4.16E-02	1.19E-14	5.60E+02	8.36E-20	6.64E-12
Pa^M	234	IT	1.60E-03	7.02E+01	9.87E-03	4.11E-13	1.62E-23	4.16E-02	6.65E-16	7.36E+01	8.36E-20	4.89E-14
U	234	Alpha	1.00E+00	7.75E+12	8.95E-14	5.31E-19	2.31E-18	5.93E+03	5.88E-20	1.38E+01	1.19E-14	8.14E-19
U	238	Alpha	1.00E+00	1.41E+17	4.92E-18	4.54E-13	3.65E-08	9.24E+13	3.67E-14	1.34E+01	1.86E-04	4.93E-13
Pu	242	Alpha	1.00E+00	1.18E+13	5.88E-14	2.93E-03	2.00E-02	4.98E+19	2.68E-04	1.38E+01	1.00E+02	3.68E-03

Table 25. Composition of the ^{242}Pu 1 year after the isotopic separation

Z	A	Type of decay	Branch	T1/2 (s)	λ (s-1)	Disint t/ns	m (g)	#atoms	#γ/ns	<Eg> (keV)	% of atoms	<Eγ>I *(#γ/ns)i (keV/ns)
Th	230	Long T1/2		2.38E+12	2.91E-13	1.49E-22	1.95E-22	5.12E-01			1.03E-18	0.00E+00
Th	234	Beta	1.00E+00	2.08E+06	3.33E-07	2.27E-12	2.65E-18	6.82E+03	3.49E-13	6.04E+01	1.37E-14	2.11E-11
Pa	234	Beta	1.00E+00	2.41E+04	2.87E-05	2.95E-15	3.99E-23	1.03E-01	6.33E-15	6.70E+02	2.06E-19	4.24E-12
Pa^M	234	Beta	9.98E-01	7.02E+01	9.87E-03	2.27E-12	8.94E-23	2.30E-01	6.55E-14	5.60E+02	4.62E-19	3.67E-11
Pa^M	234	IT	1.60E-03	7.02E+01	9.87E-03	2.27E-12	8.94E-23	2.30E-01	3.68E-15	7.36E+01	4.62E-19	2.70E-13
U	234	Alpha	1.00E+00	7.75E+12	8.95E-14	1.56E-17	6.78E-17	1.74E+05	1.73E-18	1.38E+01	3.50E-13	2.39E-17
U	238	Alpha	1.00E+00	1.41E+17	4.92E-18	2.27E-12	1.83E-07	4.62E+14	1.83E-13	1.34E+01	9.28E-04	2.47E-12
Pu	242	Alpha	1.00E+00	1.18E+13	5.88E-14	2.93E-03	2.00E-02	4.98E+19	2.68E-04	1.38E+01	1.00E+02	3.68E-03

Table 26. Composition of the ^{242}Pu 5 years the isotopic separation

Z	A	Type of decay	Branch	T1/2 (s)	λ (s-1)	Disint /ns	m (g)	#atoms	#γ/ns	<Eg> (keV)	%atoms	<Eγ>I *(#γ/ns)i (keV/ns)
Th	230	Long T1/2		2.38E+12	2.91E-13	5.29E-20	6.93E-20	1.81E+02			3.65E-16	0.00E+00
Th	234	Beta	1.00E+00	2.08E+06	3.33E-07	1.36E-11	1.59E-17	4.09E+04	2.10E-12	6.04E+01	8.23E-14	1.27E-10
Pa	234	Beta	1.00E+00	2.41E+04	2.87E-05	1.77E-14	2.40E-22	6.17E-01	3.80E-14	6.70E+02	1.24E-18	2.54E-11
Pa^M	234	Beta	9.98E-01	7.02E+01	9.87E-03	1.36E-11	5.36E-22	1.38E+00	3.93E-13	5.60E+02	2.77E-18	2.20E-10
Pa^M	234	IT	1.60E-03	7.02E+01	9.87E-03	1.36E-11	5.36E-22	1.38E+00	2.21E-14	7.36E+01	2.77E-18	1.62E-12
U	234	Alpha	1.00E+00	7.75E+12	8.95E-14	5.75E-16	2.50E-15	6.43E+06	6.37E-17	1.38E+01	1.29E-11	8.81E-16
U	238	Alpha	1.00E+00	1.41E+17	4.92E-18	1.36E-11	1.10E-06	2.77E+15	1.10E-12	1.34E+01	5.57E-03	1.48E-11
Pu	242	Alpha	1.00E+00	1.18E+13	5.88E-14	2.93E-03	2.00E-02	4.98E+19	2.68E-04	1.38E+01	1.00E+02	3.68E-03

Table 27. Composition of the ^{242}Pu 30 years after the isotopic separation

^{241}Am

Z	A	Type of decay	Branch	T1/2 (s)	λ (s-1)	Disint /ns	m (g)	#atoms	#γ/ns	<Eg> (keV)	% of atoms	<Eγ>i *(#γ/ns)i (keV/ns)
Th	229	Alpha	1.00E+00	2.49E+11	2.79E-12	4.85E-17	6.62E-18	1.74E+04	1.29E-17	1.37E+02	2.79E-14	1.77E-15
Pa	233	Beta	1.00E+00	2.33E+06	2.97E-07	9.16E-07	1.19E-12	3.08E+09	1.38E-06	1.45E+02	4.94E-09	2.01E-04
U	233	Alpha	1.00E+00	5.02E+12	1.38E-13	1.81E-12	5.07E-12	1.31E+10	1.00E-13	1.68E+01	2.10E-08	1.68E-12
Np	237	Alpha	1.00E+00	6.77E+13	1.02E-14	1.03E-06	3.94E-05	1.00E+17	1.06E-06	3.23E+01	1.60E-01	3.42E-05
Am	241	Alpha	1.00E+00	1.36E+10	5.08E-11	3.17E+00	2.50E-02	6.24E+19	2.55E+00	3.47E+01	9.98E+01	8.88E+01

Table 28. Composition of the ^{241}Am 1 year after the isotopic separation.

Z	A	Type of decay	Branch	T1/2 (s)	λ (s-1)	Disint /ns	m (g)	#atoms	#γ/ns	<Eg> (keV)	% of atoms	<Eγ>i *(#γ/ns)i (keV/ns)
Tl	209	Beta	1.00E+00	1.32E+02	5.25E-03	1.84E-16	1.22E-26	3.50E-05	5.76E-16	6.84E+02	5.61E-23	3.94E-13
Pb	209	Beta	1.00E+00	1.19E+04	5.83E-05	8.51E-15	5.07E-23	1.46E-01	0.00E+00	0.00E+00	2.34E-19	0.00E+00
Bi	209	Stable					1.08E-19	3.12E+02			4.99E-16	0.00E+00
Bi	213	Beta	9.79E-01	2.74E+03	2.53E-04	8.51E-15	1.19E-23	3.36E-02	2.81E-15	3.85E+02	5.38E-20	1.08E-12
Bi	213	Alpha	2.09E-02	2.74E+03	2.53E-04	8.51E-15	1.19E-23	3.36E-02	2.68E-17	2.56E+02	5.38E-20	6.86E-15
Po	213	Alpha	1.00E+00	4.20E-06	1.65E+05	8.33E-15	1.79E-32	5.05E-11	4.00E-19	7.79E+02	8.08E-29	3.11E-16
At	217	Beta	1.00E-04	3.23E-02	2.15E+01	8.51E-15	1.43E-28	3.97E-07	0.00E+00	0.00E+00	6.35E-25	0.00E+00
At	217	Alpha	1.00E+00	3.23E-02	2.15E+01	8.51E-15	1.43E-28	3.97E-07	5.82E-18	3.17E+02	6.35E-25	1.85E-15
Fr	221	Beta	1.00E-03	2.88E+02	2.41E-03	8.51E-15	1.30E-24	3.54E-03	4.49E-19	5.42E+01	5.66E-21	2.44E-17
Fr	221	Alpha	1.00E+00	2.88E+02	2.41E-03	8.51E-15	1.30E-24	3.54E-03	1.48E-15	1.69E+02	5.66E-21	2.51E-13
Ra	225	Beta	1.00E+00	1.28E+06	5.42E-07	8.51E-15	5.87E-21	1.57E+01	2.68E-15	3.87E+01	2.52E-17	1.04E-13
Ac	225	Alpha	1.00E+00	8.64E+05	8.02E-07	8.51E-15	3.97E-21	1.06E+01	3.48E-15	4.17E+01	1.70E-17	1.45E-13
Th	229	Alpha	1.00E+00	2.49E+11	2.79E-12	8.51E-15	1.16E-15	3.05E+06	2.27E-15	1.37E+02	4.89E-12	3.10E-13
Pa	233	Beta	1.00E+00	2.33E+06	2.97E-07	5.11E-06	6.66E-12	1.72E+10	7.73E-06	1.45E+02	2.75E-08	1.12E-03
U	233	Alpha	1.00E+00	5.02E+12	1.38E-13	5.90E-11	1.66E-10	4.28E+11	3.27E-12	1.68E+01	6.85E-07	5.50E-11
Np	237	Alpha	1.00E+00	6.77E+13	1.02E-14	5.11E-06	1.96E-04	4.99E+17	5.28E-06	3.23E+01	7.99E-01	1.71E-04
Am	241	Alpha	1.00E+00	1.36E+10	5.08E-11	3.15E+00	2.48E-02	6.20E+19	2.54E+00	3.47E+01	9.92E+01	8.82E+01

Table 29. Composition of the ^{241}Am 5 years after the isotopic separation.

Z	A	Type of decay	Branch	T1/2 (s)	λ (s-1)	Disint /ns	m (g)	#atoms	#γ/ns	<Eg> (keV)	% of atoms	<Eγ>i *(#γ/ns)i (keV/ns)
Tl	209	Beta	1.00E+00	1.32E+02	5.25E-03	3.79E-14	2.50E-24	7.21E-03	1.19E-13	6.84E+02	1.15E-20	8.11E-11
Pb	209	Beta	1.00E+00	1.19E+04	5.83E-05	1.75E-12	1.04E-20	3.01E+01	0.00E+00	0.00E+00	4.81E-17	0.00E+00
Bi	209	Stable					1.45E-16	4.16E+05			6.67E-13	0.00E+00
Bi	213	Beta	9.79E-01	2.74E+03	2.53E-04	1.75E-12	2.45E-21	6.93E+00	5.78E-13	3.85E+02	1.11E-17	2.22E-10
Bi	213	Alpha	2.09E-02	2.74E+03	2.53E-04	1.75E-12	2.45E-21	6.93E+00	5.53E-15	2.56E+02	1.11E-17	1.41E-12
Po	213	Alpha	1.00E+00	4.20E-06	1.65E+05	1.72E-12	3.68E-30	1.04E-08	8.24E-17	7.79E+02	1.66E-26	6.41E-14
Rn	217	Alpha	1.00E+00	5.40E-04	1.28E+03	0.00E+00	0.00E+00	0.00E+00	0.00E+00	0.00E+00	0.00E+00	0.00E+00
At	217	Beta	1.00E-04	3.23E-02	2.15E+01	1.75E-12	2.95E-26	8.17E-05	0.00E+00	0.00E+00	1.31E-22	0.00E+00
At	217	Alpha	1.00E+00	3.23E-02	2.15E+01	1.75E-12	2.95E-26	8.17E-05	1.20E-15	3.17E+02	1.31E-22	3.80E-13
Ra	221	Alpha	1.00E+00	2.80E+01	2.48E-02	0.00E+00	0.00E+00	0.00E+00	0.00E+00	9.19E+01	0.00E+00	0.00E+00
Fr	221	Beta	1.00E-03	2.88E+02	2.41E-03	1.75E-12	2.68E-22	7.29E-01	9.26E-17	5.42E+01	1.17E-18	5.02E-15
Fr	221	Alpha	1.00E+00	2.88E+02	2.41E-03	1.75E-12	2.68E-22	7.29E-01	3.05E-13	1.69E+02	1.17E-18	5.16E-11
Ra	225	Beta	1.00E+00	1.28E+06	5.42E-07	1.75E-12	1.21E-18	3.24E+03	5.53E-13	3.87E+01	5.18E-15	2.14E-11
Ac	225	Alpha	1.00E+00	8.64E+05	8.02E-07	1.75E-12	8.17E-19	2.19E+03	7.18E-13	4.17E+01	3.50E-15	2.99E-11
Th	229	Alpha	1.00E+00	2.49E+11	2.79E-12	1.75E-12	2.39E-13	6.29E+08	4.67E-13	1.37E+02	1.01E-09	6.38E-11
Pa	233	Beta	1.00E+00	2.33E+06	2.97E-07	3.01E-05	3.92E-11	1.01E+11	4.54E-05	1.45E+02	1.62E-07	6.61E-03
U	233	Alpha	1.00E+00	5.02E+12	1.38E-13	1.98E-09	5.54E-09	1.43E+13	1.10E-10	1.68E+01	2.29E-05	1.84E-09
Np	237	Alpha	1.00E+00	6.77E+13	1.02E-14	3.01E-05	1.15E-03	2.93E+18	3.11E-05	3.23E+01	4.70E+00	1.00E-03
Am	241	Alpha	1.00E+00	1.36E+10	5.08E-11	3.03E+00	2.38E-02	5.95E+19	2.44E+00	3.47E+01	9.53E+01	8.47E+01

Table 30. Composition of the ^{241}Am 30 years after the isotopic separation.

^{243}Am

Z	A	Type of decay	Branch	T1/2 (s)	λ (s-1)	Disint /ns	m (g)	#atoms	#γ/ns	<Eg> (keV)	% of atoms	<Eγ>i *(#γ/ns)i (keV/ns)
Pa	231	Alpha	1.00E+00	1.03E+12	6.70E-13	1.82E-20	1.04E-20	2.72E+01	1.11E-20	6.64E+01	4.39E-17	7.34E-19
Th	231	Beta	1.00E+00	9.19E+04	7.54E-06	2.59E-15	1.32E-22	3.43E-01	3.45E-15	2.08E+01	5.54E-19	7.16E-14
U	235	Alpha	1.00E+00	2.22E+16	3.12E-17	2.59E-15	3.24E-11	8.30E+10	5.39E-15	8.65E+01	1.34E-07	4.66E-13
Pu	239	Alpha	1.00E+00	7.61E+11	9.11E-13	5.26E-06	2.29E-06	5.77E+15	2.62E-07	1.48E+01	9.32E-03	3.89E-06
Np	239	Beta	1.00E+00	2.04E+05	3.41E-06	1.85E-01	2.15E-08	5.42E+13	3.20E-01	1.02E+02	8.75E-05	3.27E+01
Am	243	Alpha	1.00E+00	2.33E+11	2.98E-12	1.85E-01	2.50E-02	6.19E+19	1.79E-01	5.97E+01	1.00E+02	1.07E+01

Table 31. Composition of the ^{243}Am 1 year after the isotopic separation.

Z	A	Type of decay	Branch	T1/2 (s)	λ (s-1)	Disint /ns	m (g)	#atoms	#γ/ns	<Eg> (keV)	% of atoms	<Eγ>i *(#γ/ns)i (keV/ns)
Pa	231	Alpha	1.00E+00	1.03E+12	6.70E-13	2.31E-18	1.32E-18	3.44E+03	1.40E-18	6.64E+01	5.55E-15	9.27E-17
Th	231	Beta	1.00E+00	9.19E+04	7.54E-06	6.52E-14	3.32E-21	8.64E+00	8.68E-14	2.08E+01	1.39E-17	1.80E-12
U	235	Alpha	1.00E+00	2.22E+16	3.12E-17	6.52E-14	8.16E-10	2.09E+12	1.36E-13	8.65E+01	3.37E-06	1.17E-11
Pu	239	Alpha	1.00E+00	7.61E+11	9.11E-13	2.65E-05	1.15E-05	2.91E+16	1.32E-06	1.48E+01	4.69E-02	1.96E-05
Np	239	Beta	1.00E+00	2.04E+05	3.41E-06	1.85E-01	2.15E-08	5.42E+13	3.20E-01	1.02E+02	8.75E-05	3.27E+01
Am	243	Alpha	1.00E+00	2.33E+11	2.98E-12	1.85E-01	2.50E-02	6.19E+19	1.79E-01	5.97E+01	1.00E+02	1.07E+01

Table 32. Composition of the ^{243}Am 5 years after the isotopic separation.

Z	A	Type of decay	Branch	T1/2 (s)	λ (s-1)	Disint /ns	m (g)	#atoms	#γ/ns	<Eg> (keV)	% of atoms	<Eγ>i *(#γ/ns)i (keV/ns)
Tl	207	Beta	1.00E+00	2.86E+02	2.42E-03	9.89E-17	1.40E-26	4.08E-05	2.68E-19	8.69E+02	6.59E-23	2.33E-16
Pb	207	Stable					6.56E-21	1.91E+01			3.08E-17	0.00E+00
Po	211	Alpha	1.00E+00	5.16E-01	1.34E+00	3.01E-19	7.86E-32	2.24E-10	3.43E-21	7.18E+02	3.62E-28	2.46E-18
Bi	211	Beta	2.80E-03	1.28E+02	5.42E-03	9.91E-17	6.41E-27	1.83E-05	1.01E-20	5.58E+01	2.95E-23	5.62E-19
Bi	211	Alpha	9.97E-01	1.28E+02	5.42E-03	9.91E-17	6.41E-27	1.83E-05	1.64E-17	2.86E+02	2.95E-23	4.70E-15
Pb	211	Beta	1.00E+00	2.17E+03	3.20E-04	9.91E-17	1.09E-25	3.10E-04	1.21E-17	5.28E+02	5.00E-22	6.38E-15
Po	215	Beta	2.30E-06	1.78E-03	3.89E+02	9.91E-17	9.09E-32	2.55E-10	0.00E+00	0.00E+00	4.11E-28	0.00E+00
Po	215	Alpha	1.00E+00	1.78E-03	3.89E+02	9.91E-17	9.09E-32	2.55E-10	3.96E-15	4.39E+02	4.11E-28	1.74E-12
Rn	219	Alpha	1.00E+00	3.96E+00	1.75E-01	9.91E-17	2.06E-28	5.66E-07	1.65E-16	3.16E+02	9.14E-25	5.22E-14
Ra	223	Alpha	1.00E+00	9.88E+05	7.02E-07	9.91E-17	5.23E-23	1.41E-01	1.11E-16	1.23E+02	2.28E-19	1.37E-14
Fr	223	Beta	1.00E+00	1.31E+03	5.30E-04	1.37E-18	9.56E-28	2.58E-06	7.50E-19	8.78E+01	4.17E-24	6.58E-17
Fr	223	Alpha	6.00E-05	1.31E+03	5.30E-04	1.37E-18	9.56E-28	2.58E-06	9.03E-26	1.91E+01	4.17E-24	1.72E-24
Th	227	Alpha	1.00E+00	1.62E+06	4.29E-07	9.78E-17	8.60E-23	2.28E-01	7.74E-17	1.52E+02	3.68E-19	1.17E-14
Ac	227	Beta	9.86E-01	6.87E+08	1.01E-09	9.92E-17	3.71E-20	9.83E+01	3.62E-20	1.20E+01	1.59E-16	4.34E-19
Ac	227	Alpha	1.38E-02	6.87E+08	1.01E-09	9.92E-17	3.71E-20	9.83E+01	3.85E-20	1.24E+02	1.59E-16	4.76E-18
Pa	231	Alpha	1.00E+00	1.03E+12	6.70E-13	4.97E-16	2.85E-16	7.42E+05	3.01E-16	6.64E+01	1.20E-12	2.00E-14
Th	231	Beta	1.00E+00	9.19E+04	7.54E-06	2.35E-12	1.19E-19	3.11E+02	3.13E-12	2.08E+01	5.03E-16	6.49E-11
U	235	Alpha	1.00E+00	2.22E+16	3.12E-17	2.35E-12	2.94E-08	7.53E+13	4.89E-12	8.65E+01	1.21E-04	4.23E-10
Pu	239	Alpha	1.00E+00	7.61E+11	9.11E-13	1.59E-04	6.92E-05	1.74E+17	7.93E-06	1.48E+01	2.82E-01	1.18E-04
Np	239	Beta	1.00E+00	2.04E+05	3.41E-06	1.84E-01	2.15E-08	5.41E+13	3.19E-01	1.02E+02	8.72E-05	3.26E+01
Am	243	Alpha	1.00E+00	2.33E+11	2.98E-12	1.84E-01	2.49E-02	6.18E+19	1.78E-01	5.97E+01	9.97E+01	1.06E+01

Table 33. Composition of the ^{243}Am 30 years after the isotopic separation.

^{245}Cm

Z	A	Type of decay	Branch	T1/2 (s)	λ (s-1)	Disint /ns	m (g)	#atoms	#γ/ns	<Eγ> (keV)	% of atoms	<Eγ>I *(#γ/ns)i (keV/ns)
Pa	233	Beta	1.00E+00	2.33E+06	2.97E-07	2.04E-13	2.65E-19	6.86E+02	3.08E-13	1.45E+02	2.79E-15	4.48E-11
U	233	Alpha	1.00E+00	5.02E+12	1.38E-13	2.08E-19	5.84E-19	1.51E+03	1.15E-20	1.68E+01	6.14E-15	1.94E-19
U	237	Beta	1.00E+00	5.83E+05	1.19E-06	7.35E-08	2.43E-14	6.18E+07	1.38E-07	7.51E+01	2.52E-10	1.03E-05
Np	237	Alpha	1.00E+00	6.77E+13	1.02E-14	2.73E-13	1.05E-11	2.67E+10	2.83E-13	3.23E+01	1.09E-07	9.13E-12
Pu	241	Beta	1.00E+00	4.53E+08	1.53E-09	3.00E-03	7.83E-07	1.96E+15	0.00E+00	0.00E+00	7.96E-03	0.00E+00
Pu	241	Alpha	2.50E-05	4.53E+08	1.53E-09	3.00E-03	7.83E-07	1.96E+15	4.07E-04	1.27E+02	7.96E-03	5.16E-02
Am	241	Alpha	1.00E+00	1.36E+10	5.08E-11	2.42E-06	1.91E-08	4.76E+13	1.95E-06	3.47E+01	1.94E-04	6.78E-05
Cm	245	Alpha	1.00E+00	2.68E+11	2.58E-12	6.35E-02	1.00E-02	2.46E+19	9.21E-02	7.15E+01	1.00E+02	6.59E+00

Table 34. Composition of the ^{245}Cm 1 year after the isotopic separation.

Z	A	Type of decay	Branch	T1/2 (s)	λ (s-1)	Disint /ns	m (g)	#atoms	#γ/ns	<Eγ> (keV)	% of atoms	<Eγ>i *(#γ/ns)i (keV/ns)
Pb	209	Beta	1.00E+00	1.19E+04	5.83E-05	5.83E-28	3.47E-36	1.00E-14	0.00E+00	0.00E+00	4.07E-32	0.00E+00
Bi	209	Stable					6.58E-27	1.90E-05			7.71E-23	0.00E+00
At	217	Beta	1.00E-04	3.23E-02	2.15E+01	1.63E-20	2.74E-34	7.60E-13	0.00E+00	0.00E+00	3.09E-30	0.00E+00
At	217	Alpha	1.00E+00	3.23E-02	2.15E+01	1.63E-20	2.74E-34	7.60E-13	1.11E-23	3.17E+02	3.09E-30	3.53E-21
Fr	221	Beta	1.00E-03	2.88E+02	2.41E-03	1.63E-20	2.49E-30	6.77E-09	8.61E-25	5.42E+01	2.76E-26	4.66E-23
Fr	221	Alpha	1.00E+00	2.88E+02	2.41E-03	1.63E-20	2.49E-30	6.77E-09	2.77E-21	1.72E+02	2.76E-26	4.77E-19
Ra	225	Beta	1.00E+00	1.28E+06	5.42E-07	1.63E-20	1.12E-26	3.01E-05	5.14E-21	3.87E+01	1.22E-22	1.99E-19
Ac	225	Alpha	1.00E+00	8.64E+05	8.02E-07	1.63E-20	7.59E-27	2.03E-05	6.67E-21	4.17E+01	8.27E-23	2.78E-19
Th	229	Alpha	1.00E+00	2.49E+11	2.79E-12	1.63E-20	2.23E-21	5.85E+00	4.35E-21	1.37E+02	2.38E-17	5.93E-19
Pa	233	Beta	1.00E+00	2.33E+06	2.97E-07	3.15E-11	4.10E-17	1.06E+05	4.75E-11	1.45E+02	4.31E-13	6.91E-09
U	233	Alpha	1.00E+00	5.02E+12	1.38E-13	1.85E-16	5.18E-16	1.34E+06	1.02E-17	1.68E+01	5.44E-12	1.72E-16
U	237	Beta	1.00E+00	5.83E+05	1.19E-06	3.34E-07	1.11E-13	2.81E+08	6.26E-07	7.51E+01	1.14E-09	4.70E-05
Np	237	Alpha	1.00E+00	6.77E+13	1.02E-14	3.14E-11	1.21E-09	3.07E+12	3.25E-11	3.23E+01	1.25E-05	1.05E-09
Pu	241	Beta	1.00E+00	4.53E+08	1.53E-09	1.36E-02	3.56E-06	8.90E+15	0.00E+00	0.00E+00	3.62E-02	0.00E+00
Pu	241	Alpha	2.50E-05	4.53E+08	1.53E-09	1.36E-02	3.56E-06	8.90E+15	1.85E-03	1.27E+02	3.62E-02	2.35E-01
Am	241	Alpha	1.00E+00	1.36E+10	5.08E-11	5.67E-05	4.46E-07	1.12E+15	4.57E-05	3.47E+01	4.54E-03	1.59E-03
Cm	245	Alpha	1.00E+00	2.68E+11	2.58E-12	6.35E-02	1.00E-02	2.46E+19	9.21E-02	7.15E+01	1.00E+02	6.59E+00

Table 35. Composition of the ^{245}Cm 5 years after the isotopic separation.

Z	A	Type of decay	Branch	T1/2 (s)	λ (s-1)	Disint /ns	m (g)	#atoms	#γ/ns	<Eγ> (keV)	%atoms	<Eγ>i *(#γ/ns)i (keV/ns)
Tl	209	Beta	1.00E+00	1.32E+02	5.25E-03	2.11E-18	1.40E-28	4.02E-07	6.62E-18	6.84E+02	1.64E-24	4.53E-15
Pb	209	Beta	1.00E+00	1.19E+04	5.83E-05	9.78E-17	5.82E-25	1.68E-03	0.00E+00	0.00E+00	6.82E-21	0.00E+00
Bi	209	Stable					5.50E-21	1.58E+01			6.44E-17	0.00E+00
Bi	213	Beta	9.79E-01	2.74E+03	2.53E-04	9.78E-17	1.37E-25	3.86E-04	3.24E-17	3.83E+02	1.57E-21	1.24E-14
Bi	213	Alpha	2.09E-02	2.74E+03	2.53E-04	9.78E-17	1.37E-25	3.86E-04	3.08E-19	2.56E+02	1.57E-21	7.89E-17
Po	213	Alpha	1.00E+00	4.20E-06	1.65E+05	9.57E-17	2.05E-34	5.80E-13	4.59E-21	7.79E+02	2.36E-30	3.58E-18
Rn	217	Alpha	1.00E+00	5.40E-04	1.28E+03	0.00E+00	0.00E+00	0.00E+00	0.00E+00	0.00E+00	0.00E+00	0.00E+00
At	217	Beta	1.00E-04	3.23E-02	2.15E+01	9.78E-17	1.64E-30	4.56E-09	0.00E+00	0.00E+00	1.85E-26	0.00E+00
At	217	Alpha	1.00E+00	3.23E-02	2.15E+01	9.78E-17	1.64E-30	4.56E-09	6.69E-20	3.17E+02	1.85E-26	2.12E-17
Ra	221	Alpha	1.00E+00	2.80E+01	2.48E-02	0.00E+00	0.00E+00	0.00E+00	0.00E+00	9.19E+01	0.00E+00	0.00E+00
Fr	221	Beta	1.00E-03	2.88E+02	2.41E-03	9.78E-17	1.49E-26	4.06E-05	5.16E-21	5.42E+01	1.65E-22	2.80E-19
Fr	221	Alpha	1.00E+00	2.88E+02	2.41E-03	9.78E-17	1.49E-26	4.06E-05	1.66E-17	1.72E+02	1.65E-22	2.86E-15
Ra	225	Beta	1.00E+00	1.28E+06	5.42E-07	9.78E-17	6.74E-23	1.80E-01	3.08E-17	3.87E+01	7.34E-19	1.19E-15
Ac	225	Alpha	1.00E+00	8.64E+05	8.02E-07	9.78E-17	4.55E-23	1.22E-01	4.00E-17	4.17E+01	4.96E-19	1.67E-15
Th	229	Alpha	1.00E+00	2.49E+11	2.79E-12	9.78E-17	1.33E-17	3.51E+04	2.61E-17	1.37E+02	1.43E-13	3.56E-15
Pa	233	Beta	1.00E+00	2.33E+06	2.97E-07	5.11E-09	6.65E-15	1.72E+07	7.72E-09	1.45E+02	6.99E-11	1.12E-06
U	233	Alpha	1.00E+00	5.02E+12	1.38E-13	1.77E-13	4.97E-13	1.28E+09	9.82E-15	1.68E+01	5.22E-09	1.65E-13
U	237	Beta	1.00E+00	5.83E+05	1.19E-06	1.19E-06	3.94E-13	1.00E+09	2.23E-06	7.51E+01	4.07E-09	1.67E-04
Np	237	Alpha	1.00E+00	6.77E+13	1.02E-14	5.10E-09	1.96E-07	4.98E+14	5.28E-09	3.23E+01	2.03E-03	1.70E-07
Pu	241	Beta	1.00E+00	4.53E+08	1.53E-09	4.85E-02	1.27E-05	3.17E+16	0.00E+00	0.00E+00	1.29E-01	0.00E+00
Pu	241	Alpha	2.50E-05	4.53E+08	1.53E-09	4.85E-02	1.27E-05	3.17E+16	6.60E-03	1.27E+02	1.29E-01	8.36E-01
Am	241	Alpha	1.00E+00	1.36E+10	5.08E-11	1.42E-03	1.12E-05	2.79E+16	1.14E-03	3.47E+01	1.13E-01	3.96E-02
Cm	245	Alpha	1.00E+00	2.68E+11	2.58E-12	6.34E-02	9.98E-03	2.45E+19	9.19E-02	7.15E+01	9.98E+01	6.57E+00

Table 36. Composition of the ^{245}Cm 30 years after the isotopic separation.

Appendix III.
Counting rates of ^{197}Au, ^{233}U, ^{237}Np, ^{240,242}Pu, ^{241,243}Am and ^{245}Cm at n_TOF

The expected counting rates for the different samples described in Table 1 are shown in Figure 33, Figure 34, Figure 36, Figure 37, Figure 38, Figure 39 and Figure 40.

- **^{197}Au**

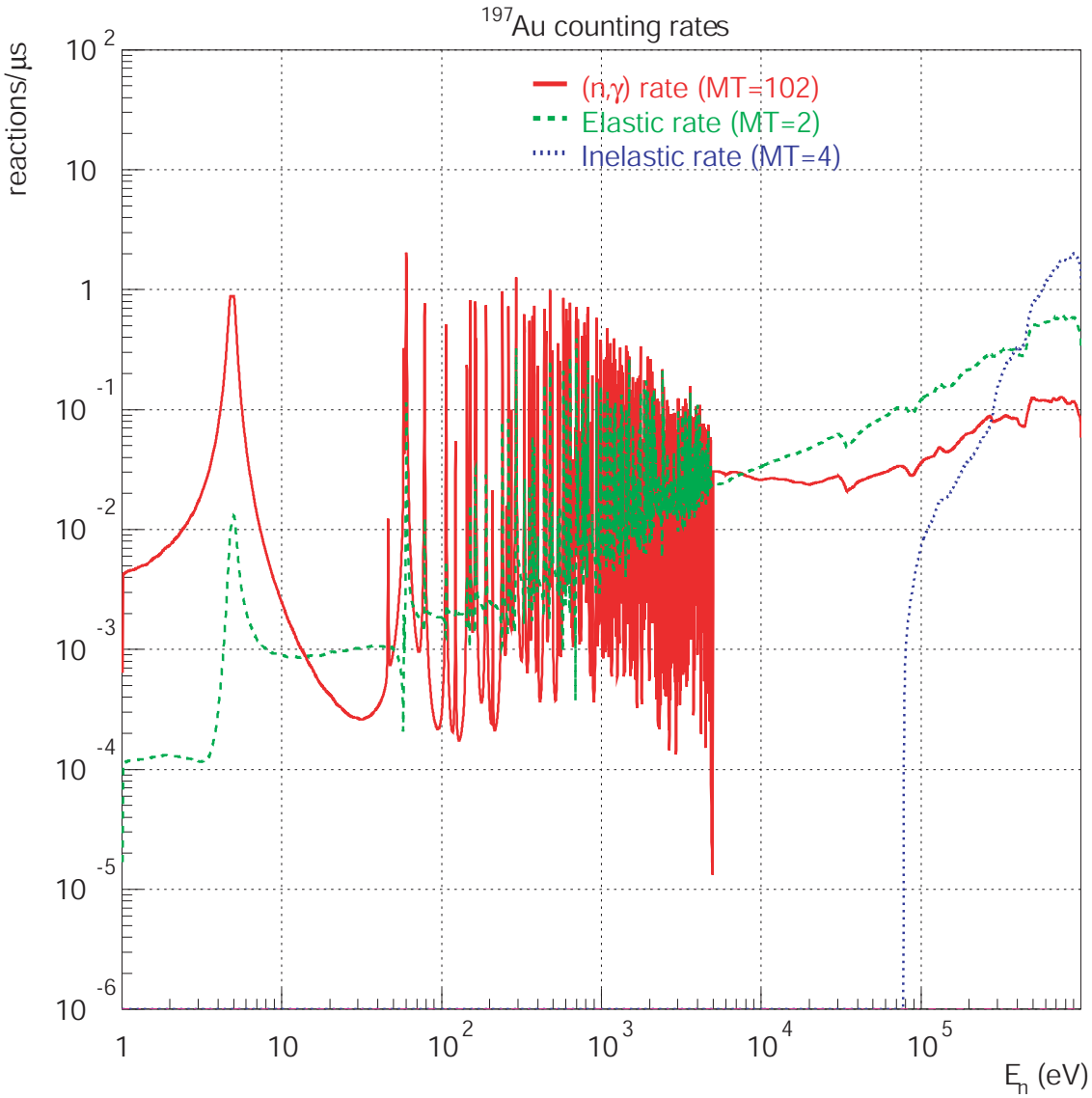

Figure 33. Expected counting rates of the capture, elastic and inelastic reaction channels for ^{197}Au.

- ^{233}U

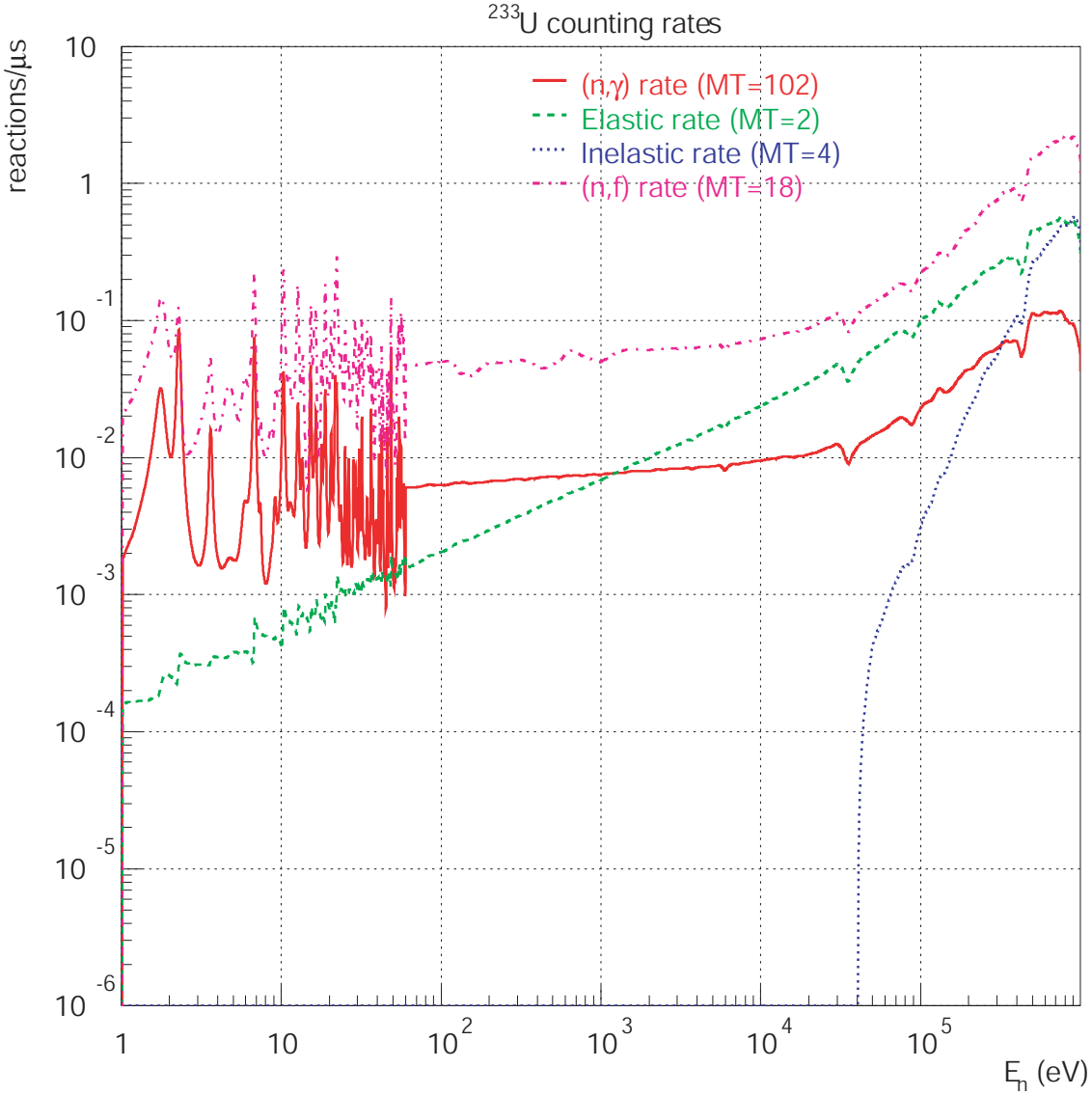

Figure 34. Expected counting rates of the capture, fission, elastic and inelastic reaction channels for ^{233}U.

- **^{237}Np**

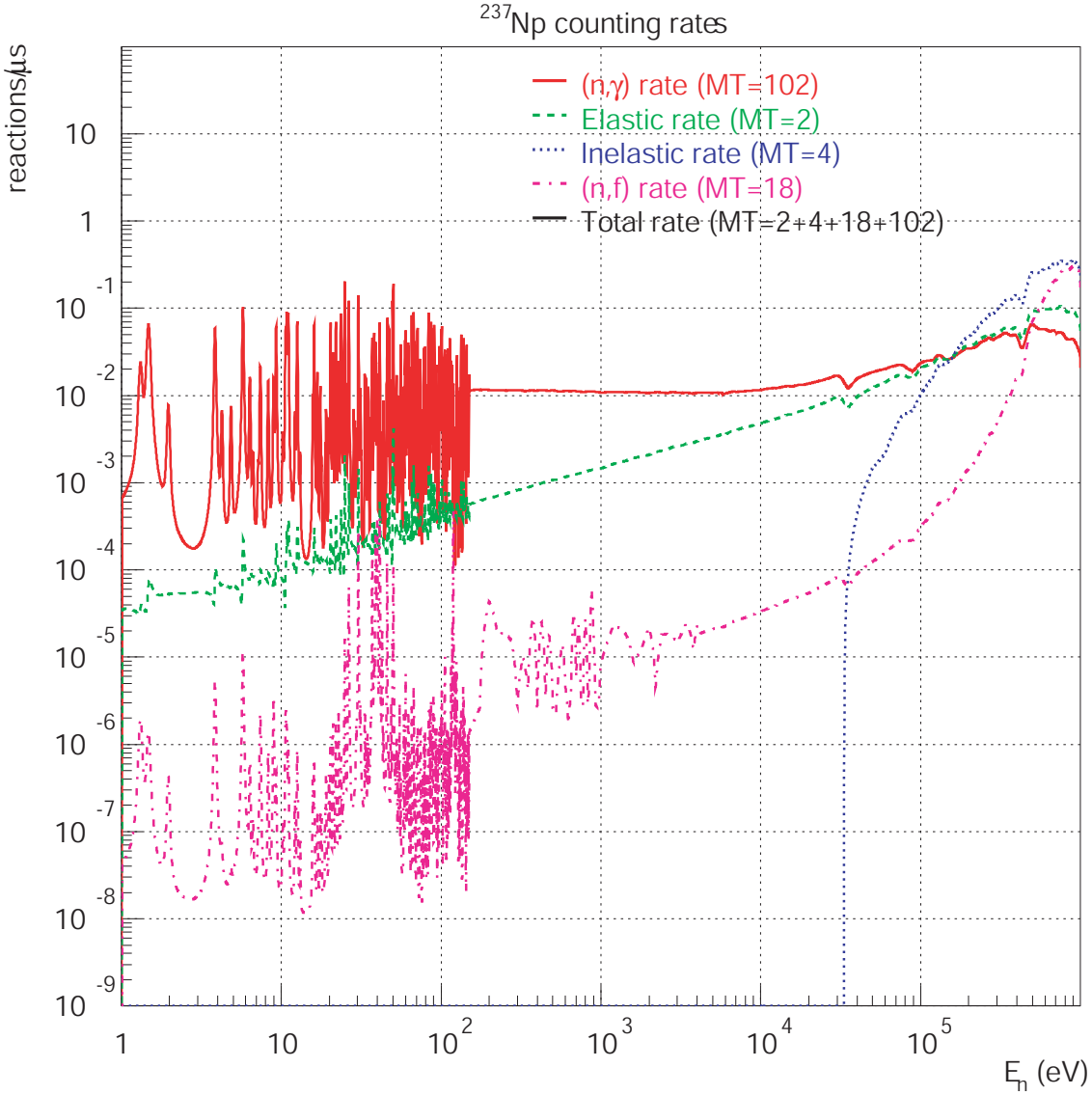

Figure 35. Expected counting rates of the capture, fission, elastic and inelastic reaction channels for ^{237}Np.

- **^{240}Pu**

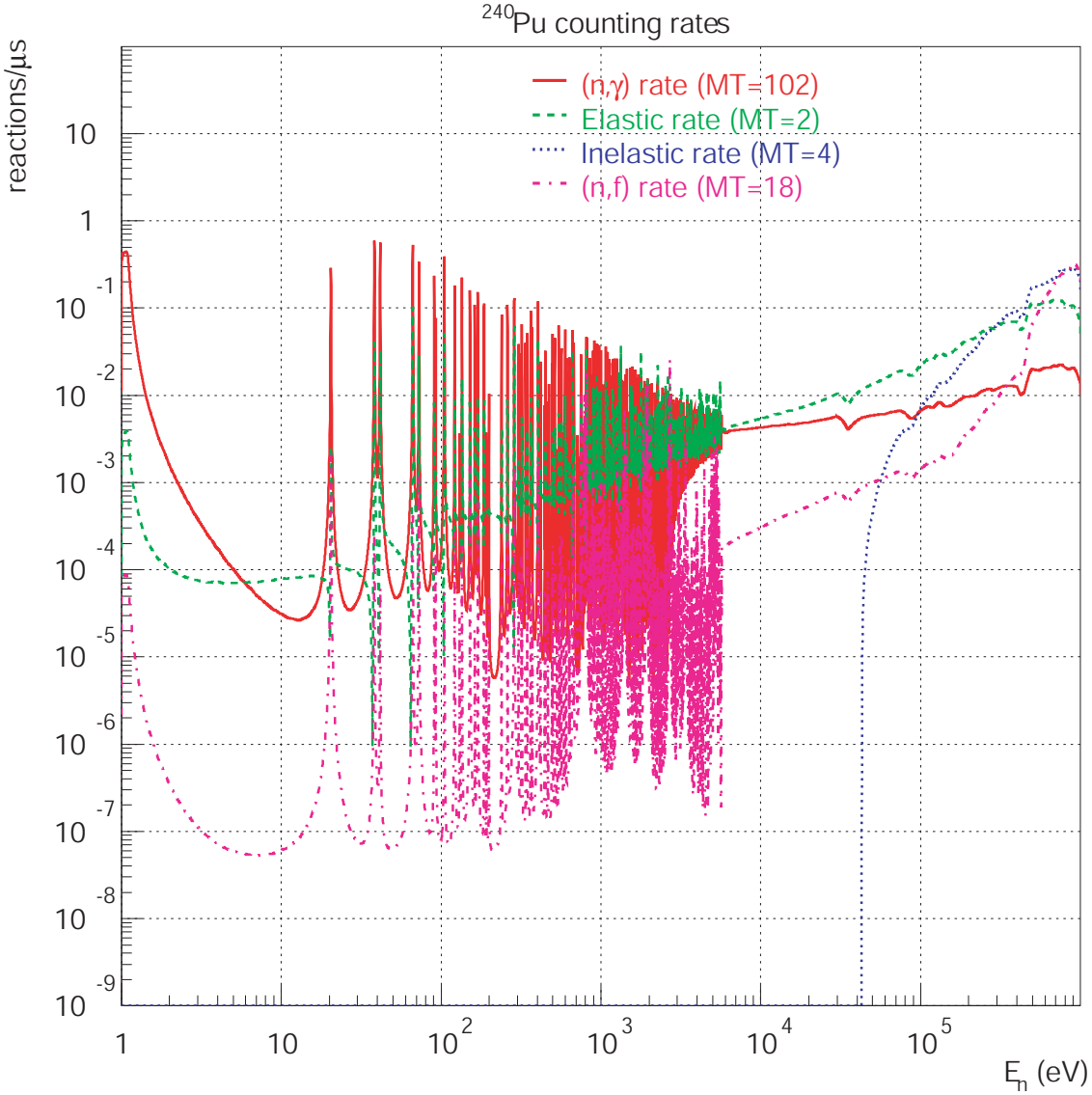

Figure 36. Expected counting rates of the capture, fission, elastic and inelastic reaction channels for ^{240}Pu.

- **^{242}Pu**

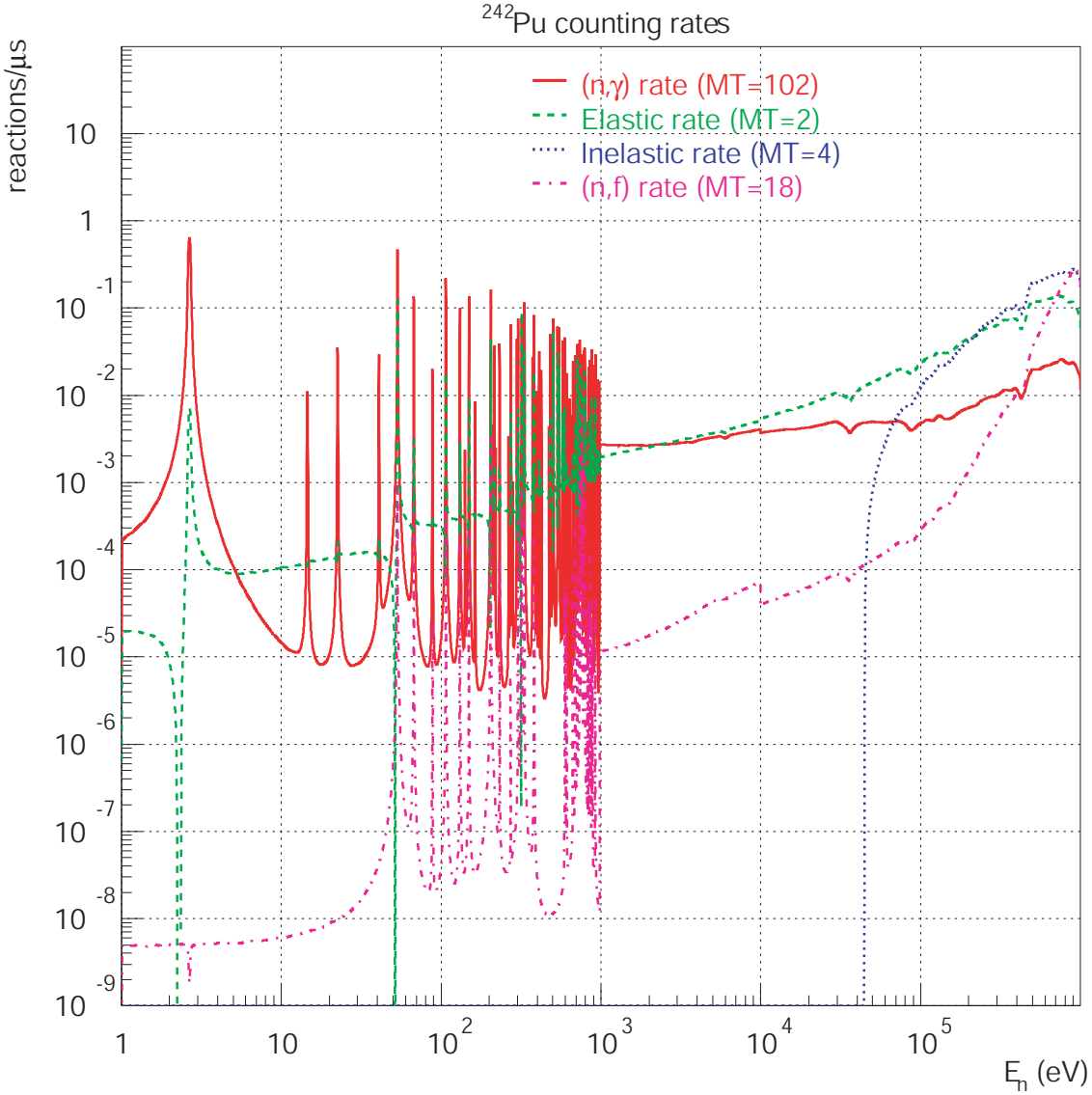

Figure 37. Expected counting rates of the capture, fission, elastic and inelastic reaction channels for ^{242}Pu.

- **^{241}Am**

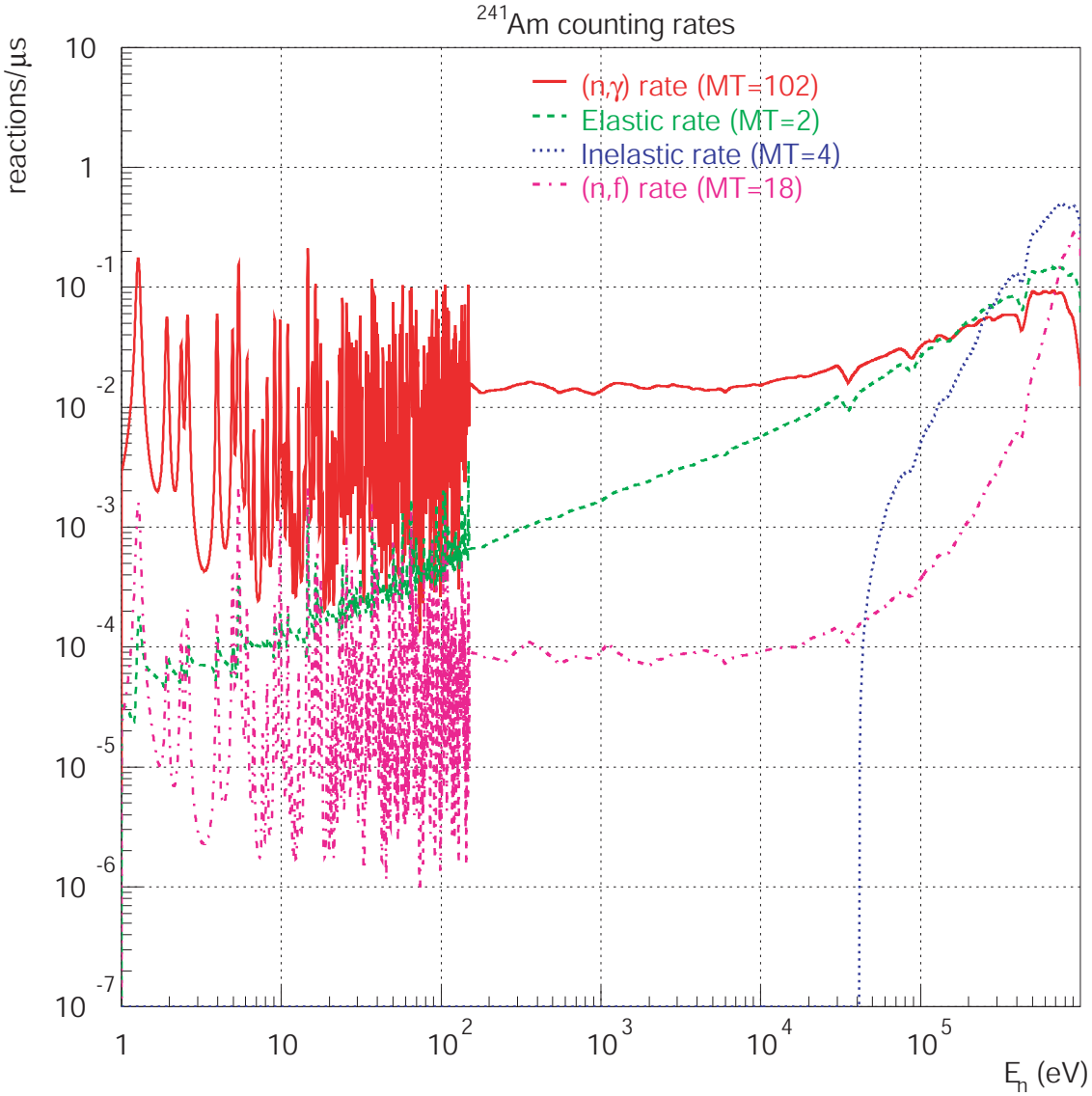

Figure 38. Expected counting rates of the capture, fission, elastic and inelastic reaction channels for ^{241}Am.

- **^{243}Am**

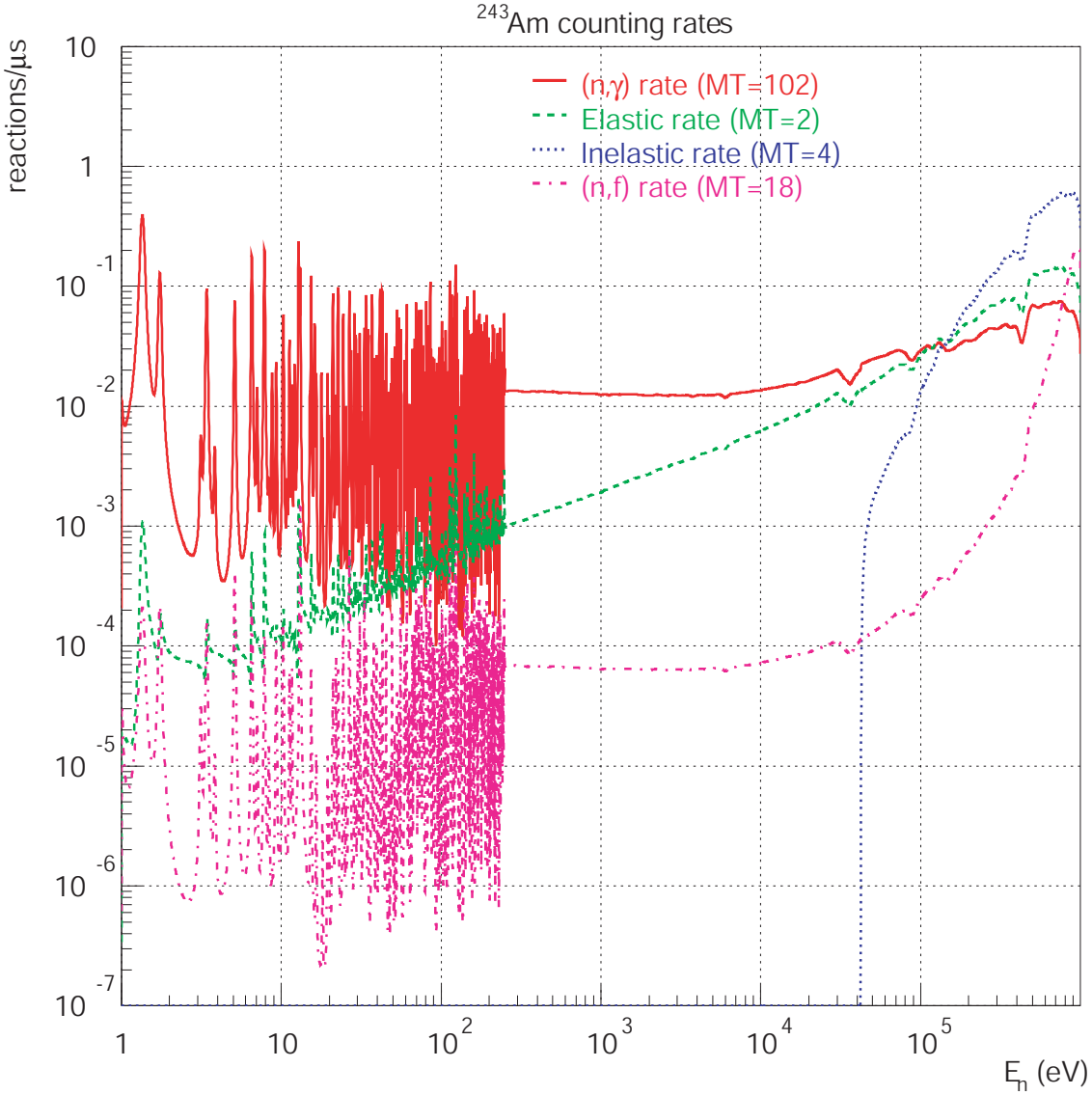

Figure 39. Expected counting rates of the capture, fission, elastic and inelastic reaction channels for ^{243}Am.

- **^{245}Cm**

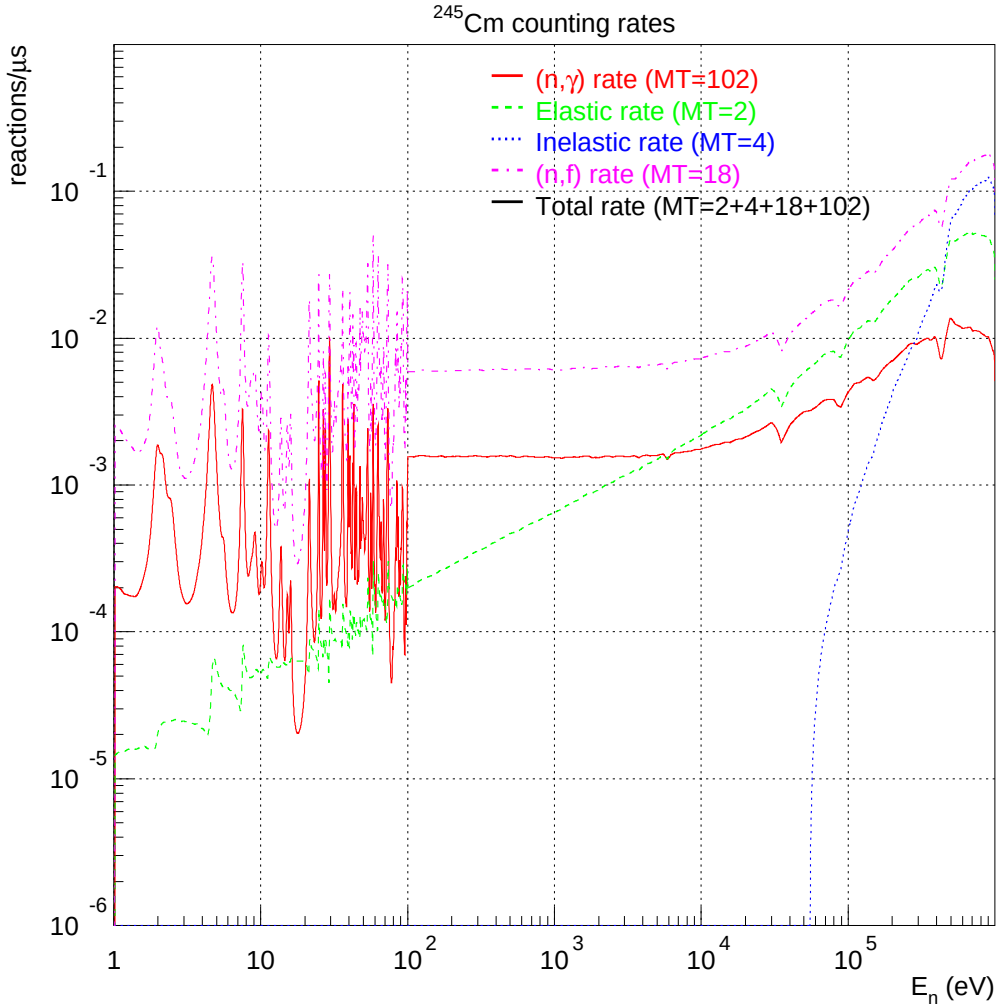

Figure 40. Expected counting rates of the capture, fission, elastic and inelastic reaction channels for ^{245}Cm.